

A FORWARD GENETIC APPROACH TO IDENTIFYING NOVEL
CALCIUM REGULATORS IN *TOXOPLASMA GONDII*

Kaice Arminda LaFavers

Submitted to the faculty of the University Graduate School

in partial fulfillment of the requirements

for the degree

Doctor of Philosophy

in the Department of Pharmacology and Toxicology,

Indiana University

November 2017

Accepted by the Graduate Faculty of Indiana University, in partial fulfillment of the requirements for the degree of Doctor of Philosophy.

Doctoral Committee

Gustavo Arrizabalaga, Ph.D., Chair

Nickolay Brustovetsky, Ph.D.

Theodore Cummins, Ph.D.

Stacey Gilk, Ph.D.

July 25, 2017

William Sullivan, Ph.D.

Acknowledgements

I would like to thank Dr. Vern Carruthers for sharing the Rh Δ Ku80 strain used for endogenous tagging and generation of the *gra41* knockout as well as the *gra2* knockout strains along with its parental and complemented strains and the MIC2 antibody, Dr. Peter Bradley for the GRA7 and ROP1 antibodies, Dr. John Boyle for the Pru Δ Ku80 strain used for endogenous tagging and the generation of the *gra41* Type II knockout strain, Dr. Barry Stein for valuable training and advice in obtaining the transmission electron microscopy of the *gra41* parental, knockout and complemented strains and Dr. Sanofar Abdeen for training and advice in recombinant protein purification. I would like to thank Karla Marquez Noguera, in the laboratory of Dr. Silvia Moreno at University of Georgia for conducting the calcium measurement experiments, Dr. Isabelle Coppens at Johns Hopkins for conducting the immunoelectron microscopy imaging, and Dr. Gustavo Arrizabalaga and Erin Garrison for the sequencing of the forward genetic mutant. I would also like to thank all members of Arrizabalaga and Sullivan labs for scientific and personal support. Finally, I would like to thank all of the members of my research committee, Drs. Brustovetsky, Cummins, Gilk and Sullivan, along with my mentor, Dr. Arrizabalaga, for their continued mentorship and support throughout my graduate career. This research has been funded by NIH grants R21AI119516, R01AI123457, and RO3AI101624 to Gustavo Arrizabalaga as well as an NIH training grant AI060519 and a fellowship from the American Heart Association 16PRE27260042 to Kaice LaFavers.

Kaice Arminda LaFavers

A FORWARD GENETIC APPROACH TO IDENTIFYING NOVEL
CALCIUM REGULATORS IN TOXOPLASMA GONDII

Toxoplasma gondii is an obligate intracellular eukaryotic pathogen that causes severe neurologic disease in immunocompromised adults and congenitally infected neonates. Events critical to the propagation of *T. gondii*, such as invasion and egress, are regulated by calcium-dependent signaling. In order to identify unique components of the parasite's calcium signaling networks, members of the Arrizabalaga laboratory have used a forward genetics approach to isolate mutants with altered sensitivity to the calcium ionophore A23187. Exposing extracellular parasites to A23187 induces protein secretion, motility and cytoskeletal rearrangements and prolonged treatment causes exhaustion of factors required for invasion, which results in what is referred to as ionophore induced death (iiDeath). Mutants capable of surviving this treatment were isolated from a chemically mutagenized population. Whole genome sequencing of one such mutant, MBD2.1, identified a nonsense mutation in a protein of unknown function (TGGT1_069070, ToxoDBv7.2) Complementation of MBD 2.1 with a wild-type copy of TGGT1_069070 restored sensitivity to iiDeath treatment. Endogenous tagging of this locus revealed that the encoded protein is secreted from a unique parasite secretory organelle known as the dense granule into the parasitophorous vacuole, leading to its designation as TgGRA41. Complete knockout of TgGRA41 recapitulates the resistance to iiDeath observed in MBD2.1 but also exhibits a

dramatic decrease in propagation in tissue culture not seen in the original mutant. The knockout shows defects in multiple steps of the lytic including compromised invasion efficiency and premature egress of parasites from host cells. Cytosolic calcium measurements of extracellular parasites show enhanced uptake of calcium in the knockout strain as compared to parental and complemented, suggesting that the loss of TgGra41 results in calcium dysregulation. Together, these results provide a novel insight into the role that the parasitophorous vacuole of *T. gondii* plays in calcium homeostasis and calcium-dependent signaling processes.

Gustavo Arrizabalaga, Ph.D., Chair

Table of Contents

List of Tables	x
List of Figures	xi
List of Abbreviations	xiii
Chapter 1 : Introduction	1
Specific Aims	1
Clinical Significance	3
<i>T. gondii</i> Life Cycle	6
<i>T. gondii</i> Lytic Cycle	9
Cell Biology of <i>T. gondii</i>	12
Calcium Signaling in <i>T. gondii</i>	22
Chapter 2 : Methods	29
Parasite propagation	29
Genome sequencing and complementation	29
iiDeath survival assay	30
Micronemal secretion assay	31
Generation of Type I endogenously tagged GRA41 line	32
Immunofluorescence assays	32
Western blot analysis	33
Triton-X 114 membrane partitioning	34
Electron microscopy	35
Generation of Type I <i>GRA41</i> knockout strain	36
Generation of <i>GRA41</i> knockout complemented clones	39

Parasite growth assays	40
Parasite egress assays	40
Parasite invasion assays	40
Calcium measurements	41
Recombinant protein production	42
Calcium thermal shift assays	43
Immunoprecipitation.....	44
Yeast two hybrid screen.....	46
Generation of Type II endogenously tagged GRA41 line.....	47
Generation of Type II <i>GRA41</i> knockout strain	48
Bradyzoite differentiation assays	49
Mouse studies of chronic toxoplasmosis.....	50
Chapter 3 : Identification and Characterization of GRA41	54
Nonsense mutation in novel gene is responsible for iiDeath ⁻ phenotype of MBD2.1	54
TGGT1_069070 encodes a novel dense granule protein, GRA41.....	58
Complete knockout of GRA41 recapitulates iiDeath ⁻ phenotype.....	62
Complete knockout of <i>GRA41</i> results in decreased plaquing efficiency	65
Complementation of <i>GRA41</i> knockout with the parental gene rescues both iiDeath sensitivity and lytic cycle defects	66
Complete knockout of <i>GRA41</i> affects timing of natural egress.....	70
Chapter 4 : Functional Analysis of GRA41	75

Ionophore induced death is due to decreased attachment and decreased stimulated microneme secretion	75
Complete knockout of <i>GRA41</i> leads to dysregulation of parasite calcium	78
Complete knockout of <i>GRA41</i> disrupts vacuolar morphology	79
Complete knockout of <i>GRA41</i> leads to altered structure of the tubulovesicular network	82
Incubation of recombinant GRA41 with calcium does not affect protein melting temperature	84
Attempts to identify interactors of GRA41 by immunoprecipitation yield inconsistent results	86
GRA41 has several high confidence interactions in yeast two hybrid screen ..	88
Chapter 5 : Characterization of GRA41 During Parasite Differentiation	92
TgGRA41 is expressed in a Type II strain and localizes to the wall of bradyzoite tissue cysts	93
Knockout of <i>GRA41</i> in a Type II Strain recapitulates resistance to ionophore induced death	95
Preliminary Data on Impact of GRA41 Loss on Tissue Cyst Development	97
Chapter 6 : Discussion	102
Chapter 7 : Conclusion and Future Directions	119
Conclusion	119
Future Directions	122
Does the loss of GRA41 impact calcium levels within the parasitophorous vacuole?	122

How does GRA41 localize to the tubulovesicular network?	123
What parts of the protein are necessary for the different functions of GRA41?	124
What are the protein interaction partners of GRA41? Can any of these explain the phenotypes associated with its loss?.....	125
Are there differences between the Type I and Type II GRA41 proteins that could provide insight into protein function or parasite biology?	127
Does the knockout of GRA41 in a Type II strain lead to a defect in bradyzoite cyst maintenance?	128
Chapter 8 : References	131
Curriculum Vitae	

List of Tables

Table 2.1 Name and sequence of primers used in this study. All sequences are 5' to 3'.....	39
Table 4.1 Proteins identified following immunoprecipitation of GRA41 from whole cell lysates.....	87
Table 4.2 GRA41 Potential Interactors from Yeast Two Hybrid Analysis	90

List of Figures

Figure 1.1 Life cycle of <i>T. gondii</i>	8
Figure 1.2 Lytic Cycle of <i>T. gondii</i>	10
Figure 1.3 <i>T. gondii</i> tachyzoite with selected organelles drawn and identified. .	21
Figure 1.4 Key steps in the lytic cycle of <i>T. gondii</i> are accompanied by fluctuations in calcium within the parasite and host cell.....	23
Figure 1.5 Conservation of Calcium Signaling in <i>T. gondii</i>	24
Figure 3.1 Sequencing of TgGT1_069070	55
Figure 3.2 The iiDeath ⁻ phenotype of MBD2.1 is due to the introduction of a premature stop codon in TGGT1_069070.	57
Figure 3.3 TGGT1_069070 encodes a novel dense granule protein, GRA41	60
Figure 3.4 Western Blot Analysis of Triton-X 114 partitioning of parasite lysates from the GRA41 endogenously HA-tagged strain.	62
Figure 3.5 Complete knockout of <i>GRA41</i> recapitulates the iiDeath ⁻ phenotype seen in MBD2.1 mutant.	64
Figure 3.6 Complete knockout of <i>GRA41</i> results in reduced plaquing efficiency which is rescued by complementation.	67
Figure 3.7 Complete knockout of <i>GRA41</i> results in decreased invasion efficiency	70
Figure 3.8 Complete knockout of <i>GRA41</i> leads to premature egress of parasites.....	71
Figure 4.1 Ionophore treatment of extracellular parasites causes a decrease in host cell attachment and microneme secretion.....	77

Figure 4.2 <i>GRA41</i> knockout parasites exhibit enhanced uptake of extracellular calcium.	79
Figure 4.3 <i>GRA41</i> knockout parasites have altered vacuole morphology and division pattern.	81
Figure 4.4 <i>GRA41</i> knockout parasites show altered morphology and size of tubulovesicular network (TVN) as compared to the parental and complemented strains	83
Figure 4.5 Ionophore induced death phenotype of <i>Gra2</i> parental, knockout and complemented strains.....	84
Figure 4.6 Melt curve analysis of <i>GRA41</i> recombinant protein incubated with calcium	85
Figure 5.1 <i>GRA41</i> is expressed in a type II strain and localizes to the wall of bradyzoite tissue cysts	94
Figure 5.2 Complete knockout of <i>GRA41</i> in a Type II Strain recapitulates the iiDeath phenotype seen in Type I Knockout.....	97
Figure 5.3 Differentiation of Type II <i>Gra41</i> Knockout.....	100
Figure 6.1 Proposed model for phenotypes associated with Loss of <i>GRA41</i> in Type I Strain	113

List of Abbreviations

Abbreviation	Definition
ADP	Adenosine diphosphate
AM ester	Acetoxymethyl ester
AMA1	Apical Membrane Antigen 1
ATP	Adenosine triphosphate
BME	Beta-mercaptoethanol
Bp	Basepairs
BSA	Bovine serum albumin
Ca ⁺⁺ /Ca ²⁺	Calcium ion
CBA/J	CBA Jackson
cDNA	Complementary deoxyribonucleic acid
CDPK3	Calcium-dependent Protein Kinase 3
COPI	Coat protein I
COPII	Coat protein II
CPL	Cathepsin protease L
DAPI	4',6-Diamidino-2-Phenylindole
DBA	<i>Dolichos biflorus</i> agglutinin
DG	Dense granule
DMEM	Dulbecco's modified Eagle medium
DMP-30	2,4,6-Tris(dimethylaminomethyl)phenol
DMSO	Dimethylsulfoxide
DTT	Dithiothreitol
EM	Electron microscopy
ER	Endoplasmic reticulum
FBS	Fetal bovine serum
GPI	Glycosylphosphatidylinositol
GPN	glycyl-L-phenylalanine-naphthylamide
GRA1	Dense Granule protein 1
GRA2	Dense Granule protein 2
GRA3	Dense Granule protein 3
GRA9	Dense Granule protein 9
GRA22	Dense Granule protein 22
GRA41	Dense Granule protein 41
H ⁺	Hydrogen ion, proton
HA	Hemagglutinin
HBSS	Hank's buffered salt solution
HEPES	4-(2-hydroxyethyl)-1-piperazineethanesulfonic acid
HFF	Human foreskin fibroblast
HXGPRT	Hypoxanthine-xanthine-guanine phosphoribosyl transferase
iiDeath	Ionophore induced Death
iiEgress	Ionophore induced Egress
IP ₃	Inositol triphosphate

IP ₃ R	Inositol triphosphate Receptor
IPTG	Isopropyl β-D-1-thiogalactopyranoside
ISC6	IMC Sutures Component 6
K ⁺	Potassium ion
kD	kiloDaltons
LB	Lysogeny broth
Mbp	Mega basepairs
MIC2	Microneme Protein 2
MOI	Multiplicity of infection
MW	Molecular Weight
MYOA	Myosin A
PBS	Phosphate buffered saline OR Predicted biological score
PCR	Polymerase chain reaction
PLV	Plant-like vacuole
PM	Plasma membrane
PV	Parasitophorous vacuole
PVM	Parasitophorous vacuole membrane
qPCR	Quantitative polymerase chain reaction
RIPA Buffer	Radioimmunoprecipitation assay buffer
RON2	Rhoptry Neck Protein 2
RON4	Rhoptry Neck Protein 4
RON5	Rhoptry Neck Protein 5
RON8	Rhoptry Neck Protein 8
ROP1	Rhoptry Protein 1
ROP40	Rhoptry Protein 40
ROP5	Rhoptry Protein 5
ROP7	Rhoptry Protein 7
ROP8	Rhoptry Protein 8
RPMI Medium	Roswell Park Memorial Institute Medium
RyR	Ryanodine receptor
SDS-PAGE	Sodium dodecyl sulfate – polyacrylamide gel electrophoresis
SNV	Single nucleotide variant
SORTL	Sortilin-like Receptor
<i>T. gondii</i>	<i>Toxoplasma gondii</i>
TBS	Tris-buffered saline
TBST	Tris-buffered saline with tween
TVN	Tubulovesicular network
TX-100	Triton X-100
TX-114	Triton X-114
VAC	Vacuole, refers to same organelle as plant-like vacuole
YFP	Yellow fluorescent protein

Chapter 1 : Introduction

Specific Aims

Toxoplasma gondii is an obligate intracellular eukaryotic pathogen responsible for potentially fatal infections in immunocompromised individuals and neonates. Current treatments for clinical Toxoplasmosis exhibit high rates of toxicity and cannot clear the chronic form of the disease (Luft and Remington 1992). The identification and characterization of processes and proteins that are both unique to the parasite and crucial for its survival is key for the discovery of new drug targets. In this context, calcium-dependent signaling represents an ideal target since it controls key aspects of the parasite's life cycle, and depends on many proteins that are unique to the parasite and absent in the mammalian host (Arrizabalaga and Boothroyd 2004, Nagamune 2009, Lourido and Moreno 2015). In order to identify novel calcium signaling factors, members of the Arrizabalaga laboratory have used a forward genetic approach to isolate mutants able to resist prolonged extracellular exposure to the calcium ionophore A23187. Ionophore treatment of extracellular parasites induces excessive secretion of invasion-related proteins, rendering parasites non-invasive, a phenomenon termed ionophore induced death (iiDeath). Members of the Arrizabalaga and Boothroyd laboratories were able to isolate a mutant, MBD 2.1, which remains invasive after this treatment. This mutant is also hypersensitive to the chelation of intraparasitic calcium by BAPTA-AM, suggesting that it may have dysregulated calcium homeostasis (Black, Arrizabalaga et al. 2000). Whole genome sequencing of the mutant and its parental strain identified multiple single nucleotide variants, two of

which lead to changes in the primary sequence of encoded proteins. Given that the common thread between the phenotype by which the MBD 2.1 mutant was isolated (iiDeath resistance) and this sensitivity to the calcium chelator BAPTA-AM is calcium, I hypothesize that identifying the causative mutation for iiDeath resistance in MBD2.1 will allow us to identify a novel protein regulator of calcium homeostasis within the parasite. I will test this hypothesis through the following aims:

Specific Aim 1: Determine the causative mutation in mutant MBD2.1 and characterize the protein responsible for resistance to iiDeath. Chemical mutagenesis and selection of the $RH\Delta h x g p r t$ strain led to the isolation of MBD2.1, which exhibits resistance to iiDeath. Whole genome sequencing of the mutant and parental strains identified candidate single nucleotide variants that could be responsible for this phenotype. To identify the causative mutation, I will attempt to complement the iiDeath⁻ phenotype by transfecting in wild-type copies of the mutated genes. Upon identification of the causative mutation, I will endogenously tag the responsible gene to determine the localization of the encoded protein. Additionally, I will generate a complete knockout of the responsible gene to verify that this recapitulates the resistance to iiDeath and to further characterize any phenotypes associated with the loss of this protein.

Specific Aim 2: Determine the mechanistic role of the iiDeath protein. Based on the resistance to iiDeath and hypersensitivity to BAPTA-AM seen in mutant MBD2.1, it is likely that the iiDeath protein impacts calcium homeostasis within the parasite. With this in mind, I will utilize the iiDeath protein knockout

generated in Aim 1 to test calcium levels in the parasite cytosol under normal and stimulated conditions. I will also generate recombinant iiDeath protein to investigate whether this protein is capable of binding calcium. In parallel I will explore the function of the iiDeath protein in an unbiased approach by identifying interacting proteins. I will also examine the morphology of the iiDeath protein knockout to look for any structural defects.

Specific Aim 3: Determine the impact of the iiDeath protein on the establishment and progression of infection *in vivo*. The forward genetic approach used to generate the MBD2.1 mutant was conducted in a highly virulent strain that does not establish a chronic infection and cannot be used to determine the full spectrum of the iiDeath protein's role during infection. Accordingly, I will generate a knockout of the iiDeath protein in a strain suitable for *in vivo* and developmental studies. This will allow us to test the role of this novel protein in the generation of chronic stage cysts in tissue culture and *in vivo* and development of acute and chronic infection *in vivo*.

Clinical Significance

T. gondii is an obligate intracellular parasite of the phylum Apicomplexa that causes widespread infection among many vertebrates, including humans (San Miguel, Gutierrez-Exposito et al. 2016). It is estimated that approximately a third of the world's human population is infected with this opportunistic pathogen. Humans become infected congenitally or by ingestion of either environmental oocysts, which are shed in the feces of cats, or tissue cysts, found in the undercooked meat of infected animals (Pappas, Roussos et al. 2009).

Though immunocompetent individuals will not generally experience symptoms during infection, *T. gondii* can be particularly devastating in immunocompromised individuals and those infected congenitally (Mazzillo, Shapiro et al. 2013, Oray, Ozdal et al. 2015). During the acute stage of the infection, *T. gondii* propagates through repeated lytic cycles of host cell invasion, growth and egress as a rapidly dividing form known as the tachyzoite, resulting in significant host cell death (Black and Boothroyd 2000). The tissue damage elicited by parasite propagation is normally limited by an immune response that relies on both CD4⁺ and CD8⁺ T cells, which induces conversion to the cyst-forming bradyzoite stage and the establishment of a chronic infection (Landrith, Harris et al. 2015).

In immunocompromised individuals and lymphoma patients, new infections or rupture of pre-existing tissue cysts can lead to toxoplasmic encephalitis (Luft and Remington 1992, Israelski and Remington 1993, Slavin, Meyers et al. 1994). Toxoplasmic encephalitis can be a difficult diagnosis to make; the most common associated symptoms are nonspecific headache, confusion and fever. However, this can progress to coma and death if left untreated and in a small minority of treated patients as well (Porter and Sande 1992). Neuropathological analysis of toxoplasmic encephalitis by magnetic resonance imaging (MRI) shows visible lesions that are the result of tissue damage caused by lysis of host cells by the parasite (Neuen-Jacob, Figge et al. 1993). Current anti-retroviral treatments directed at the human immunodeficiency virus (HIV) have reduced the overall incidence and mortality of toxoplasmic encephalitis in the HIV-infected population,

one of the largest population groups at risk for developing this severe complication. However, toxoplasmic encephalitis remains an important cause of morbidity and mortality in the subset of this population whose HIV infection remains undetected for prolonged periods of time, referred to as late presenters (Martin-Iguacel, Ahlstrom et al. 2017). Toxoplasmic encephalitis continues to remain a concern for other immunosuppressed patients, such as those who have received organ transplants (Greenway, Sacco et al. 2017). Another important immunocompromised population includes those individuals who are infected congenitally, who may experience severe neurological problems or even death as a result of *T. gondii* infection of the central nervous system, given the immature nature of the fetal immune system (Wilson, Remington et al. 1980).

In all patient populations, *T. gondii* infection can result in the development of eye infections to the retina (ocular toxoplasmosis) that can cause scarring, blurred vision or even loss of sight. Though it was originally thought that the majority of ocular toxoplasmosis cases were acquired congenitally, recent studies show that many cases are acquired postnatally (Gilbert and Stanford 2000). Current evidence suggests that both types of exposure lead to infection of the eye tissue from parasites circulating in the blood rather than from the nervous system (Park 2012). Despite this, they have very different clinical presentations if left untreated, with postnatally acquired cases often resulting in a focal necrotizing retinitis that may not dramatically impair vision (Cochereau-Massin, LeHoang et al. 1992), and congenitally acquired infections causing widespread lesions throughout

the retina, which often results in damage to the macula and vision loss (Mets, Holfels et al. 1997).

T. gondii Life Cycle

The *T. gondii* life cycle is a complex one, utilizing both a definitive host in which sexual reproduction may occur and intermediate hosts where the parasite can only reproduce asexually (Figure 1.1, below). The definitive host of *T. gondii* is the cat and the feline intestine is capable of supporting both asexual and sexual reproduction of the parasite. Initial replication within the feline gut occurs asexually before parasites switch to production of micro- and macrogametes in response to as yet uncharacterized signals (Weiss and Kim 2014). Though these gametes are capable of generating cross-fertilized parasites (Pfefferkorn and Pfefferkorn 1980), the actual fertilization event has not been observed. The resulting oocysts produced by the sexual stages are shed for 1-2 weeks in the feces of the cat and are capable of initiating an acute infection in animals that consume them (Frenkel, Dubey et al. 1970). Though domesticated cats play a key role in disease transmission among humans, all tested felids are capable of producing oocysts. *T. gondii* has been able to establish infections in a large variety of vertebrates worldwide in any area where infected felines are present (Jewell, Frenkel et al. 1972).

The oocyst is the only stage in the life cycle of *T. gondii* capable of undergoing development outside of a host cell (extracellular growth). After the oocyst is shed in the feces of the cat its contents differentiate from a single cytoplasmic mass known as the sporoblast to two sporocysts. Each sporocyst

contains four sporozoites capable of invading host cells and generating an acute infection in the intermediate host (Birch-Andersen, Ferguson et al. 1976). The oocysts are highly stable in the environment and can last from months to years, depending on the moisture content and temperature of the soil; they are particularly stable under cool, damp conditions (Lelu, Villena et al. 2012). Upon ingestion, the sporozoites will excyst from the oocyst and are able to infect host cells. Though the process of excystation has not been monitored *in vivo*, *in vitro* studies show that a fluid containing trypsin and bile salts can stimulate this process, suggesting that the trigger for excystation is the host digestive tract (Speer, Clark et al. 1998). Within 1-2 lytic cycles of the sporozoite invading the host, the sporozoite will convert to the rapidly replicating form of the parasite known as the tachyzoite, which characterizes the acute infection in the intermediate host (Speer, Tilley et al. 1995).

The tachyzoite life stage is responsible for the tissue damage, rapid dissemination to distant tissues and symptomology seen in the acute stage of *T. gondii* infection. Repeated cycles of host cell invasion, parasite replication and egress by the tachyzoite result in the lysis and death of the host cell. In immunocompetent individuals, the acute infection is rapidly cleared by the immune system as described previously. The tachyzoite form of the parasite is not often responsible for transmission of infections to a new host, except in the case of congenital transmission or more rarely as a result of laboratory accidents or blood transfusions (Parker and Holliman 1992, Karimi, Mardan et al. 2014). A mother who is infected for the first time during pregnancy can transmit the disease to her

fetus as the tachyzoite can cross the placental barrier (Jones, Lopez et al. 2003). The rate of fetal seroconversion and health outcomes vary over the course of pregnancy and are inversely correlated with one another, with infection in the first trimester relatively rare, but associated with severe birth defects and potential miscarriage, and infection in the third trimester much more likely but with limited impact on the fetus (Montoya and Liesenfeld 2004).

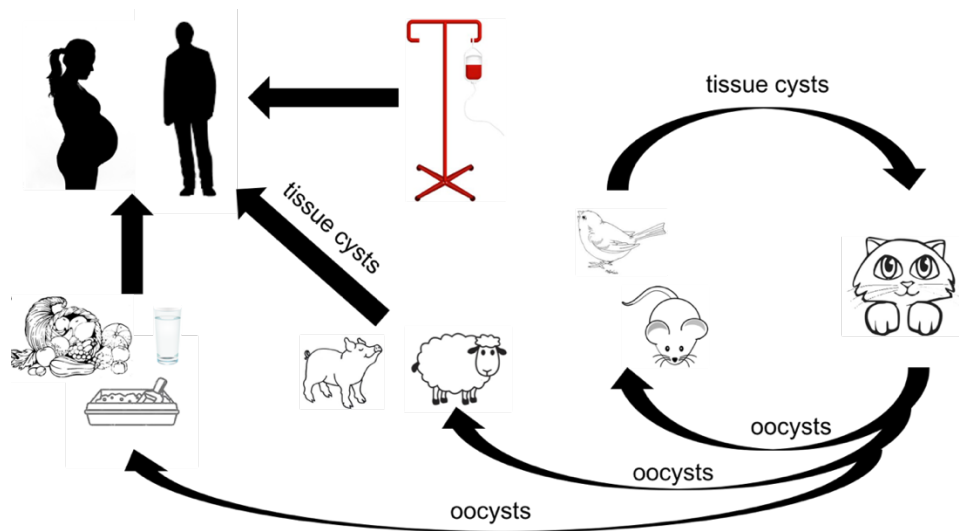


Figure 1.1 Life cycle of *T. gondii*

The complete life cycle of *T. gondii* occurs in felids and their prey. Highly infectious oocysts are shed in the feces of the felid and are ingested by prey. Following acute infection, the parasite will form tissue cysts, which are highly infectious to felids. Humans can be infected by exposure to oocysts and tissue cysts, congenitally, or via organ transplant/blood transfusion.

The tachyzoite converts to a slower growing, tissue cyst-forming stage known as the bradyzoite in response to immune system pressure in the intermediate host (Weiss and Kim 2000). The tissue cyst formed by the bradyzoite is protected by a cyst wall, which is dependent on extensive glycosylation of its components for tissue cyst persistence in a mouse model (Caffaro, Koshy et al. 2013). During the initial stages of tissue cyst formation and bradyzoite maturation,

the parasites continue to replicate slowly, but this replication becomes relatively rare in mature cysts (Ferguson and Hutchison 1987). The bradyzoite is the final life cycle stage observed in the immunocompetent intermediate host, but it is a crucial one for propagation to a new host. In order to complete its life cycle, the parasite must return to its definitive host, and evidence suggests that the most infectious form of *T. gondii* for cats is the bradyzoite (Dubey 2006). Bradyzoite cysts are also infectious to other intermediate hosts and cysts in raw or undercooked meat are an important source of infection for humans (Tenter, Heckeroth et al. 2000).

T. gondii Lytic Cycle

The lytic cycle of the *T. gondii* tachyzoite (Figure 1.2, below), which is at the center of its propagation and pathogenesis, begins with the active attachment and invasion of parasites into host cells, a process that is dependent on the secretion of proteins from specialized secretory organelles known as the micronemes and rhoptries (Carruthers and Sibley 1997). Invasion initiates the formation of a parasitophorous vacuole (PV) through the invagination of the host cell membrane (Suss-Toby, Zimmerberg et al. 1996). Following parasite growth within the PV, the cycle is reinitiated after the parasites actively egress the host cell and invade neighboring host cells. In recent years, many of the key molecular players in the lytic cycle have been identified. Unique proteins with adhesive properties are first released from the micronemes, where they interact with both the plasma membrane of the parasite and the host cell surface (Carruthers and Sibley 1997, Garcia-Reguet, Lebrun et al. 2000). Active invasion of the host cell is dependent

on a micronemal protein, Apical Membrane Antigen 1 (AMA1), along with proteins secreted from the rhoptries, rhoptry neck proteins 2, 4, 5 and 8 (RONs 2,4,5,8). These proteins assemble to form a moving junction, where RONs 2, 4,5, and 8 are associated with the host cell plasma membrane and AMA1 is associated with the parasite plasma membrane. A high affinity interaction between AMA1 and RON2 brings the parasite into close contact with the host cell plasma membrane and is necessary for rapid invasion of the host cell as the parasite moves through the moving junction into the host cytosol (Alexander, Mital et al. 2005, Lebrun, Michelin et al. 2005, Alexander, Arastu-Kapur et al. 2006, Beck, Chen et al. 2014). Invading parasites do not cross the host cell plasma membrane and instead cause it to invaginate; the parasite then uses this membrane to form the membrane of the

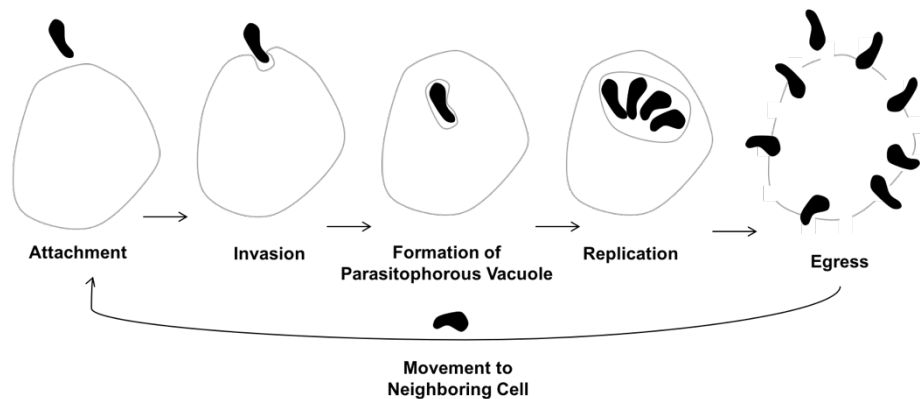


Figure 1.2 Lytic Cycle of *T. gondii*

The lytic cycle begins with the active attachment of a parasite (shown in black) to a new host cell (outlined in grey). The parasite then actively invades the host cell and invaginates the host cell membrane to create the parasitophorous vacuole. It then replicates within this vacuole before actively egressing from the host cell and moving to a nearby cell to begin the cycle again.

parasitophorous vacuole. During invasion, this membrane is stripped of the majority of host cell transmembrane proteins, though GPI-anchored host proteins

have been found in the resulting vacuole membrane (Mordue, Desai et al. 1999). Once the parasite is completely internalized, proteins secreted from the rhoptries and a third secretory organelle, the dense granule, traffic to both the newly formed vacuole and the host cell to create a niche for parasite replication (Carruthers and Sibley 1997).

Once inside the host cell, tachyzoites replicate by a process known as endodyogeny, in which a single mother parasite replicates its entire genome and organelles before dividing into two daughter parasites. This process results in ageometric expansion in parasite number, with doublings occurring every 5-9 hours *in vitro*, depending on the strain (Radke, Striepen et al. 2001). The number of doublings that a parasite undergoes before leaving a single host cell depends on a number of factors, including the size and type of host cell, the average number of parasites per host cell (multiplicity of infection or MOI) and the presence of signaling molecules (Nagamune, Hicks et al. 2008). When grown in human foreskin fibroblasts (HFFs) *in vitro*, parasites typically complete 5-7 division cycles over the course of 2-3 days before egressing (Black and Boothroyd 2000). *In vivo*, tachyzoites are found replicating within immune cells shortly after the initiation of an acute infection, where they typically only divide a few times before egressing (Tomita, Yamada et al. 2009). Thus, it is possible that the kinetics of parasite propagation in the mouse are quite different from what is seen in tissue culture.

In both natural and induced egress observed *in vitro*, the parasites actively leave the cell in a coordinated manner that requires activation of the parasite motility machinery. The parasite relies on an actin/myosin-based motility system

that is anchored just beneath the parasite membrane in a series of flattened sacs known as the inner membrane complex (IMC). This complex, known as the glideosome, consists of multiple IMC-bound proteins that act as an anchor for a myosin motor protein which interacts with filamentous actin to generate a motive force (Frenal, Polonais et al. 2010). Recent work from our lab demonstrates that the activation of a calcium-dependent protein kinase (CDPK3) following an increase in calcium levels within the parasite leads to the phosphorylation of the glideosome's myosin motor MYOA. This phosphorylation is required for maximal activation of MYOA, which is required for efficient and rapid host cell egress (Gaji, Johnson et al. 2015). Once this motility machinery is engaged, the parasites will leave the cell and travel to a neighboring cell where they can reinitiate the process of host cell attachment and invasion (Black and Boothroyd 2000).

Cell Biology of *T. gondii*

DNA-containing Organelles

T. gondii houses the majority of its genomic material in a large, centrally located nucleus (Figure 1.3, below). The haploid genome (approximately 69 Mbp) is spread among 14 chromosomes and encodes more than 8,000 genes (Lau, Lee et al. 2016). Curated versions of the *T. gondii* genome are maintained online at ToxoDB.org. *T. gondii* has two additional DNA-containing organelles, the mitochondrion, found in all eukaryotes, and a plastid-like organelle known as the apicoplast (Figure 1.3, below). As has been accepted to be the case for eukaryotic mitochondria, the apicoplast is also thought to be the result of engulfment of an endosymbiont (Gray 2017). Though the genome of the parasite's single

mitochondrion remains unresolved, it has been shown that the parasite mitochondrion is functional (i.e. generates a membrane potential through the activity of the electron transport chain) in both intra and extracellular parasites (Melo, Attias et al. 2000). Recent work has demonstrated that the parasite mitochondrion imports proteins using components of the TOM complex, which has been well characterized in model eukaryotes (Fukasawa, Oda et al. 2017). Conditional knockdown of proteins in this complex block parasite replication *in vitro*, suggesting that mitochondrial function is absolutely required for the tachyzoite stage of the life cycle (van Dooren, Yeoh et al. 2016). The apicoplast is a plastid-like organelle that is likely the result of a secondary endosymbiotic event wherein the ancestor of the parasite engulfed a red algal photosynthetic eukaryote to establish the chromalveolate lineage (Gould, Waller et al. 2008). Though many chromalveolates retain photosynthetic capabilities within their plastids, members of the apicomplexan phylum that have evolved as parasitic organisms have lost this function (McFadden and Yeh 2017). In fact, it appears that the only reason that the apicoplast is essential for *T. gondii* growth is due to the production of precursors of the isoprenoid pathway that takes place inside this organelle (Nair, Brooks et al. 2011).

Plasma Membrane and Associated Organelles

Just underneath the plasma membrane of *T. gondii* and all other alveolates (apicomplexans, dinoflagellates and ciliates) is a series of flattened sacs called alveoli (Ruggiero, Gordon et al. 2015). In *T. gondii*, these sacs come together to form the inner membrane complex (IMC), which covers the entirety of the plasma

membrane with the notable exception of the apical tip (Vivier and Petitprez 1969). The sacs are restricted to the area beneath a structure called the apical polar ring, leaving the apical tip of the parasite free, perhaps to facilitate secretion (Tran, de Leon et al. 2010). In addition to acting as a starting point for the IMC, the apical polar ring also acts as an anchor for 22 subpellicular microtubules that extend out from the ring in a spiral (Russell and Burns 1984). The microtubules line up with the IMC sacs to form a structure that helps the parasite to maintain its typical banana shape (Nichols and Chiappino 1987).

In addition to its role in maintaining parasite morphology, the IMC also houses the parasite motility machinery, called the glideosome (Opitz and Soldati 2002). Many of the proteins associated with the glideosome (Glideosome Associated Proteins or GAPs) are anchored in the membranes of the IMC through transmembrane domains (Bullen, Tonkin et al. 2009). They anchor the actin/myosin motor complex that propels the parasite forward in its typical gliding motion (Frenal, Polonais et al. 2010). Evidence also suggests that the IMC is capable of storing calcium (Bonhomme, Pingret et al. 1993), which would make it a convenient potential store for the calcium that is required for activation of glideosome components by calcium-dependent protein kinases (Gaji, Johnson et al. 2015).

The apical tip of the parasite contains a unique structure known as the conoid, which is composed of microtubules arranged in a specific structure (Hu, Roos et al. 2002). Normally the conoid is retracted within the apical polar ring that demarcates the beginning of the IMC, but is extended during invasion (Del

Carmen, Mondragon et al. 2009) and in response to artificial induction of calcium fluxes within the parasite (Mondragon and Frixione 1996). Though the exact function of the conoid is unknown, it is plausible that this structure plays a key role in parasite attachment and/or invasion. In fact, supporting this notion, non-apicomplexan alveolates with an incomplete conoid and apical secretory organelles use these structures to either partially or fully invade other free-living protozoa to obtain nutrients required for growth (Beis, Andre et al. 2002, Brugerolle, Bricheux et al. 2002, Leander, Kuvardina et al. 2003).

Secretory Organelles

The apical end of the parasite is also home to two unique secretory organelles, the small oval micronemes and the long club-shaped rhoptries (Figure 1.3, below), whose contents are released at specific times during the lytic cycle (Carruthers and Sibley 1997) and are essential for attachment, invasion, egress and modulation of the host immune system (Huynh, Rabenau et al. 2003, Huynh and Carruthers 2006, El Hajj, Lebrun et al. 2007, Fentress and Sibley 2011, Tyler and Boothroyd 2011, Niedelman, Gold et al. 2012). The micronemes release multiple adhesive proteins (MICs) responsible for forming the initial attachment of the parasite to a new host cell prior to invasion (Carruthers, Giddings et al. 1999, Cerede, Dubremetz et al. 2005). A complex known as the moving junction is then formed from micronemal and rhoptry-derived proteins. It is through this structure that the parasite will travel through to invade the host cell (Alexander, Mital et al. 2005, Straub, Peng et al. 2011, Beck, Chen et al. 2014). This complex and its role in invasion are described in more detail in the *T. gondii* lytic cycle section. The

rhoptries will continue to release their contents (ROPs for proteins secreted from the body of the rhoptry, RONs for those secreted from the rhoptry neck) into the newly formed parasitophorous vacuole and even into the host cell to modulate host cell immune responses (Boothroyd and Dubremetz 2008).

The dense granules are an additional secretory organelle that are found throughout the parasite (Figure 1.3, below) which release their contents constitutively throughout the parasite lytic cycle (Chaturvedi, Qi et al. 1999). When dense granule proteins are secreted from an intracellular parasite, they may be trafficked to one or more of four locations: the lumen of the parasitophorous vacuole, the parasitophorous vacuole membrane (PVM), the membranes of the tubulovesicular network (TVN), found throughout the vacuolar space or beyond the vacuole into the host cell (Sibley, Niesman et al. 1995, Lecordier, Mercier et al. 1999, Rome, Beck et al. 2008, Bougdour, Durandau et al. 2013). The majority of dense granule proteins share no sequence homology with characterized proteins from other organisms and homologs are often restricted to closely related species (i.e. those in the subfamily Toxoplamatinae), and are missing from other well-studied apicomplexans, such as *Plasmodium* species, suggesting that this group of proteins has evolved to specifically support *T. gondii*'s lifestyle (Mercier, Adjogble et al. 2005). The NTPases that are secreted from the dense granules into the parasitophorous vacuole are one notable exception to this rule with a conserved NTPase domain that has been shown to be enzymatically active (Asai, O'Sullivan et al. 1983, Bermudes, Peck et al. 1994, Sibley, Niesman et al. 1994). Though most dense granule proteins studied thus far are dispensable for *in vitro*

growth, they have been shown to play key roles in *in vivo* virulence, vacuole structure, host cell immune response and antigen presentation (Mercier, Cesbron-Delauw et al. 1998, Mercier, Howe et al. 1998, Travier, Mondragon et al. 2008). Other GRA proteins that are trafficked to the host cell have been shown to play important roles in strain-specific activation of the NFkB pathway (Rosowski, Lu et al. 2011), regulation of the p53 tumor suppressor pathway to enhance parasite virulence (Bougdour, Durandau et al. 2013), and regulation of the p38a MAPK pathway (Braun, Brenier-Pinchart et al. 2013).

Parasitophorous Vacuole

The parasite creates a parasitophorous vacuole during invasion by invaginating the host cell plasma membrane and stripping it of the majority of its proteins, rendering it non-fusogenic with the host cell endolysosomal system (Mordue, Hakansson et al. 1999). Parasite secreted proteins, whose identities were only recently identified, are trafficked into the vacuole membrane where they form a pore which allows molecules less than 1300 daltons to pass from the host cell cytosol to the parasitophorous vacuole lumen, allowing the parasite access to host cell nutrients (Schwab, Beckers et al. 1994, Gold, Kaplan et al. 2015). Also localized to the vacuole membrane are multiple rhoptry-derived kinases that are key determinants of virulence in a mouse model due to their ability to phosphorylate and inactivate the immunity-related GTPases used by mice to control intracellular pathogens (Etheridge, Alaganan et al. 2014). Though the export of multiple parasite proteins into the host cell suggests that the PVM must also contain a complex capable of transporting proteins across this membrane, the

molecular components of such a complex have yet to be identified. An attempt to identify *T. gondii* homologues to the components of the PV protein export complex of its apicomplexan relative, *Plasmodium*, identified the nutrient pore described above, suggesting that mechanisms for protein export across the PV membrane within these two parasites evolved independently (Gold, Kaplan et al. 2015).

Within the vacuole is found a network of membranous tubules known as the tubulovesicular network (TVN). The network is formed following the secretion of multi-lamellar vesicles from the basal end of the parasite shortly after host cell infection. These vesicles then fuse together to form the long membranous tubules of the TVN, which are 40-60 nm in diameter and may extend up to 1 μ M long. Electron microscopy analysis of the TVN shows that some, but not all of the tubules are continuous with the PVM (Sibley, Niesman et al. 1995). Multiple dense granule proteins are required for the formation of the TVN, and genetic disruption of these proteins leads to the accumulation of membranous material or partially formed tubules within the vacuole. Though vacuoles without a TVN are capable of growth *in vitro*, they show dramatically decreased virulence in a mouse model of infection (Mercier, Howe et al. 1998).

Endomembrane Trafficking Organelles

Proteins are trafficked to their final destinations through an endomembrane system that consists of a single perinuclear endoplasmic reticulum (ER) and a single Golgi stack (Figure 1.3, below). Secretory proteins are targeted to this system by a signal recognition particle-dependent translocation pathway, which has been shown to be partially conserved between *T. gondii* and eukaryotic model

organisms (Sheiner and Soldati-Favre 2008). It is likely that transport between the ER and Golgi is mediated by COPI/COPII coated vesicles as in model eukaryotes, based on the functional conservation of sequences for targeting to these two compartments (Hoppe and Joiner 2000), though these proteins have not been characterized within the parasite. In contrast to higher eukaryotes, which can have hundreds of Golgi stacks, *T. gondii* maintains a single stack of 3-5 Golgi cisternae that is located directly adjacent to the ER exit site (Pelletier, Stern et al. 2002). From the Golgi, the default secretory pathway will take proteins either to the dense granules, discussed above, or the parasite plasma membrane (Karsten, Qi et al. 1998, Striepen, He et al. 1998). Proteins targeted to the apicomplexan specific secretory organelles, the micronemes and rhoptries (discussed below) are recognized by a transmembrane Golgi protein, the sortilin-like receptor TgSORTL, which prevents them from following the default secretory pathway. This receptor recruits components of the protein transport machinery that instead allows these proteins to reach their final destination in the micronemes or rhoptries (Sloves, Delhaye et al. 2012). While transport into the mitochondrion occurs post-translationally through translocons located in the mitochondrial membrane, transport to the other endosymbiont-derived organelle, the apicoplast, begins in the ER/golgi. Apicoplast proteins are targeted via a bipartite signal sequence that contains both a signal peptide to direct them to the ER and a transit peptide that directs them to the apicoplast (Yung and Lang-Unnasch 1999). Preliminary characterization of translocons localized to membranes of the apicoplast suggest that this organelle imports proteins using translocons similar to those found in

chloroplast membranes, as would be expected (van Dooren, Tomova et al. 2008, Sheiner, Fellows et al. 2015). For remaining organelles, such as the acidocalcisomes or the plant-like vacuole (PLV), it remains unclear how proteins are targeted to these locations, though at least one PLV-localized protein contains a predicted signal peptide, suggesting proteins targeted to this organelle also pass through the ER/golgi secretory system (LaFavers, Alveal, and Arrizabalaga, unpublished data).

Ion Storage Organelles

T. gondii contains multiple organelles that play important roles in ion homeostasis (Figure 1.3, below). The first of these, the acidocalcisome, is found in many other species including prokaryotes and eukaryotes and contains large amounts of oxygen, sodium, chlorine, potassium, zinc, phosphate, and magnesium in addition to the calcium that gives it its name (Luo, Vieira et al. 2001, Docampo, de Souza et al. 2005). The calcium stores within this organelle have been shown to be released in response to alkalinizing agents such as NH_4Cl or proton ionophores such as nigericin or monensin (Moreno and Zhong 1996). Though the exact function of the acidocalcisome is unclear, the genetic ablation of a Ca^{2+} -ATPase localized to the acidocalcisome results in elevated cytosolic calcium and decreased invasion of host cells, leading to decreased virulence *in vivo*, suggesting this organelle plays an important role in sequestering parasite calcium from the cytosol (Luo, Ruiz et al. 2005).

The plant-like vacuole (PLV or VAC) is another organelle important for ion homeostasis. Proteins localized to this large vacuole include multiple proteases

hypothesized to be important for digestion of material acquired from the host cell by ingestion (Dou and Carruthers 2011), a Na⁺/H⁺ exchanger shown to be critical for normal calcium-dependent signaling processes (Francia, Wicher et al. 2011), a vacuolar proton pyrophosphatase (Rodrigues, Scott et al. 2000, Liu, Pace et al. 2014), a vacuolar proton ATPase (Rodrigues, Ruiz et al. 2002) and a transporter with homology to the chloroquine resistance transporter found in *Plasmodium*'s digestive vacuole (Warring, Dou et al. 2014). It has been proposed that the PLV acts as an additional store for calcium due to the release of calcium into the cytosol in response to glycyl-L-phenylalanine-naphthylamide (GPN) (Moreno and Zhong 1996). GPN is used in higher eukaryotes to measure lysosomal Ca²⁺ release since it is specifically hydrolyzed by cathepsin proteases found in lysosomes (Haller, Volkl et al. 1996, Srinivas, Ong et al. 2002). In *T. gondii*, these cathepsin

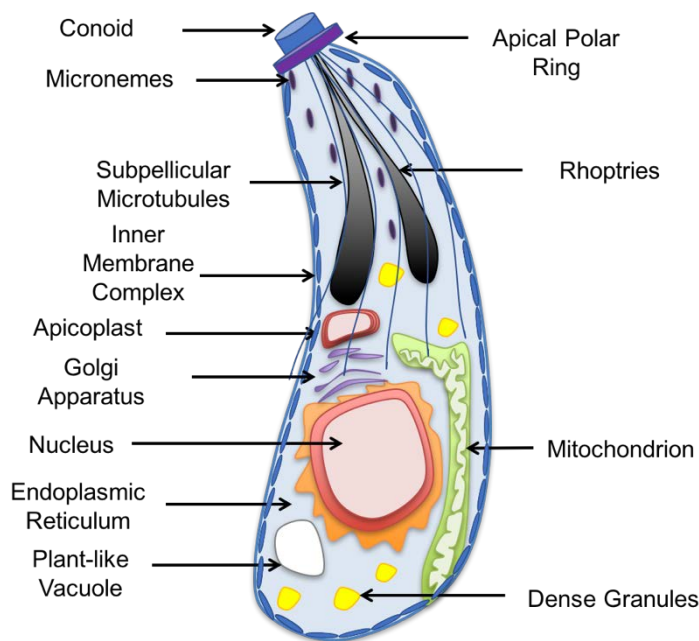


Figure 1.3 *T. gondii* tachyzoite with selected organelles drawn and identified.

proteases are found in the PLV, making it a likely source of Ca²⁺ release in response to GPN (Parussini, Coppens et al. 2010, Dou and Carruthers 2011). Phenotypes associated with disruption of PLV localized proteins can vary widely with genetic disruption of the Na⁺/H⁺ exchanger of the PLV resulting in increased sensitivity to osmotic stress (Francia, Wicher et al. 2011), while disruption of the L- type cathepsin protease (TgCPL) of the PLV results in accumulation of undigested host cell protein material (Dou, McGovern et al. 2014). Together these disparate phenotypes suggest that the PLV is a multifunctional organelle that not only plays an important role in ion homeostasis but also in digesting proteins ingested from the host cell cytosol.

Calcium Signaling in *T. gondii*

Many of the events in *T. gondii*'s lytic cycle such as egress, motility, invasion and micronemal protein secretion are accompanied by and dependent on calcium fluxes within both the parasite and the host cell (Arrizabalaga and Boothroyd 2004). Calcium levels increase in the host cell, the PV and the parasite cytoplasm just prior to the initiation of parasite egress from its host cell (Borges-Pereira, Budu et al. 2015). Oscillations in parasite calcium, which are enhanced in the presence of extracellular calcium, have been observed during periods of parasite motility using both chemical and genetically encoded calcium indicators (Lovett and Sibley 2003, Borges-Pereira, Budu et al. 2015). Secretion of proteins from the micronemes, which are required for parasite attachment to a host cell, can be stimulated by artificially inducing calcium fluxes (Carruthers and Sibley 1999).

The parasite can access the calcium required for these signaling events from both intraparasitic calcium stores and the extracellular milieu once it has egressed from its host cell (Moreno, Ayong et al. 2011). *T. gondii* has been shown by transmission electron microscopy of precipitated calcium to store intracellular calcium within the perinuclear endoplasmic reticulum (ER) as well large

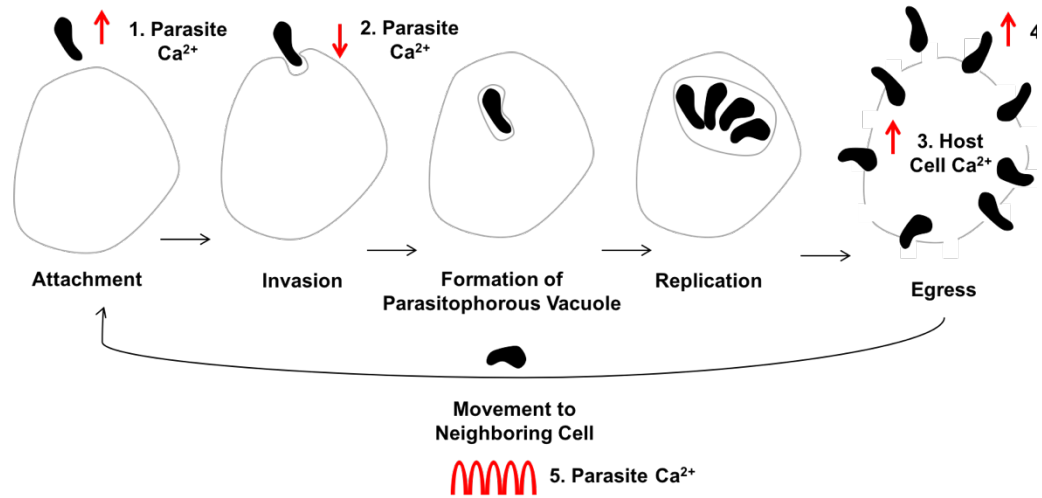


Figure 1.4 Key steps in the lytic cycle of *T. gondii* are accompanied by fluctuations in calcium within the parasite and host cell

1. Parasite cytosolic calcium increases stimulate the release of micronemal proteins required for efficient host cell attachment. 2. Invasion of the parasite is accompanied by a dramatic drop in parasite cytosolic calcium. 3. Host cell cytosolic calcium and 4. parasite cytosolic calcium increase just prior to egress of parasites to host cells. 5. The active motility of the parasite is accompanied by oscillations in parasite cytosolic calcium.

cytoplasmic vacuoles, which likely are what has been referred to as plant like vacuoles (PLV), (Miranda, Pace et al. 2010), and within the flattened sacs of the inner membrane complex that lie just beneath the parasite plasma membrane (Bonhomme, Pingret et al. 1993). The localization of calcium stores within the ER is supported by pharmacological studies using triggers of ER calcium release, such as thapsigargin, which induce invasion related events including protein secretion and cytoskeletal rearrangement of the apical end of the parasite (Moreno and

Zhong 1996, Carruthers and Sibley 1999). Though the target of thapsigargin, the sarco-endoplasmic reticulum calcium ATPase, is conserved in *T. gondii* and localizes to the ER as predicted (Nagamune, Beatty et al. 2007), it is unclear whether or not additional channels involved in calcium release from the ER in higher eukaryotes have homologues in

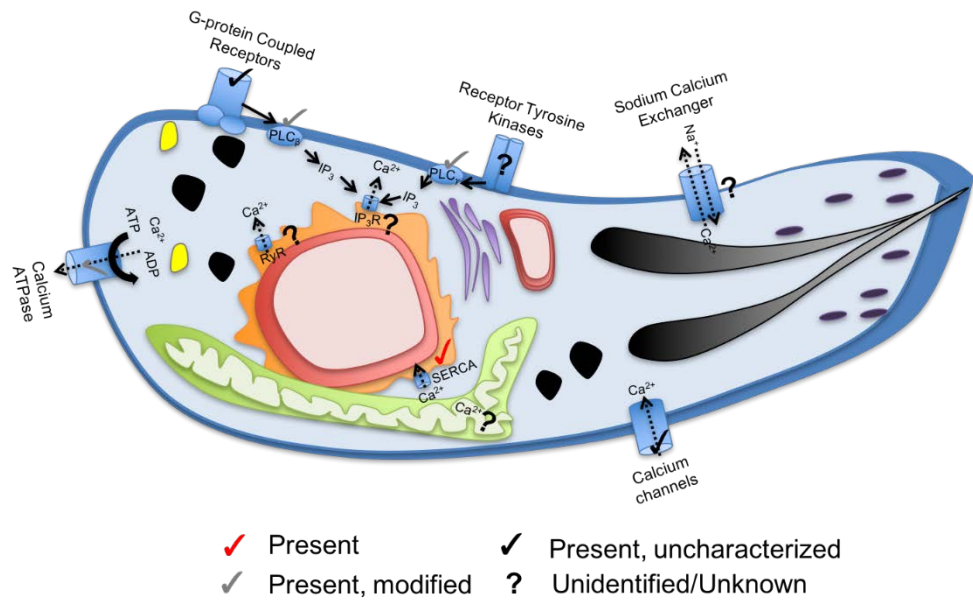


Figure 1.5 Conservation of Calcium Signaling in *T. gondii*
 ATP - adenosine triphosphate, ADP - adenosine diphosphate, RyR - Ryanodine Receptor, IP₃- Inositol trisphosphate, IP₃R - IP₃ Receptor

the parasite (Figure 1.5, above). For example, the IP₃ and Ryanodine (RyR) receptors that reside within and release calcium from the ER of eukaryotes from yeast to human do not have sequence homologues in *T. gondii*, despite the organism's ability to respond to pharmacological agents that target these proteins in other species (Moreno, Ayong et al. 2011, Prole and Taylor 2011). As described above, there is pharmacological evidence to support calcium storage within the PLV and acidocalcisomes (Moreno and Zhong 1996). The parasites can also

access calcium when extracellular; this calcium is likely taken up by a nifedipine-sensitive calcium channel in the parasite plasma membrane, though the channel responsible for this uptake has not been identified (Pace, McKnight et al. 2014). Once inside a cell, the parasite divides within the PV, where it is presumed to have access to the host cell calcium through the presence of a nonselective pore in the PVM, though the exact molecular mechanism for calcium import from the PV lumen across the parasite plasma membrane has yet to be elucidated (Gold, Kaplan et al. 2015). Interestingly, electron microscopy analysis of intracellular tachyzoites suggests that calcium is concentrated within the TVN (Bonhomme, Pingret et al. 1993). Whether this accumulation of calcium within the TVN is an active process or if it plays a role in the parasite's biology is not known. Calcium levels within the parasite and the PV are thought to remain relatively constant during the replicative phase of the parasite life cycle, with levels within the host cell, PV and parasite spiking just prior to egress to activate protein secretion and parasite motility and begin the lytic cycle over again (Borges-Pereira, Budu et al. 2015). Interestingly, some PV-localized proteins seem to play a role in calcium-dependent signaling processes, such as egress. GRA1 was initially identified as a highly abundant, calcium-binding protein found in the lumen of the PV, though its exact function is unclear since genetic disruption of this gene has not been successful (Cesbron-Delauw, Guy et al. 1989). An additional GRA protein, GRA22, that has not been shown to bind calcium directly, has nevertheless been shown to play a role in the timing of natural egress, as the loss of this protein results in early egress of parasites from host cells (Okada, Marmansari et al. 2013).

Though many of the key molecular mechanisms and factors that respond to calcium during the invasion and egress of *T. gondii* have been identified, how the parasite detects and regulates the calcium fluxes is not completely understood. In this context, ionophores such as ionomycin, A23187, and nigericin have been instrumental in studying calcium signaling in *T. gondii* (Mondragon and Frixione 1996, Pingret, Millot et al. 1996, Stommel, Ely et al. 1997, Black, Arrizabalaga et al. 2000, Arrizabalaga, Ruiz et al. 2004, Fruth and Arrizabalaga 2007, Caldas, de Souza et al. 2010). These ionophores are carrier ionophores which can exchange Ca^{2+} (ionomycin, A23187) or K^{+} (nigericin) ions for H^{+} ions across membranes until the ions reach electrochemical equilibrium (Pressman 1976). Brief (<2 minute) treatment of intracellular parasites with the calcium ionophores ionomycin or A23187 results in rapid exit from the host cell, a process known as ionophore induced egress (iiEgress). In contrast, treatment of intracellular parasites with nigericin requires a much longer treatment of 30 minutes before 100% of vacuoles have left their host cells, but it is likely that nigericin causes the activation of signaling pathways that lead to the eventual release of calcium to trigger egress, since mutants delayed in responding to calcium fluxes do not undergo egress in response to nigericin (Fruth and Arrizabalaga 2007). Brief treatment (2-5 min) of extracellular parasites with calcium ionophore A23187 induces micronemal secretion and parasite motility (Carruthers and Sibley 1999). When treatment with ionophore A23187 is prolonged (45-60 min for Type I strains), the parasites lose their ability to attach and invade host cells, resulting in parasite death (ionophore induced death, iiDeath) (Mondragon and Frixione 1996, Black, Arrizabalaga et al.

2000). In an effort to identify the proteins that allow *T. gondii* to respond to calcium, former members of the Arrizabalaga and Boothroyd laboratories have exploited these calcium ionophore induced phenomena to isolate mutants with altered sensitivity to A23187. From a series of selections and screens six independent mutants have been isolated that fall into three phenotypic categories: delay in iiEgress and resistance to iiDeath, delay in iiEgress but normal sensitivity to iiDeath, and resistance to iiDeath but normal iiEgress (Black, Arrizabalaga et al. 2000, Lavine, Knoll et al. 2007). Members of the Arrizabalaga laboratory have previously reported that all mutants that are both delayed in iiEgress and resistant to extracellular ionophore death have causative mutations in a calcium dependent protein kinase, TgCDPK3, which regulates egress by phosphorylating the major motor driving *T. gondii* motility (Garrison, Treeck et al. 2012, Gaji, Johnson et al. 2015).

To understand how *T. gondii* responds to calcium fluxes I focused our attention to the mutant strain MBD2.1, which is able to survive prolonged exposure to the ionophore while extracellular, but has no delay in iiEgress. Besides ionophore resistance, this mutant strain also exhibited hypersensitivity to treatment of extracellular parasites with the intracellular calcium chelator BAPTA-AM, suggesting that it has altered calcium homeostasis or sensitivity (Black, Arrizabalaga et al. 2000). Here I describe how these phenotypes are due to a nonsense mutation in a previously uncharacterized protein, GRA41, which localizes to the parasites' secretory organelles known as dense granules and is secreted into the PV, where it associates with the TVN. Importantly, I also show

that GRA41 is critical for calcium homeostasis and the timing of natural non-induced egress. In conjunction, our findings suggest a connection between the TVN and ion homeostasis within parasite, and thus a novel role for the vacuole of this important pathogen.

Chapter 2 : Methods

Parasite propagation

T. gondii tachyzoites were propagated by passaging in human foreskin fibroblasts (HFFs, purchased from the American Tissue Culture Collection, ATCC) in a humidified incubator maintained at a temperature of 37°C and 5% CO₂ concentration. Normal growth medium used was Dulbecco's Modified Eagle Medium (DMEM) with 10% fetal bovine serum (FBS), 2 mM L-glutamine and 50 µg/mL penicillin-streptomycin.

Genome sequencing and complementation

Preparation of genomic DNA was done by previous members of the Arrizabalaga laboratory. Extracellular parasites from strains MBD2.1 and RHΔ*hxgprt* (the parental strain) were purified through a 3 µm filter to eliminate human cell contamination. Genomic DNA from both strains was isolated using the DNeasy Blood and Tissue Kit (Qiagen). Sample preparation, sequencing, genome assembly, and annotation was performed at the University of Idaho IBEST Genomics Resources Core facility. Genomic DNA libraries were constructed using the Illumina TruSeq library kit and quantified with rtPCR using the Kapa Illumina library quantification kit. 100bp paired-end Illumina sequencing was used to an estimated > 100x coverage per genome. Mapping of Illumina sequence was performed using GMAP to the TGGT1 reference sequence from ToxoDB (Gajria, Bahl et al. 2008) with output to SAM format files for further processing. Genomic variants in the mutant strains in comparison to the reference sequence were detected and extracted from the mapped data using the Broad institutes GATK

toolkit. Data was exported as a variant call format (VCF) file, which listed each genomic variant, its position in the genome, and the quality of sequence data for that particular region. In total 14 SNVs were detected between the mutant and parental strain. The two SNVs that resulted in missense or nonsense mutations in MBD2.1 were confirmed by sequencing fragments of genomic DNA amplified by PCR from both the parental and mutant strains and that spanned regions with putative mutations.

To determine which of the identified variants in the mutant was responsible for the phenotype, a cosmid-based complementation approach was used. Cosmids generated from the RH (Type I strain) containing the genomic regions of interest were identified on ToxoDB.org and were graciously provided by Dr. David Sibley at Washington University, St. Louis. For TGGT1_069070 cosmid TOXO119 was linearized by digestion with NotI (New England Biolabs), purified and electroporated into *T. gondii* tachyzoites of the MBD 2.1 mutant according to established protocols (Kim, Soldati et al. 1993, Soldati and Boothroyd 1993). Transfected parasites were maintained in the presence of 1 μ M pyrimethamine prior to cloning by limiting dilution to select for stable transformants.

iiDeath survival assay

The iiDeath survival assay was performed as described previously (Black, Arrizabalaga et al. 2000). In brief, intracellular parasites were harvested by passage through a 27 gauge needle three times before dilution and treatment with either 1 μ M A23187 or DMSO solvent control for 45 or 60 minutes (10 or 30 minutes for Type II strains) in a humidified incubator at 37°C and 5% CO₂

concentration. At each time point, 500 parasites were removed from the treatment and allowed to infect a confluent monolayer of HFFs in a twelve well plate format for two hours before changing the media to remove uninvaded parasites. Parasites were allowed to grow and form plaques for 6 days before the cultures were fixed and scored. Each combination of treatment and time point was the average of a minimum of three technical replicates per experiment and the experiments were performed a minimum of three times for statistical analysis. The percent survival for each strain and time point was calculated as a ratio of the number of plaques scored in the wells infected with treated parasites as compared to the wells infected with untreated (DMSO solvent control) parasites.

Micronemal secretion assay

Micronemal protein secretion was assessed by suspending extracellular parasites at a concentration of 1×10^9 /mL in complete DMEM. Calcium ionophore A23187 or DMSO control was added to each sample to a final concentration of 1 μ M and incubated at 37°C for one hour. Parasites were separated from secreted proteins in the media by centrifugation at 3,000 x g's for 3 minutes at 4°C. The resulting supernatant was subjected to a second spin under the same conditions to ensure all of the parasite pellet was removed from the sample. The pellets were resuspended in 2X Laemmli Sample Buffer (Bio-Rad) with 5% freshly added betamercaptoethanol (BME) to a final concentration of 1×10^9 /mL and treated as described in Western Blot analysis (below). Supernatants were combined with 4X Laemmli Sample Buffer (Bio-Rad) with 10% freshly added BME and treated as described in Western blot analysis. The resulting Western blots were probed with

mouse anti-MIC2 antibody to detect endogenous MIC2 protein (Wan, Carruthers et al. 1997) and visualized as described in Western Blot analysis.

Generation of Type I endogenously tagged GRA41 line

For the expression of GRA41 tagged with hemagglutinin at the carboxyl terminal of the encoded protein, an 800 base pair fragment of parasite genomic DNA was amplified by PCR with specific primers GRA41 Tag.FOR and GRA41 Tag.REV (see Table 2.1, for sequence of all primers used in this study) and directionally cloned into the *PacI* site of the 3xHA.Lic.DHFR-TS plasmid using In-Fusion Cloning (Clontech). The 3xHA.LIC.DHFR-TS plasmid is a derivative of the YFP.LIC.DHFR-TS plasmid (Huynh and Carruthers 2009) with the YFP coding sequence replaced by a triple hemagglutinin tag. The resulting construct was verified by restriction digestion and sequencing. The plasmid construct was linearized with the restriction enzyme *XcmI*, which cuts within the region containing the insert and allows for integration of the construct by single homologous recombination when transfected into the RH Δ *ku80* strain (Huynh and Carruthers 2009). *T. gondii* tachyzoites were transfected with the linearized vector by electroporation according to established protocols (Soldati and Boothroyd 1993). Transfected parasites were maintained in the presence of 1 μ M pyrimethamine prior to cloning by limiting dilution to select for stable transformants.

Immunofluorescence assays

For immunofluorescence assays, HFFs grown on glass coverslips infected 18-24 hours prior were fixed with 3.5% methanol-free formaldehyde in PBS, blocked in PBS/3% BSA and permeabilized in PBS/3% BSA/0.2% TX-100.

Samples were then incubated in primary antibodies (Rabbit anti-HA, Cell Signaling Technology, mouse anti-Gra1, Biotem) diluted in PBS/3% BSA/0.2% TX-100, washed and then incubated in secondary antibodies (goat anti-mouse/rabbit Alexafluor 488/594 conjugated, Invitrogen) diluted in PBS/3% BSA. Coverslips were mounted onto microscope slides with Vectashield mounting media containing DAPI (Vector Laboratories). IFAs were inspected using a Nikon Eclipse E100080i microscope and images captured with a Hamamatsu C4742-95 charge-coupled device camera using NIS elements software.

Western blot analysis

To examine protein expression by Western blot, parasites were lysed in 150 mM NaCl, 50 mM Tris-Cl, pH 7.5, 0.1% NP-40 for a minimum of twenty minutes. Samples were centrifuged at 14,000 x g's for 20 minutes to remove insoluble proteins before combining with an equal amount of 2X Laemmli Sample Buffer (Bio-Rad) with freshly added 5% BME (Thermo Scientific) and heating at ~95°C for 5 minutes. Samples were separated on a 4-20% gradient SDS-PAGE gel (Bio-Rad) before transferring to a nitrocellulose membrane using a Trans-Blot semi-dry transfer cell (Bio-Rad). Nitrocellulose membranes were blocked for a minimum of 30 minutes in Tris-buffered saline/tween (TBST) with 5% non-fat dry milk (NFDM) before being probed with Rabbit anti-HA at a dilution of 1:5000 (Cell Signaling Technologies), mouse anti-ROP1 at a dilution of 1:5000 (Schwartzman and Krug 1989) or mouse anti-SAG1 at a dilution of 1:5000 (Genway) for a minimum of one hour. They were then washed a minimum of three times for ten minutes with TBST before incubating with the appropriate horse radish peroxidase conjugated

secondary antibody (Sigma) for one hour. Membranes were washed again before incubating with SuperSignal West Femto Maximum Sensitivity Substrate (Thermo Scientific) for five minutes. Blots were imaged using the FluorChem E system (Protein Simple) for analysis of chemiluminescent Western blots.

Triton-X 114 membrane partitioning

Membrane partitioning of lysates with Triton-X 114 (Sigma-Aldrich) was performed as described previously (Rome, Beck et al. 2008). Briefly, parasites were lysed in 10% Triton-X 114, 10 mM Tris, pH 7.4, 5 mM NaCl on ice for 30 minutes, before centrifuging the samples at 2500 x g's for five minutes before removing the supernatant to a new tube for partitioning. Lysates were incubated at 30°C for five minutes, followed by centrifugation at 3,000 x g's for 5 minutes to separate samples into the aqueous and detergent phases. The aqueous phase was re-extracted by incubating with 10% Triton-X 114, 10 mM Tris, pH 7.4, 5 mM NaCl on ice for 5 minutes, then at 30°C for five minutes, followed by centrifugation as described above. The detergent phase was re-extracted by incubating with PBS on ice for 5 minutes, then at 30°C for five minutes, followed by centrifugation as described above. Proteins were precipitated from the final aqueous and detergent phases by adding two volumes of ice cold acetone to each sample and incubating at -20°C for a minimum of two hours, followed by centrifugation at 15,000 x g's for ten minutes. The resulting pellets were washed once more with ice cold acetone before they were resuspended in 2X Laemlli Sample Buffer (Bio-Rad) with freshly added 5% BME (Thermo Scientific) and processed for Western blot analysis as described above.

Electron microscopy

For transmission electron microscopy, confluent monolayers of HFFs were infected with parasites of the strain of interest 24 hours prior to sample preparation. Infected cells were washed four times with PBS before fixing for one hour in freshly prepared 2.5% glutaraldehyde in 100 mM sodium cacodylate, pH 7.4 buffer in the dark. Fixative was then removed and samples were washed three times with PBS before being harvested by gentle scraping followed by centrifugation at 3,000xg's for 10 minutes. The pellets were then incubated in 1% osmium tetroxide in 100 mM sodium cacodylate pH 7.4 buffer that had been reduced by adding solid potassium ferrocyanide to a final concentration of 1.5% (w/v) and incubated in the dark at 4 °C for one hour. The pellets were washed three times with 100 mM sodium cacodylate, pH 7.4 buffer before dehydration in a series of ethanol washes. Pellets were dehydrated with five minute incubations in 30%, 50%, 70%, 90% and 95% ethanol followed by four five minute washes of 100% ethanol. The samples were infiltrated with Embed-812/Araldite 502 resin (Electron Microscopy Sciences), at a dilution of 1:1 resin with 100% ethanol and in 3 changes of 100% resin. The formulation of resin used was 12.5 ml Embed-812, 7.5 ml Araldite-502, 27.5 ml Dodecenyl Succinic Anhydride, and 0.95 ml DMP-30. All resin incubations were for at least 2 hours and were done at room temperature in a rotator at low speed. After the final change the inserts were polymerized at 65 degrees Celsius. Remaining steps were done with the assistance of the Indiana University-Blomington Electron Microscopy Center (<http://iubemcenter.indiana.edu>). Thin sections were obtained using a diamond knife, mounted on copper grids and

stained with uranyl acetate and lead citrate before imaging on a JEOL 1010 transmission electron microscope. Images were captured with a 1k x 1k Gatan CCD camera (MegaScan model 794) and a tungsten filament was used as an electron source.

For immunoelectron microscopy, HFFs infected with parasites for 24-36 hours were washed three times with PBS before fixing for one hour in freshly prepared 4% paraformaldehyde (EM grade, VWR) in 250 mM HEPES pH 7.4. Fixative was then removed and replaced with a solution of 8% paraformaldehyde in 250 mM HEPES pH 7.4 for overnight incubation at 4°C. Samples were harvested by gentle scraping to detach sheets of cells followed by centrifugation at 2,000 rpm for 10 minutes. Additional steps were carried out by Dr. Isabelle Coppins of Johns Hopkins University. Infected cells were pelleted in 10% fish skin gelatin and the gelatin-embedded pellets were infiltrated overnight with 2.3 M sucrose at 4°C and frozen in liquid nitrogen. Ultrathin cryosections were incubated in PBS and 1% fish skin gelatin containing mouse anti-HA antibody at 1/250 dilution, and then exposed to the secondary antibody that were revealed with 10 nm protein A-gold conjugates. Sections were observed and images were recorded with a Philips CM120 Electron Microscope (Eindhoven, the Netherlands) under 80 kV.

Generation of Type I *GRA41* knockout strain

The *GRA41* knockout strain, RH $\Delta ku80\Delta gra41$, was generated by replacing the entire *GRA41* coding sequence with the HXGPRT selectable marker by double homologous recombination in the RH $\Delta ku80$ parental strain (Huynh and Carruthers 2009). The pGRA41KO vector was generated by cloning fragments approximately

1.5 kbp in length directly upstream (primers GRA41 KO 5' Flank.FOR and GRA41 KO 5' Flank.REV, Table 2.1) and downstream (primers GRA41 KO 3' Flank.FOR and GRA41 KO 3' Flank.REV, Table 2.1) of the *GRA41* coding sequence into the HindIII and NotI sites of the pMini vector (Donald, Carter et al. 1996) by In-Fusion cloning (Clontech). The resulting construct was verified by restriction digestion and sequencing. *T. gondii* tachyzoites were transfected with purified linearized vector by electroporation according to established protocols (Soldati and Boothroyd 1993). Transfected parasites were maintained in the presence of 50 µg/ml mycophenolic acid and 50 µg/ml xanthine prior to cloning by limiting dilution to select for stable transformants. Individual clones were screened by PCR to verify correct replacement of the *GRA41* locus with the HXGPRT selectable marker. To confirm the correct insertion, primers complementary to the 3' end of the HXGPRT selectable marker and downstream of the insertion site were used to perform a PCR analysis of genomic DNA isolated from *GRA41* knockout clones. A primer within the 3' homology region of the pGRA41KO vector (p1, Figure 3.5, GRA41 3'UTR Mid.FOR, Table 2.1) and one downstream of the insertion site (p3, Figure 3.5, GRA41 Downstream.REV, Table 2.1) were used as a positive control, while a primer within the selectable marker of the pGRA41KO vector (p2, Figure 3.5, DHFR 3'UTR End.FOR, Table 2.1) was combined with the same downstream primer (p3) to identify clones with the desired incorporation of the pGRA41KO vector. Loss of *GRA41* mRNA transcript was verified by qPCR analysis (primers GRA41 qPCR.FOR and GRA41 qPCR.REV, Table 2.1) using the SYBR Green

Primer Name	Sequence
Gra41 Tag.FOR	TACTTCCAATCCAATTTAATGCAATAGAGACGC AGCACCTTG
Gra41 Tag.REV	TCCTCCACTTCCAATTTTAGCTTCGGGTAGGTG AAGTTTAG
Gra41 qPCR.FOR	ACGGCAGCTTGAGATACCAC
Gra41 qPCR.REV	GCAGCCCTGGTATTGTATCG
Gra41 KO 5'Flank.FOR	CGGTATCGATAAGCTTTTTGGTGTGGGCCTGT CGAAT
Gra41 KO 5'Flank.REV	CGTGCTGATCAAGCTTCCACGCGTGGATTGCA GAAAA
Gra41 KO 3' Flank.FOR	AGTTCTAGAGCGGCCGCTTTTGGTACCTCCAT GGGCAAGG
Gra41 KO 3' Flank.REV	ACCGCGGTGGCGGCCGCATACAAAGGCGAGG TCATTGCTGTG
GraX 41 3'UTR Mid.FOR	GCGGATTTGTGGCTACAATACTGC
Gra41 Downstream.REV	CTGCTCTATGTCCTCTGTTTCGATGT
DHFR 3'UTR End.FOR	GGCCATTCATGCCAGTCAGT
TgGT1_236870 qPCR.FOR	TTGATGACGACGAGGATGAA
TgGT1_236870 qPCR.REV	GTATGCGGGTAACGACGAGT
TgGT1_236860 qPCR.FOR	TCTCGCGACAACATTTCAAG
TgGT1_236860 qPCR.REV	GCTTTGTCTTCGCTTCCATC
Gra41 qPCR.FOR	ACGGCAGCTTGAGATACCAC
Gra41 qPCR.REV	GCAGCCCTGGTATTGTATCG
RPL29 qPCR.FOR	GGCGAAATCAAAGAACCACAC
RPL29 qPCR.REV	TCGGACTTCATCATGCCTCTC
GRA41 pet28a.FOR	CGCGCGGCAGCCATATGGACTGTATTCCTTCG CATCAA
GRA41 pet28a.REV	GTCATGCTAGCCATATGTTATTCGGGTAGGTG AAGTTTAGA
Type II Gra41 Tag.FOR	TTCCAATCCAATTTAATTAATTGAAATACACCCT AGACGGCACAC
Type II Gra41 Tag.REV	CCACTTCCAATTTTAATTAATTTGGGTAGGTGA AGTTCAGAAAGC
Type II Gra41 KO 5' Flank.FOR	CGGTATCGATAAGCTTTTTGGTGTGGGCCTGT CGAAT
Type II Gra41 KO 5' Flank.REV	CGTGCTGATCAAGCTTCCACGCGTGGATTGCA GAAAA
Type II Gra41 KO 3' Flank. FOR	AGTTCTAGAGCGGCCGCTTTTGGTACCTCCAT GGGCAAGG

Type II Gra41 KO 3' Flank. REV	ACCGCGGTGGCGGCCGCATACAAAGGCGAGG TCATTGCTGTG
-----------------------------------	--

Table 2.1 Name and sequence of primers used in this study. All sequences are 5' to 3'.

detection reagent (Fast Syber Green Master Mix, Applied Biosystems). Relative gene expression was calculated by normalizing to levels of the housekeeping gene ribosomal protein 29 (TGGT1_2345500, Primers RPL29 qPCR.FOR and RPL29 qPCR.REV, Table 2.1) Relative transcript abundance of the genes directly flanking *GRA41* (TGGT1_236860 using primers TGGT1_236860 qPCR.FOR and TGGT1_236860 qPCR.REV and TGGT1_236870 using primers TGGT1_236870 qPCR.FOR and TGGT1_236870 qPCR.REV, Table 2.1) was also measured by qPCR analysis to ensure that their levels did not differ significantly from the parental strain.

Generation of *GRA41* knockout complemented clones

The *GRA41* knockout strain, $RH\Delta ku80\Delta gra41$ was complemented by transfecting with the cosmid TOXO119 previously utilized for the complementation of mutant MBD2.1 described above. Complemented clones were selected for integration of the gene back into its original locus by selecting against the presence of the *HXGPRT* selectable marker using 80 $\mu\text{g/ml}$ 6-thioxanthine. Following limited dilution cloning, individual clones were subjected to treatment with 50 $\mu\text{g/ml}$ mycophenolic acid and 50 $\mu\text{g/ml}$ xanthine and qPCR analysis of *GRA41* transcript levels to identify clones which were either $HXGPRT^+GRA41^-$ or $HXGPRT^-GRA41^+$. Transcript levels of *GRA41* were normalized to the levels of ribosomal protein *RPL29* as described above.

Parasite growth assays

Growth of all parasite strains was assessed by determining plaquing efficiency and growth rate as follows. Intracellular parasites were harvested from a confluent monolayer of HFFs by passage through a 27-gauge needle 2-3 times. Parasites were then diluted in normal growth medium and allowed to infect a confluent monolayer of HFFs and returned to a humidified incubator for two hours before changing the media to remove any uninvaded parasites. For plaque assays, parasites were allowed to form plaques for six days before the monolayer was fixed and stained with Crystal Violet (ACROS Organics) to visualize plaques. For doubling assays, parasites were allowed to grow for twelve, twenty-four and or thirty hours before they were fixed and stained with Hema3 Manual Staining System (Fisher) to count the number of parasites per vacuole for a minimum of 50 vacuoles per sample.

Parasite egress assays

Egress in response to DTT treatment was assessed as follows. Parasites were allowed to invade host cells for 24 hours prior to the start of the assay. Infected monolayers were washed twice with 1X PBS and once with 1X HBSS (Invitrogen) before incubating in either 5 mM DTT in 1X HBSS or buffer only control for the required time. Monolayers were then fixed with methanol and stained with Hema3 Manual Staining System (Fisher) to assess parasite egress.

Parasite invasion assays

The efficiency of attachment and invasion for various parasite strains was measured as follows. Intracellular parasites were harvested as for plaque assays.

Parasites were then diluted in normal growth medium and allowed to infect a confluent monolayer of HFFs for two hours. Unattached parasites were removed by washing with PBS three times. Cells were then fixed in 3.5% methanol-free formaldehyde before blocking in PBS/3% BSA. Prior to permeabilization, extracellular parasites were labeled with mouse anti-P30 antibody (Genway) for one hour in PBS/3% BSA. Cells were then washed to eliminate unbound antibody and permeabilized in PBS/3% BSA/0.2% TX-100 before incubation with rabbit anti-*T. gondii* (MyBioSource) for one hour. Cells were washed and then incubated with goat anti-mouse Alexa fluor 488 and goat anti-rabbit Alexa flour 594 (Invitrogen) for one hour before washing and mounting in Vectashield mounting media with DAPI (Vector Labs). Intracellular and extracellular parasites were distinguished between by the presence of dual-color staining (extracellular parasites) or single-color staining (intracellular parasites, which only stain after permeabilization). The efficiency of attachment was calculated by counting the total number of parasites for ten random fields of view and normalizing to 100% attachment for the parental strain. The efficiency of invasion was calculated as the percentage of invaded (intracellular) parasites out of the total number of parasites.

Calcium measurements

Calcium measurements of free cytosolic calcium were done by Karla Marquez-Nogueras of the Moreno laboratory at the University of Georgia. Loading of parasites with Fura-2 was performed as previously described (Moreno and Zhong, 1996). Briefly, freshly egressed parasites were washed and then centrifuged twice at 500 x g's for 10 minutes at room temperature in buffer A (116

mM NaCl, 5.4 mM KCl, 0.8 mM MgSO₄, 5.5 mM d-glucose and 50 mM HEPES, pH 7.4). Then, parasites were resuspended to a final density of 1x10⁹ parasites/ml in Ringer buffer (155 mM NaCl, 3 mM KCl, 1 mM MgCl₂, 3 mM NaH₂PO₄H₂O, 10 mM HEPES, pH 7.3, and 5 mM glucose; plus 1.5% sucrose and 5 μM of Fura-2-AM). The suspension was incubated for 26 minutes in a 26°C water bath with mild agitation. Subsequently, the parasites were washed twice with Ringer's buffer to remove extracellular dye. Parasites were resuspended to a final density of 1x10⁹ parasites/ml in Ringer's buffer and kept on ice. Parasites are known to be viable for a few hours under these conditions (Pace, McKnight et al. 2014). For fluorescence measurements, 2x10⁷ parasites/mL were added to a cuvette with 2.5 mL of Ringer's buffer. Cuvette was placed in a thermostatically controlled Hitachi F-7000 fluorescence spectrophotometer, using the conditions for Fura-2 excitation (340 and 380nm) and emission (510nm). The Fura-2 fluorescence response to intracellular Ca²⁺ concentration ([Ca²⁺]_i) was calibrated from the ratio of 340/380 nm fluorescence values after subtraction of the background fluorescence of the cells at 340 and 380 nm as previously described (Grynkiewicz et al., 1985). Changes in [Ca²⁺]_i (ΔF [Ca²⁺]) were measured by subtracting the highest peak of calcium in the first 50 seconds after addition of calcium minus the baseline.

Recombinant protein production

The GRA41 recombinant expression vector was generated by cloning the GRA41 coding sequence without the signal peptide into the pet28a (+) vector (EMD Biosciences) using In-fusion Cloning (Clontech). The GRA41 coding sequence was amplified using primers GRA41 pet28a.FOR and GRA41

pet28a.REV (Table 1) and inserted into the NdeI sites of the pet28a (+) vector. The resulting construct was verified by restriction digestion and sequencing. Rosetta (DE3) pLysS *E. coli* BL21 competent cells (Novagen) were transformed with purified vector according to the manufacturer's protocol. Transformed cells were then grown at 37°C in LB media to an O.D. of 0.6 before inducing protein expression with 1 mM IPTG for 3 hours. After induction, cells were harvested by centrifugation at 10,000 x g's for 20 minutes at 4°C. Pellets were stored at -80°C. Additional steps were done with the assistance of Dr. Sanofar Abdeen of the Johnson laboratory at Indiana University School of Medicine. Pellets were resuspended in ~100 mL of lysis buffer (50 mM Tris-HCl, pH 7.4, 10 mM MgSO₄, 1 mM beta-mercaptoethanol, 0.1% Triton-X 100, 5% glycerol) before adding lysozyme to a final concentration of 50 µg/mL and incubating for ten minutes on ice. Samples were then sonicated on ice for six minutes (10 seconds on, twenty seconds rest) before removing the insoluble portion by centrifugation at 14,000 x g's for 30 minutes at room temperature. The supernatant was filtered through a 0.45 µm filter before purifying on a 5 ml HisTrap HP Nickel column (GE) on a NGC Quest FPLC (Bio-Rad). Fractions were collected analyzed by SDS-PAGE and Western Blot to determine purity. Fractions positive for the His-tagged protein were combined and further purified using a HiLoad 26/600 Superdex 200 size exclusion column (GE).

Calcium thermal shift assays

Differential scanning fluorimetry was utilized to measure the ability of calcium ions to bind to and stabilize the secondary structures of recombinant

proteins as described in (Niesen, Berglund et al. 2007) using recombinant CDPK3 (Gaji, Johnson et al. 2015) as a positive control. N-terminally His tagged GRA41 (final concentration of 8 μ M) or CDPK3 (final concentration of 3.5 μ M) in 100 mM HEPES, pH 7.0, 150 mM NaCl was incubated with 4X Sypro Orange (Sigma Aldrich) and CaCl_2 in a two-fold dilution series ranging from 0-250 μ M. Melt curve analysis was performed from 25 to 99°C with 1°C steps on a StepOne Plus Real-Time PCR System (Applied Biosystems). Data were analyzed in Prism (GraphPad) to determine melting temperatures for each condition.

Immunoprecipitation

Human foreskin fibroblasts were infected with the strain containing an endogenous HA tag at the C terminus of GRA41 for twenty-four hours before harvesting. Samples were harvested by scraping the infected monolayer and solubilizing in RIPA buffer (10 mM Tris-Cl, pH 8.0, 1 mM EDTA, 0.5 mM EGTA, 1% Triton X-100, 0.1% sodium deoxycholate, 0.1% SDS, 140 mM NaCl) with added protease inhibitors (cOmplete Mini Protease Inhibitor Cocktail, Roche) for a minimum of twenty minutes with rotation. Samples were sonicated for ten second pulses 2-3 x, with a minimum rest on ice of twenty seconds between pulses. Insoluble material was removed by centrifuging for 20 minutes at 13,000 x g's and 4°C. The supernatant was removed and incubated with high affinity rat anti-HA antibody (Roche) overnight at 4°C with rotation. The following morning, the antibody/antigen complex was bound to Protein G-conjugated Dynabeads (Invitrogen) by incubating the supernatant/antibody mixture with freshly washed Dynabeads for ten minutes at room temperature with rotation. The precipitated

beads were isolated using a magnet and washed three times with RIPA buffer plus protease inhibitors. Proteins were eluted from the beads by adding 2X Laemmli sample buffer with 5% betamercaptoethanol to the beads and incubating at 95°C for ten minutes. The beads were isolated using a magnet and the sample buffer containing eluted antigen was removed. The sample was run on a 4-20% Mini Protean TGX Precast Gel (Bio-rad) and the gel was stained using the Pierce Silver Stain kit (ThermoFisher Scientific). Regions containing visible bands were excised with a clean razor blade and stored in PBS before mass spectrometry analysis. Additional steps were performed by the Indiana University Bloomington Laboratory for Biological Mass Spectrometry (<http://www.chem.indiana.edu/bms/>). The samples were reduced with 10 mM DTT in 10 mM ammonium bicarbonate and then alkylated with 55 mM iodoacetamide (prepared in 10 mM ammonium bicarbonate). Alkylated samples were digested by trypsin (Promega) overnight at 37°C. Digested peptides were injected onto the C18 column. Peptides were eluted with a linear gradient from 3 to 40% acetonitrile (in water with 0.1% FA) developed over 70 min at room temperature at a flow rate of 300 nL/min, and effluent was electro-sprayed into the mass spectrometer. A blank was run prior to and between the sample runs to make sure there was no significant signal from solvents, column or carryovers. Database search was carried out using Sequest™ algorithms against the UniProt database for *T. gondii*. The results were further refined by removing hits with an expect value >0.0025. Common contaminants found in other unrelated datasets were removed and the list was restricted to proteins with a predicted signal peptide.

Yeast two hybrid screen

Yeast two-hybrid screening was performed by Hybrigenics Services, S.A.S., Paris, France (<http://www.hybrigenics-services.com>). The coding sequence for *T. gondii* GRA41 (amino acids 25-179) was PCR-amplified and cloned into pB66 as a C-terminal fusion to the Gal4 DNA-binding domain (Gal4-Gra41). The construct was checked by sequencing the entire insert and used as a bait to screen a random-primed *T. gondii* wild-type RH strain cDNA library constructed into pP6. pB66 derives from the original pAS2 $\Delta\Delta$ vector (Fromont-Racine, Rain et al. 1997) and pP6 is based on the pGADGH plasmid (Bartel, Chien et al. 1993).

62.4 million clones (6-fold the complexity of the library) were screened using a mating approach with YHGX13 (Y187 *ade2-101::loxP-kanMX-loxP*, *mat-alpha*) and CG1945 (*mata*) yeast strains as previously described (Fromont-Racine, Rain et al. 1997). 337 His⁺ colonies were selected on a medium lacking tryptophan, leucine and histidine and supplemented with 0.5 mM 3-aminotriazole to handle bait autoactivation. The prey fragments of the positive clones were amplified by PCR and sequenced at their 5' and 3' junctions. The resulting sequences were used to identify the corresponding interacting proteins in the GenBank database (NCBI) using a fully automated procedure. A confidence score (PBS, for Predicted Biological Score) was attributed to each interaction as previously described (Formstecher, Aresta et al. 2005). The PBS relies on two different levels of analysis. Firstly, a local score takes into account the redundancy and independency of prey fragments, as well as the distribution of reading frames and

stop codons in overlapping fragments. Secondly, a global score takes into account the interactions found in all the screens performed at Hybrigenics using the same library. This global score represents the probability of an interaction being nonspecific. For practical use, the scores were divided into four categories, from A (highest confidence) to D (lowest confidence). A fifth category (E) specifically flags interactions involving highly connected prey domains previously found several times in screens performed on libraries derived from the same organism. Finally, several of these highly connected domains have been confirmed as false-positives of the technique and are now tagged as F. The PBS scores have been shown to positively correlate with the biological significance of interactions (Rain, Selig et al. 2001, Wojcik, Boneca et al. 2002).

Generation of Type II endogenously tagged GRA41 line

For the expression of GRA41 tagged with hemagglutinin at the carboxyl terminal of the encoded protein, an 1700 base pair fragment of Pru genomic DNA was amplified by PCR with specific primers Type II GRA41 Tag.FOR and Type II GRA41 Tag.REV (see Table 2.1, for sequence of primers used in this study) and directionally cloned into the P_{ac}I site of the 3xHA.Lic.DHFR-TS plasmid using In-Fusion Cloning (Clontech). The 3xHA.LIC.DHFR-TS plasmid is a derivative of the YFP.LIC.DHFR-TS plasmid (Huynh and Carruthers 2009) with the YFP coding sequence replaced by a triple HA tag. The resulting construct was verified by restriction digestion and sequencing. The plasmid construct was linearized with the restriction enzyme X_{cm}I, which cuts within the region containing the insert and allows for integration of the construct by single homologous recombination when

transfected into the Pru $\Delta ku80$ strain (Fox, Falla et al. 2011) stably expressing luciferase, which can be used to visualize parasite propagation in mice using a bioluminescence-based imaging system (Saeij, Boyle et al. 2005). *T. gondii* tachyzoites were transfected with the linearized vector by electroporation according to established protocols (Soldati and Boothroyd 1993). Transfected parasites were maintained in the presence of 1 μ M pyrimethamine prior to cloning by limiting dilution to select for stable transformants.

Generation of Type II *GRA41* knockout strain

The *GRA41* knockout strain, Pru $\Delta ku80\Delta gra41$, was generated by replacing the entire *GRA41* coding sequence with the HXGPRT selectable marker by double homologous recombination in the Pru $\Delta ku80\Delta hxgprt$ parental strain (Fox, Falla et al. 2011). The p*GRA41*KO-GFP vector was generated by cloning fragments approximately 1.5 kbp in length directly upstream (primers Type II *GRA41* KO 5' Flank.FOR and Type II *GRA41* KO 5' Flank.REV, Table 2.1) and downstream (primers Type II *GRA41* KO 3' Flank.FOR and Type II *GRA41* KO 3' Flank.REV, Table 2.1) of the *GRA41* coding sequence into the HindIII and NotI sites of the pmini-GFP.ht vector (Donald, Carter et al. 1996, Arrizabalaga, Ruiz et al. 2004) by In-Fusion cloning (Clontech). The resulting construct was verified by restriction digestion and sequencing. *T. gondii* tachyzoites were transfected with purified linearized vector by electroporation according to established protocols (Soldati and Boothroyd 1993). Transfected parasites were maintained in the presence of 50 μ g/ml mycophenolic acid and 50 μ g/ml xanthine prior to cloning by limiting dilution to select for stable transformants. Individual clones were screened first for the

presence of GFP by live imaging (constructs integrated by double homologous recombination should be GFP negative) and then by PCR to verify correct replacement of the *GRA41* locus with the HXGPRT selectable marker.

To confirm the correct insertion, primers complementary to the 3' end of HXGPRT selectable marker and downstream of the insertion site were used to perform a PCR analysis of genomic DNA isolated from *GRA41* knockout clones. A primer within the 3' homology region of the pGRA41KO vector (p1, Figure 5.2, GRA41 3'UTR Mid.FOR, Table 2.1) and one downstream of the insertion site (p3, Figure 5.2, GRA41 Downstream.REV, Table 2.1) were used as a positive control, while a primer within the selectable marker of the pGRA41KO vector (p2, Fig. 3, DHFR 3'UTR End.FOR, Table 2.1) was combined with the same downstream primer (p3) to identify clones with the desired incorporation of the pGRA41KO vector.

Bradyzoite differentiation assays

The ability of parasite strains to differentiate from tachyzoites to bradyzoites was assessed as follows. Intracellular parasites were harvested from a confluent monolayer of HFFs by passage through a 27-gauge needle 2-3 times. Parasites were then diluted in normal growth medium and allowed to infect a confluent monolayer of HFFs grown on glass coverslips and returned to a humidified incubator for two hours before replacing the media with RPMI switching media (RPMI 1640, Invitrogen, pH 8.1, 5% FBS, 50 mM HEPES), placing inside an airtight container and placing in a CO₂ deprivation incubator at 37°C. At 4 or 7 days, the cells were fixed, blocked, permeabilized and probed as described in the

immunofluorescence assay methods above. Rhodamine-labeled *Dolichos biflorus* agglutinin (DBA, Vector Laboratories) was added at a dilution of 1:250 during the secondary fluorophore-conjugated antibody step to stain the bradyzoite tissue cyst wall. Coverslips were mounted onto microscope slides with Vectashield mounting media that included DAPI (Vector Laboratories). IFAs were inspected using a Nikon Eclipse E100080i microscope and a minimum of 100 vacuoles for each strain and timepoint were scored as either cyst-wall positive or cyst-wall negative. The percentage of cyst wall positive vacuoles was expressed as a percentage of the total.

Mouse studies of chronic toxoplasmosis

The ability of parasites to disseminate and form tissue cysts *in vivo* was tested as follows. Intracellular parasites were washed 2-3 times with sterile PBS before being harvested from a confluent monolayer of HFFs by passage through a 27-gauge needle 2-3 times. Host cell debris was removed by passage through a 3 μ m filter. Parasites were counted and diluted in sterile PBS and transported at room temperature to the animal facility. Insulin syringes (28 gauge, Becton Dickinson) were used to deliver 100 μ l of diluted parasite intraperitoneally to female CBA/J mice. Mice were monitored daily during the acute phase of the disease (up to 14 days) and 2-3x a week thereafter for signs of sickness. Two mice were lost during the course of the study (one each in the highest dose for the parental and knockout strains), but due to injuries sustained by the mice and the lack of recently observed acute symptoms of toxoplasmosis (ruffled coats, swollen abdomen, lethargy or difficulty walking), it was deemed that these mice did not perish as a

direct result of infection and they were removed from further analysis. At 28 days post-infection, mice were anesthetized in a CO₂ chamber followed by cervical dislocation. Blood was collected for serum analysis and the brains were harvested to measure cyst burden. Brains were placed in Eppendorf tubes on ice for the remainder of the procedure. Each brain was ground in 1500 µl of ice-cold PBS using a mortar and pestle before removing 250 µl for immunofluorescence analysis. The remainder was immediately placed at -80°C for long-term storage. Samples were centrifuged at 3,000 x g's for 5 minutes at room temperature and the supernatants removed. Brain tissue was resuspended in 150 µl of freshly prepared 3% formaldehyde in PBS and let stand for 20 minutes at room temperature prior to centrifugation at 3,000 x g's for 5 minutes at room temperature. The supernatant was removed and brains were resuspended in 150 µl of 100 mM glycine in PBS and let stand for 5 minutes at room temperature prior to centrifugation at 3,000 x g's for 5 minutes at room temperature. The supernatant was removed and brains were resuspended in 150 µl of 3% BSA/0.2% TX-100 in PBS and let stand overnight at 4°C prior to centrifugation at 3,000 x g's for 5 minutes at room temperature. The supernatant was removed and brains were resuspended in 125 µl of 3% BSA/0.2% TX-100 in PBS containing a 1:250 dilution of Rhodamine-labeled DBA (Vector Laboratories) and let stand for one hour at room temperature prior to centrifugation at 3,000 x g's for 5 minutes at room temperature. The brains were washed three times by resuspending in 150 µl of wash buffer (0.2% TX-100 in PBS) followed by centrifugation at 3,000 x g's for 5 minutes at room temperature. After the final centrifugation, the supernatant was

removed and 5 μ l of brain material was pipetted onto three microscope slides per brain using a large bore pipette. Brains were gently flattened by placing a coverslip over the top and pressing down gently. Coverslips were secured with clear nail polish. The number of cysts per slide was enumerated using a Nikon Eclipse E100080i microscope. The total number of cysts for the three slides for each mouse was combined and multiplied by 26 to obtain an estimate of the total number of cysts per mouse brain as described previously (Lavine, Knoll et al. 2007).

Serum was collected by allowing the mouse blood to coagulate at room temperature for a minimum of thirty minutes in an Eppendorf tube. Serum was separated from coagulated blood cells by centrifuging twice at 4°C for 10 minutes at 5,000 x g's. The resulting serum was used in a dot blot assay to verify that mice had been successfully infected. The dot blot assay was conducted as described previously (Benmerzouga, Checkley et al. 2015). Briefly, approximately 5×10^6 freshly egressed parasites of the parental strain, *Pru Δ ku80*, were centrifuged at room temperature for 10 minutes at 1,000 x g's. All but 100 μ l of the supernatant was removed and the parasites were resuspended in the remaining volume. Approximately 8-10 μ l of resuspended parasites were pipetted onto a nitrocellulose membrane that had been soaked in PBS for 5 minutes. The resuspended parasites were allowed to dry onto the membrane before blocking the membrane with TBST/5% NFDM for 45 minutes. Individual blots were incubated with serum from a single mouse overnight at 4°C at a dilution of 1:50 in TBST/5% NFDM. The following morning, blots were washed three times with TBST for ten minutes each

before incubating with goat anti-mouse conjugated to horse radish peroxidase at a dilution of 1:5000 for a minimum of one hour at room temperature. Blots were again washed three times with TBST for ten minutes each before incubating for five minutes with SuperSignal West Femto Maximum Sensitivity Substrate (Thermo Scientific) for five minutes. Blots were imaged using the FluorChem E system (Protein Simple) for analysis of chemiluminescent Western blots. Seropositivity of individual mice was determined by comparing dot blot results with positive and negative control sera from previous experiments and seronegative mice were removed from statistical analysis of the data.

Chapter 3 : Identification and Characterization of GRA41

In this chapter, my aim is to identify and characterize the protein responsible for resistance to iiDeath in mutant MBD2.1 by sequencing the mutant to identify variations in the mutant genome and complementing these mutations with wild-type copies of the genes impacted. I then endogenously tag the protein of interest to determine its localization and generate a complete knockout to study its impact on parasite function.

Nonsense mutation in novel gene is responsible for iiDeath phenotype of MBD2.1

To identify the causative mutation in mutant strain MBD2.1, whole-genome sequencing was undertaken of both the mutant and its parental strain, RH Δ *hxgprt*. Single nucleotide variants (SNVs) between the two were mapped against the *T. gondii* genomic database (ToxoDB). In total 18 SNVs occurred between mutant and parental; 5 were in intergenic regions, 11 within introns and 2 in exons. Of the two mutations within exons, which were both confirmed by PCR and sequencing, one results in a missense mutation in the hypothetical protein TGGT1_306020 and the other in a nonsense mutation in the hypothetical protein TGGT1_069070 (ToxoDB v7.2). Although both transcriptomic and proteomic evidence could be found for TGGT1_069070 in version 7.2 of the *T. gondii* genomic database, this predicted gene has not been annotated as a gene in subsequent genome versions. Analysis of a cDNA library using 5' and 3' RACE confirmed the gene model of TGGT1_069070 shown in ToxoDBv7.2 (Figure 3.1, below). TGGT1_069070

A. gagtagtaaatgaaatgcttgtactacgtgttctttccggttttttaat
 caatatcgacagtgttgggttttctgcaatccacgcgtggatttttgggggtgcg
 atgccagaagaactggtttgtgatttttctgaatcgaggcaccctggctttcggg
 gtaacacaaagtacaatcaacATGGCACGGAAACGCGCCACGTATTTGCTGGC
 TTGCGTCGCCCTGCCTGCTATAAATGTGCTCCTTTTCGGGGACTGTATTCCTT
 CGCATCAATTGAGTATAACCAGCACAGAGCCGCCGGGCAGGAACGCATCTGTT
 CATTGAGCCTTGCCTGCCGACGTCCTGAAACAGGACGAGGACGAAACAAGCGT
 AGAGGAGGACGTTTGGCGCCCGGTTTCATACGGCAGCTTGAGATACCACCTGT
 CTGATATGGACACGACCTTCAGGTGGCCGT**C**AGAACGCCACCGAACCTCTGCA
 TTGATGCGCGATAACAATACCAGGGCTGCTGTTGGTAGCGGCTTTGGTCCTTAT
 GTCACGTAGAGCACGACCAGAGGAGGAAGAGGGAATGGTAGCACCGTTGAGCA
 TTCTGAATCAGGGGGACGTTGCCCTGCTGTGGCAGGCGAGCAGGTACAAGAA
 CGTGCTGAAAGCCCACCACCAGCATAACAGTACTGGGAACCGCGAAAGACTTC
 TCTGCTTTCTAAACTTCACCTACCCGAATAAGaatgtacatttttggtacctcc
 atgggcaaggttctctccattaactaccatcttcatacttcgtaatgcttg
 tcgagcaacacttcttcgtgcccgaacaagtttgctggagataagatgggcaa
 ccttccacagcgcgagcgtcattctctaattttttctcatgctggcgaagacgg
 agctcaaccaatatacctattttcaggggtgatgcttcttgaaatggcttgggt
 gctacgaaagttcgcgatgtgcgggtttcacgtttatcgcgttactaacgtgc
 ttgatgccgctcttctgcatttaagtacaggggtttgagaacgccgctcgtgca
 ctcatgaagggtagaaccactgtgtaggcaccagtggtggcggtggcagccat
 acgcggtggcgtcttgactgcttcaatatggcttcttgacgcctctggatgat
 aggaaaggggagctagctcatttcatatctcgtgtttatgcttcgatgactag
 ctggctcccattccgctcgtgttttctgctttattttcttttccaggctgttgt
 gttttcattcgtcggaccacaattctcctccgtatttctggctgagggcgtctc
 tatgttcacacgctcatgctaattcagatgctttcagcctgaccgcgttttgc
 cgcgctcctacttgtggggacaggatgttctgacccaaagttcaaaaggtgcc
 ccatttttaatcgagcagggcggtagcggatttggggtacaatactgcacacc
 ggtgctcacaacattagagtcttgtctccttaatgaggggataacgatggcta
 tttattgactataaagaccggaggctgggtgtcactactcttttatcatctgc
 ggcttacgccaatcacagcggcttgcccactttcgtttggatgtcttagtct
 ttcactatgtaccgctttcagatgcgggtgatgcatgctttttccgatcg
 tttctcatgctaaagttgttgggaaatgtagctttggggctaaactacgggt
 ccaagttgattcttgcagagtccaaggatagtcgagaccgctcgttgtttccc
 cgcagcctgtgatgggtgccataccactcagacatccaagcaactcgtttcac
 aagagaaatattcgggtgttcgcgcggaaagcattcgatagccta

B.

<u>MARKRATYLLACVALPAINVLLFGDCIPSHQLSITSTEPPGRNASVHSAL</u>	50
PADV TEQDEDET SVEEDVLAPGSYGLRYHLS D MDTTFRW P SERHR T SAL	100
MRDTIPGLLLVAALVLMRRARPEEEEGMVAPLSILNQGDVAPAVAGEQV	150
QERA E SPPPAYS D WEPR K T S LL S KLHLPE	179

Figure 3.1 Sequencing of TgGT1_069070
 (A) cDNA sequence with 5' and 3' untranslated regions (UTRs), which were determined by 5' and 3' RACE in lower case. Nucleotide mutated in MBD2.1 is in bold. (B) Protein sequence. Predicted signal sequence is underlined and phosphorylated amino acids are in bold, black for those phosphorylated only in intracellular parasites and red for those phosphorylated in both extra and intracellular parasites (Treeck *et al* 2011). Arrow indicates where protein is truncated in mutant MBD2.1.

encodes a putative 179 amino acid (aa) protein with an N-terminal signal sequence but no known functional domains. Though homologs of this gene are not annotated in any genomes present in the EuPathDB (EuPathDB.org) database, a tblastn search against the parasite genomes available in EuPathDB identifies potential homologs in the closely related parasites *Hammondia hammondi* (KL544038:723,066..723,587, 77% identity with TGGT1_069070) and *Neospora caninum* (FR823391:5,147,783..5,148,286, 47% identity).

The nonsense mutation in TGGT1_069070 detected in the mutant strain is a single C to G transversion, which results in the conversion of the serine at position 91 to a premature stop codon (Figure 3.2, below). To investigate whether the mutation in this gene was responsible for the observed phenotype of MBD2.1, I transfected a cosmid containing a parental copy of the gene into the mutant and generated stable clones by limiting dilution. Two independent clones (MBD2.1 Comp Clone 1 and MBD2.1 Comp Clone 7) were established and the incorporation of the parental allele was confirmed by sequencing of a PCR fragment spanning the TGGT1_069070 coding sequence. The sequence chromatogram from Clone 1 shows a mixed peak at the position of interest (Figure 3.2, below) indicating that this clone carries both a mutant and a parental copy of the gene as expected for random integration of the cosmid. On the other hand, Clone 7 contains only the wild-type copy of the gene (Figure 3.2, below), suggesting that the cosmid recombined by homologous recombination with the endogenous locus

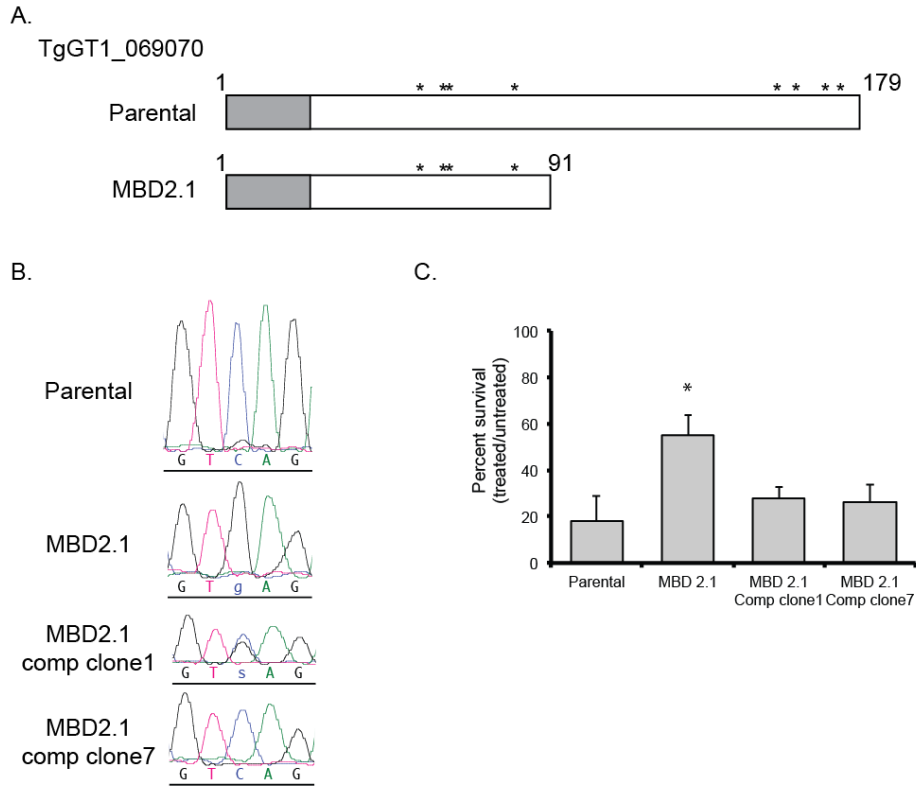


Figure 3.2 The *iiDeath* phenotype of MBD2.1 is due to the introduction of a premature stop codon in TGGT1_069070. (A) Diagrams of the protein encoded at the TGGT1_069070 locus in the parental strain (top) and the putative truncated protein encoded in MBD2.1 as a result of the nonsense mutation in TGGT1_069070 (bottom) are shown. Gray rectangle represents predicted signal peptide and asterisks indicate relative positions of known phosphorylation sites (ToxoDB proteomic databases). (B) Chromatograms from sequencing of PCR fragment spanning mutated region for the parental, MBD2.1 mutant, and two MBD2.1 clones complemented with cosmid TOXO119 (Comp clones 1 and 7) are shown. In clone 7 the mutation has been repaired to wild type base indicating allelic replacement, while in clone 1 both a mutant and wild type allele are present as observed by mixed peak for base of interest (arrow). (C) Extracellular parasites of the parental, mutant (MBD2.1) and two complemented strains were exposed to 1 μ M A23187 for 1 hour and allowed to form plaques to determine survival rate which was calculated based on survival of untreated parasites. Bars are average of three independent experiments and error bars represent standard deviation. Asterisk denotes statistical significance based on the results of an unpaired Student's t-test with a p-value of <0.05.

resulting in an allelic replacement event. I have confirmed that Clone 7 still carries the missense mutation in TGGT1_306020 corroborating that it is indeed a derivative of the mutant strain MBD2.1 (data not shown).

Importantly, regardless of whether by random integration or by allelic replacement, introduction of wildtype TGGT1_069070 restored ionophore sensitivity to MBD2.1 (Figure 3.2, above). Treatment of extracellular parasites with A23187 followed by plaque assay to determine number of viable parasites showed that, while mutant MBD2.1 has increased survivability ($54\% \pm 9\%$, $p < 0.05$) as compared to a parental strain ($18\% \pm 11\%$), both MBD2.1 Comp Clone 1 and MBD2.1 Comp Clone 7, were statistically as sensitive to iiDeath as the parental strain ($28\% \pm 5\%$ and $26\% \pm 8\%$ respectively, Figure 3.2, above). Thus, presence of a wildtype copy of TGGT1_069070 restores ionophore sensitivity to mutant MBD2.1. Based on this result and those described below I have focused my studies on the protein product of TGGT1_069070 and have not as of yet explored the role of the mutation found in TGGT1_306020 as it is unlikely to influence iiDeath.

TGGT1_069070 encodes a novel dense granule protein, GRA41

In order to confirm the expression of TGGT1_069070 at the protein level and to determine its localization, sequences encoding a carboxy-terminal (C-terminal) triple-hemagglutinin (HA) tag were introduced into the endogenous locus in the *RH Δ ku80 Δ hxgprt* strain just before the stop codon, using a previously described approach (Huynh and Carruthers 2009). Western blot analysis of protein extract from the endogenously tagged strain revealed a doublet migrating at

approximately 30 kDa, which is higher than the predicted molecular weight of the tagged protein, 24 kDa (Figure 3.3A, below). The doublet pattern was consistently observed in extracts from both intracellular and extracellular parasites (Figure 3.3A, below). At present the reason for the migration pattern is not known, although the protein is predicted to be phosphorylated, which could account for size differences as it does for other *T. gondii* proteins such as GRA7 (Dunn, Ravindran et al. 2008). The resulting strain grows normally in culture and does not exhibit resistance to ionophore induced death, indicating that the tag does not interfere with the protein's function (Figure 3.3B, below). To explore the localization of TGGT1_069070, I performed an immunofluorescence analysis (IFA) and found that the encoded protein appears to localize within the PV, where it colocalizes with the PV localized protein, GRA7 (Fischer, Stachelhaus et al. 1998, Jacobs, Dubremetz et al. 1998) (Figure 3.3C, below). IFA of the engineered parasites with antibodies against the parasite surface antigen SAG1 (Kasper, Bradley et al. 1984) confirmed that the majority of the HA-tagged protein is present within the PV and not within the parasites (Figure 3.3D, below). The majority of proteins in the PV are secreted by intracellular parasites from the dense granules, whose contents are more easily detected in extracellular parasites. To determine if TGGT1_069070 is also a dense granule protein, I performed an IFA of extracellular parasites with anti-HA antibodies to detect TGGT1_069070 and antibodies to dense granule marker GRA7, which shows co-localization of both signals within intracellular vesicles consistent with dense granules (Figure 3.3F, below). To confirm and refine the results from immunofluorescence analysis, I,

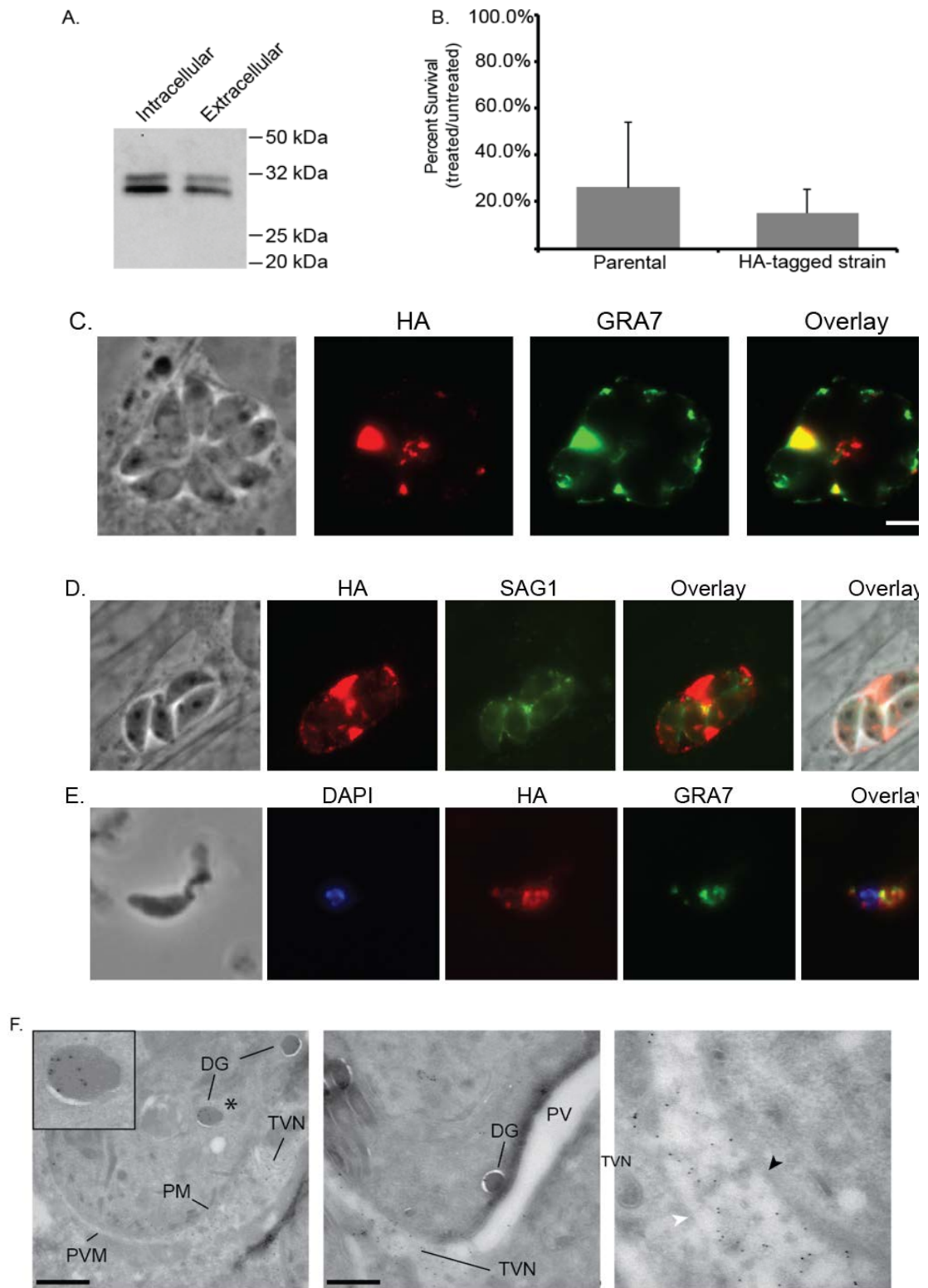


Figure 3.3 TGGT1_069070 encodes a novel dense granule protein, GRA41

A strain in which an 3xHA tag is expressed at the C terminus of the endogenous TGGT1_069070 protein was generated and analyzed for protein expression and localization. (A) Expression of HA tagged TGGT1_069070 was confirmed by Western blot in both intracellular and extracellular parasites. TGGT1_069070 migrates as a protein doublet of approximately 30 kDa (predicted molecular weight ~ 24 kDa). (B) Tagging of endogenous locus does not impact susceptibility to ionophore induced death (C-D) Intracellular parasites were analyzed by Immunofluorescence Assay (IFA) using anti-HA antibodies to detect TGGT1_069070 (in red) and antibodies against either the dense granule/parasitophorous marker GRA7 (C, in green) or the surface antigen SAG1 (D, in green). Scale bars, 5 μ m (E) Extracellular parasites were analyzed by IFA using HA antibodies to detect TGGT1_069070 within the parasite and with antibodies against the dense granule marker GRA7 (in green). DAPI stain was used to detect the nucleus. Scale bar, 2 μ m (F) Immunoelectron microscopy was used to confirm the localization of TGGT1_069070, which is designated GRA41, to the dense granule and parasitophorous vacuole. Antibodies directed against HA conjugated to gold particles were used to detect protein. Inset in left panel is magnification of the dense granule marked with asterisk in image. Middle panel focuses on vacuolar space and shows that staining is confined to regions where tubulovesicular network (TVN) is present. Right panel is magnification of region of the middle panel where TVN is present. Black arrow head points at parasite membrane, white arrow head at parasitophorous vacuole membrane. DG= dense granule, PM = parasite membrane, PVM = parasitophorous vacuole membrane, TVN = tubulovesicular network. Scale bars, 500 nm. Immunoelectron microscopy analysis conducted by Isabelle Coppens, Johns Hopkins University.

along with our collaborator, Dr. Isabelle Coppens of Johns Hopkins University, performed immunoelectron microscopy using anti-HA antibodies to detect the tagged protein (Figure 3.3F, above). Within the parasite cytoplasm, the signal is detected predominantly within the membrane bound electron dense structures whose morphology and location are consistent with that of dense granules, confirming our observations from IFA. Within the PV the protein is exclusively found associated with the vesicles and tubules of the TVN and not free in the vacuole lumen or membrane (Figure 3.3F, above). Consistent with this

membranous localization, partitioning with TX-114 showed the tagged protein partitions almost exclusively with the detergent phase, consistent with a membrane-associated protein (Figure 3.4, below). Based on these results, I have concluded that the protein encoded at the TGGT1_069070 locus is a dense granule derived protein that is secreted from the parasite into the PV where it associates with the TVN. According to the currently published literature, the dense granule proteins have been named from GRA1 to 40 so TGGT1_069070 is designated as GRA41.

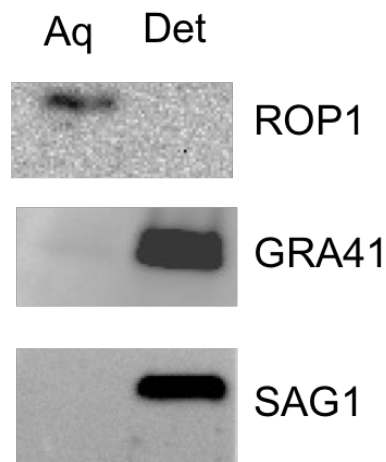


Figure 3.4 Western Blot Analysis of Triton-X 114 partitioning of parasite lysates from the GRA41 endogenously HA-tagged strain. GRA41 (detected with Rabbit anti-HA antibody) primarily partitions with the detergent (Det) rather than the aqueous (Aq) phase. ROP1 (detected with mouse anti-ROP1 antibody) was used as soluble protein control to label the aqueous phase and SAG1 (detected with mouse anti-SAG1 antibody) was used as a membrane protein control to label the detergent phase.

Complete knockout of GRA41 recapitulates iiDeath⁻ phenotype

To further study the role of GRA41 in the parasite's life cycle, I generated a knockout of the gene by replacing the entire coding sequence with the selectable marker hypoxanthine-guanine phosphoribosyltransferase (HXGPRT) through

double homologous recombination into the $RH\Delta ku80\Delta hxgp\text{rt}$ strain, hereafter referred to as $RH\Delta ku80$ (Huynh and Carruthers 2009) (Figure 3.5A, below). Parasites transfected with the knockout vector (pGRA41KO) and stably expressing HXGPRT were selected by resistance to mycophenolic acid and xanthine and cloned by limiting dilution. Through two separate attempts to generate knockout strains, I established two independent clones ($RH\Delta ku80\Delta gra41-1$, aka KO1 and $RH\Delta ku80\Delta gra41-2$, aka KO2) that were shown to have correct integration of the construct by PCR (Figure 3.5B, below). To confirm that the genetic disruption of the locus resulted in a functional knockout of GRA41, I measured relative transcript abundance by quantitative PCR (qPCR), which failed to detect *GRA41* message in either of the knockout clones (Figure 3.5C, below). In addition, through qPCR, I determined that the genetic disruption did not affect transcript levels of the genes immediately upstream and downstream of *GRA41* (Figure 3.5C, below). Based on the nature of the genetic disruption expected from double recombination of the knockout construct (pGRA41KO, Figure 3.5A, below) and the lack of detectable transcript (Figure 3.5C, below), the two established clones represent functional knockouts and are unlikely to produce any GRA41 protein. I then assessed whether or not the complete knockout of *GRA41* recapitulated the iiDeath phenotype seen in GRA41 truncation mutant MBD 2.1. Both $RH\Delta ku80\Delta gra41-1$ ($45\% \pm 16\%$ versus $11\% \pm 12\%$ for the parental strain, $p < 0.05$, Figure 3.5D, below) and $RH\Delta ku80\Delta gra41-2$ ($25\% \pm 5\%$ versus $7\% \pm 5\%$ for the parental strain, $p < 0.05$, Figure 3.5D, below) showed statistically significant increases in survival as compared to the parental strain after 60 minutes of treatment with A23187. Thus,

the recapitulation of the phenotype seen in the mutant MBD2.1 by the complete lack of *GRA41* suggests that the iiDeath phenotype of MBD2.1 is likely due to the absence of full-length *GRA41* product and not a dominant negative effect imparted by a possible truncated protein.

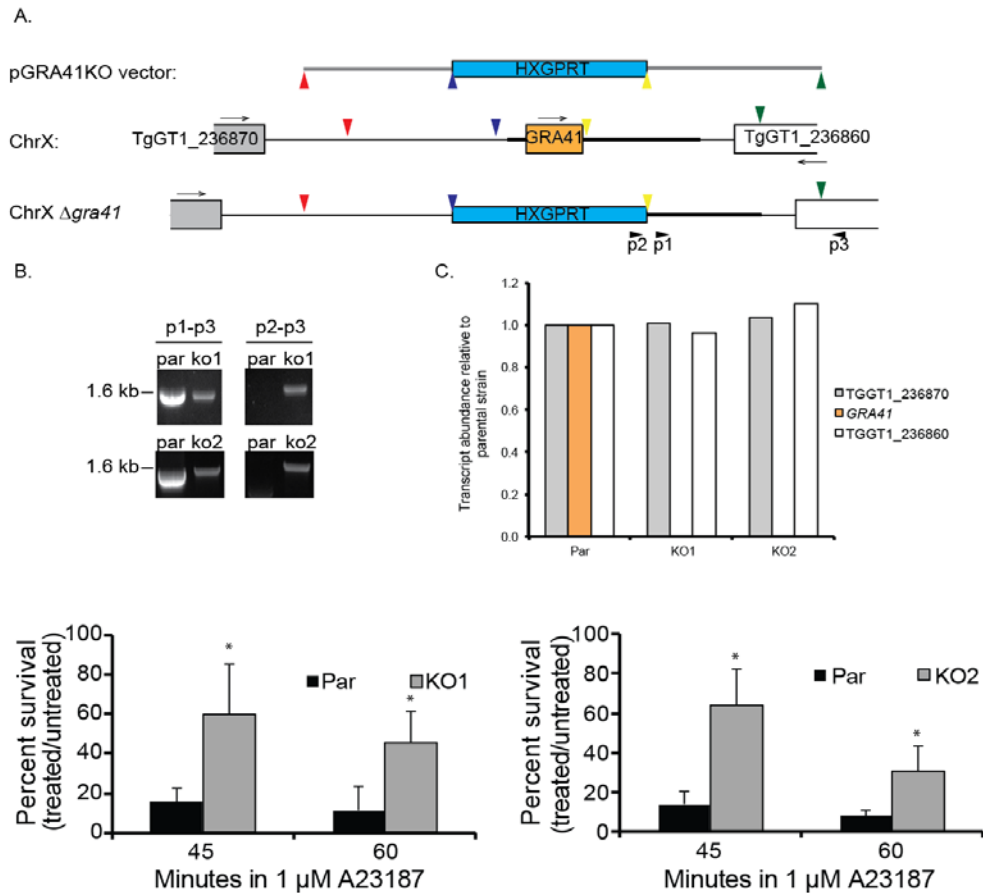


Figure 3.5 Complete knockout of *GRA41* recapitulates the iiDeath phenotype seen in MBD2.1 mutant.

(A) Diagram shows strategy used to knockout *GRA41* by double homologous recombination replacing the *GRA41* locus with the HXGPRT selectable marker. Colored arrow heads indicate beginning and end of genomic regions used to drive homologous recombination of pGRA41KO vector with target locus in chromosome X (ChrX). Arrows indicate relative direction of transcription of the three genes depicted and black arrow heads represent primers p1, 2 and 3 used to corroborate integration. (B) PCR analysis of DNA from parental strain (Par) and two independent putative knockouts KO1 (top panels) and KO2 (bottom panels) using either a primer pair expected to produce an

amplicon in both parental and knock strains (p1-p2, left panels) or a test primer pair that would produce a product only if the *GRA41* gene were replaced (p2-p3, right panels). (C) qPCR analysis was used to monitor transcript levels of *GRA41* and the two flanking genes *TGGT1_236870* and *TGGT1_236860* in the parental (Par) and two knockout strains (KO1 and KO2). Data is expressed as $\Delta\Delta C_t$ of each relative to that of parental and represents average of 3 independent experiments (D) Extracellular parasites of the parental and KO1 (left) and KO2 (right) mutant (MBD2.1 were exposed to 1 μ M A23187 for 45 or 60 minutes and survival rate was determined as in Fig. 1. Bars are average of three independent experiments and error bars represent standard deviation. Asterisk denotes statistical significance based on the results of an unpaired Student's t-test with a p-value of <0.05.

Complete knockout of *GRA41* results in decreased plaquing efficiency

While performing the iiDeath assays described above I noted that, although the same number of untreated parasites were used for all strains, the knockout parasites consistently established fewer plaques (discrete areas of host cell destruction resulting from the invasion of a single parasite followed by multiple lytic cycles) as compared to the parental. To determine whether the knockout strains truly had reduced plaquing efficiency, which would suggest a defect in the lytic cycle of the parasite, I infected cells with an equal number of freshly harvested, untreated parasites of the parental and knockout strains and allowed them to invade for two hours before removing extracellular parasites. Intracellular parasites were allowed to form plaques, which were quantitated on the sixth day post infection. Both clones showed a statistically significant decrease in the number of plaques as compared to the parental without any noticeable differences in plaque size (18% \pm 12% of parental efficiency for RH $\Delta ku80\Delta gra41$ -1, 63% \pm 9% for RH $\Delta ku80\Delta gra41$ -2, $p < 0.05$), although the phenotype of the second independently generated clone was attenuated compared to the first (Figure 3.6A, below).

Consistent with this apparently variable phenotype, I observed that continuous passage of the RH $\Delta ku80\Delta gra41-1$ in *in vitro* culture results in a relative loss of phenotype over the course of a few weeks. Plaque assays conducted over the course of two weeks showed the gradual increase in plaquing efficiency from 11% to 56% for clone RH $\Delta ku80\Delta gra41-1$ (Figure 3.6B, below). Continued passage of adapted parasites in culture resulted in a strain that grows robustly, exhibiting more and larger-sized plaques as compared to the parental strain (data not shown). Thus, the loss of *GRA41* resulted in reduced plaquing efficiency of tachyzoites, and the parasites adapted to this phenotype during continuous passage in culture, suggesting a defect in one or more steps of the lytic cycle that is either lost or compensated for over time.

Complementation of *GRA41* knockout with the parental gene rescues both
iiDeath sensitivity and lytic cycle defects

While the fact that two independent knockout strains exhibited the same plaquing phenotype support the idea that the lack of *GRA41* affects parasite propagation, there is always the possibility that secondary mutations are responsible for the observed phenotype. The introduction of a wild-type allele of *GRA41*, as was done for *MBD2.1*, would address this issue. However, the rapidity with which this strain adapts to *in vitro* culture would complicate the interpretation of phenotypic complementation, and a return to wild type levels of plaquing by a complemented strain could be due to either the addition of the wild type allele or simply to adaptation during the complementation process, which can take several

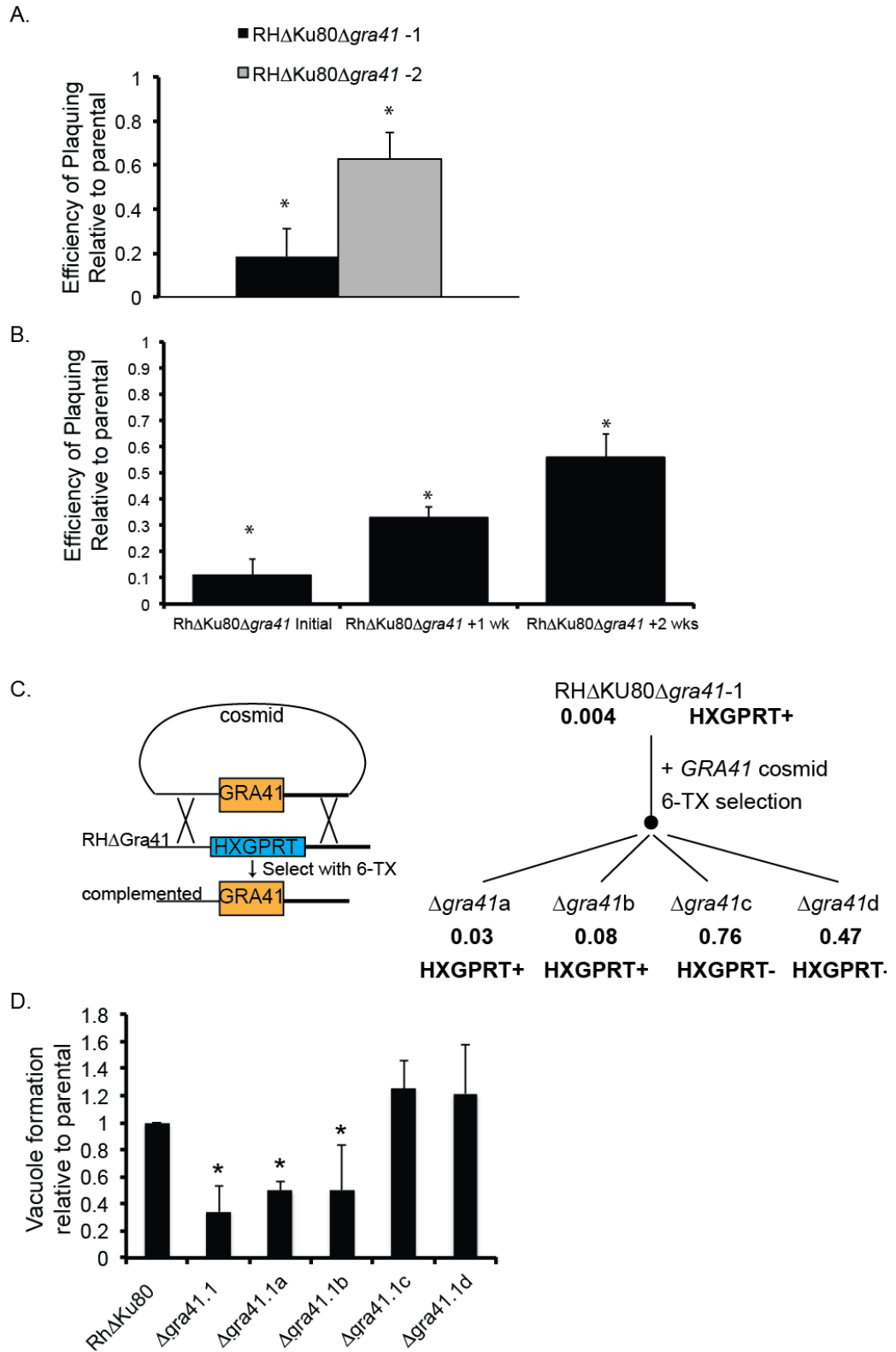


Figure 3.6 Complete knockout of *GRA41* results in reduced plaquing efficiency which is rescued by complementation.

(A) Extracellular parasites of the parental and knockout strains were allowed to form plaques to assess plaquing efficiency, which was calculated by dividing the number of plaques formed for each knockout strain by that formed by the parental strain. (B) Extracellular parasites of RH $\Delta ku80\Delta gra41-1$, which had been maintained in culture for different amounts of time, were allowed to form plaques as in (A) to determine if knockout parasites were able to adapt to loss of *GRA41* in respect to plaquing efficiency. (C) Diagram (left) shows the strategy for complementation of *gra41* knockout by double homologous recombination of cosmid TOXO119 into the target locus. Parasites transformed with cosmid were exposed to 6-thioxanthine to select for loss of the HXGPRT cassette. Flow chart (right) shows the isolation of resulting clones. Indicated below each clone is the relative transcript level of *gra41* (as described in Figure 3) and the presence/absence of the HXGPRT cassette, which was determined by sensitivity to MPA. (D) Extracellular parasites of the parental, knockout and complemented clones were allowed to grow for twenty-four hours before fixing and counting the number of vacuoles per field of view (vacuole formation). Bars are average of three independent experiments and errors bars represent standard deviation. Asterisk denotes statistical significance based on the results of an unpaired Student's t-test with a p-value of <0.05.

weeks. Thus, a complementation strategy was devised that could control for adaptation based on repairing the disrupted *GRA41* locus by homologous recombination using the same cosmid utilized to complement mutant MBD2.1 (Figure 3.6C, above). This approach took advantage of the fact that the HXGPRT marker, which was used to replace *GRA41* in the knockout strains (Figure 3.5A, above), can be selected against with 6-thioxanthine (Donald, Carter et al. 1996). Because 6-thioxanthine's effect is static and not cidal (Pfefferkorn, Bzik et al. 2001) I was able to transfect the knockout strain with the cosmid containing *GRA41*, select for lack of HXGPRT for 2 weeks, clone by limiting dilution and obtain two types of randomly selected clones: those with detectable levels of *GRA41* transcript by qPCR and still HXGPRT⁺ as demonstrated by resistance to MPA/XAN treatment ($\Delta gra41A$ and B in Figure 3.6C, above), and those with measurable

levels of *GRA41* transcript and now HXGPRT⁻ ($\Delta gra41C$ and D in Figure 3.6C, above). Since all clones, both the ones with *GRA41* and those without, had gone through the same manipulations and been in culture for the same amount of time, direct comparison of phenotypes could be performed with some control over possible adaptation. Though the knockout strain also differs from the parental and the complemented strain by the presence of HXGPRT, previous work has shown that the loss of HXGPRT does not play a role in iiEgress, iiDeath or parasite propagation (Arrizabalaga, Ruiz et al. 2004), supporting the conclusion that any differences seen are due to the loss of *GRA41*. The ability of these parasites to grow efficiently in *in vitro* culture was assessed by allowing parasites to infect a confluent monolayer of host cells for two hours, then allowing them to grow for an additional 22 hours before fixing them and counting the number of vacuoles per field of view. The number of vacuoles formed by the KO clones over that by the parental strain was used to convey the relative efficiency of vacuole formation. While both clones still lacking *GRA41* ($\Delta gra41a$ and $\Delta gra41b$) showed a significantly decreased frequency of vacuole formation ($49\% \pm 7\%$ and $50\% \pm 33\%$ respectively, $p < 0.05$), the two clones in which *GRA41* expression was restored ($\Delta gra41c$ and $\Delta gra41d$) had significantly enhanced ability to establish vacuoles ($125\% \pm 20\%$ and $121\% \pm 37\%$ respectively, Figure 3.6D, above). Thus, *GRA41* plays a role in the efficiency of the parasite's propagation cycle in addition to sensitivity to iiDeath treatment.

Complete knockout of *GRA41* affects timing of natural egress

To better define the phenotype of *GRA41* loss of function I probed the ability of *RHΔku80Δgra41-1* to complete the various steps of the lytic cycle. I first performed a 30 minute post-invasion assay as described previously (Carruthers, Giddings et al. 1999) to measure the parasite's ability to attach and invade host cells. A slight but statistically significant reduction in the percentage of invaded parasites was seen from 63%±5% in the parental strain to 45%±11% in *RHΔku80Δgra41-1*, though no difference was seen in attachment efficiency of the *GRA41* knockout strain (Figure 3.7, below). Thus, loss of *GRA41* leads to a small

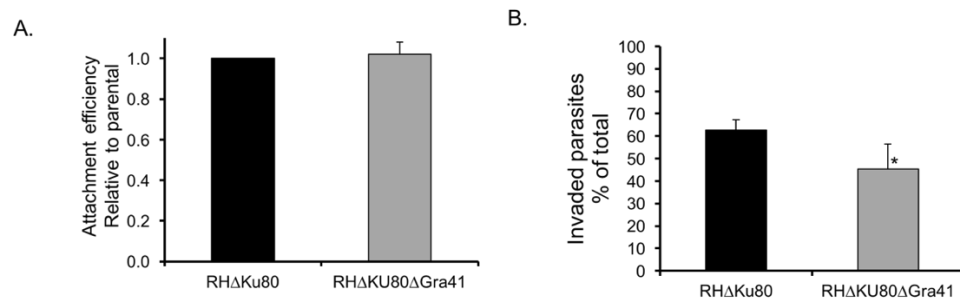


Figure 3.7 Complete knockout of *GRA41* results in decreased invasion efficiency

(A) Attachment efficiency of *RHΔKu80ΔGRA41* strain relative to parental (B) Percent of total parasites present in culture that successfully invaded. Average of three independent replicates. Error bars represent standard deviation. *, $p < 0.05$

reduction in invasion efficiency. Since the level of reduction in invasion efficiency is not sufficient to explain the 50 to 80% reduction plaquing efficiency, I looked at post-invasion lytic cycle steps to determine why parasites were inefficient in forming plaques after successful initial invasion. From the vacuole formation assay used to assess successful complementation, it was apparent that there was a decrease in the number of vacuoles present as early as 24 hours post-infection, so I chose to see what was occurring before and after this time point during

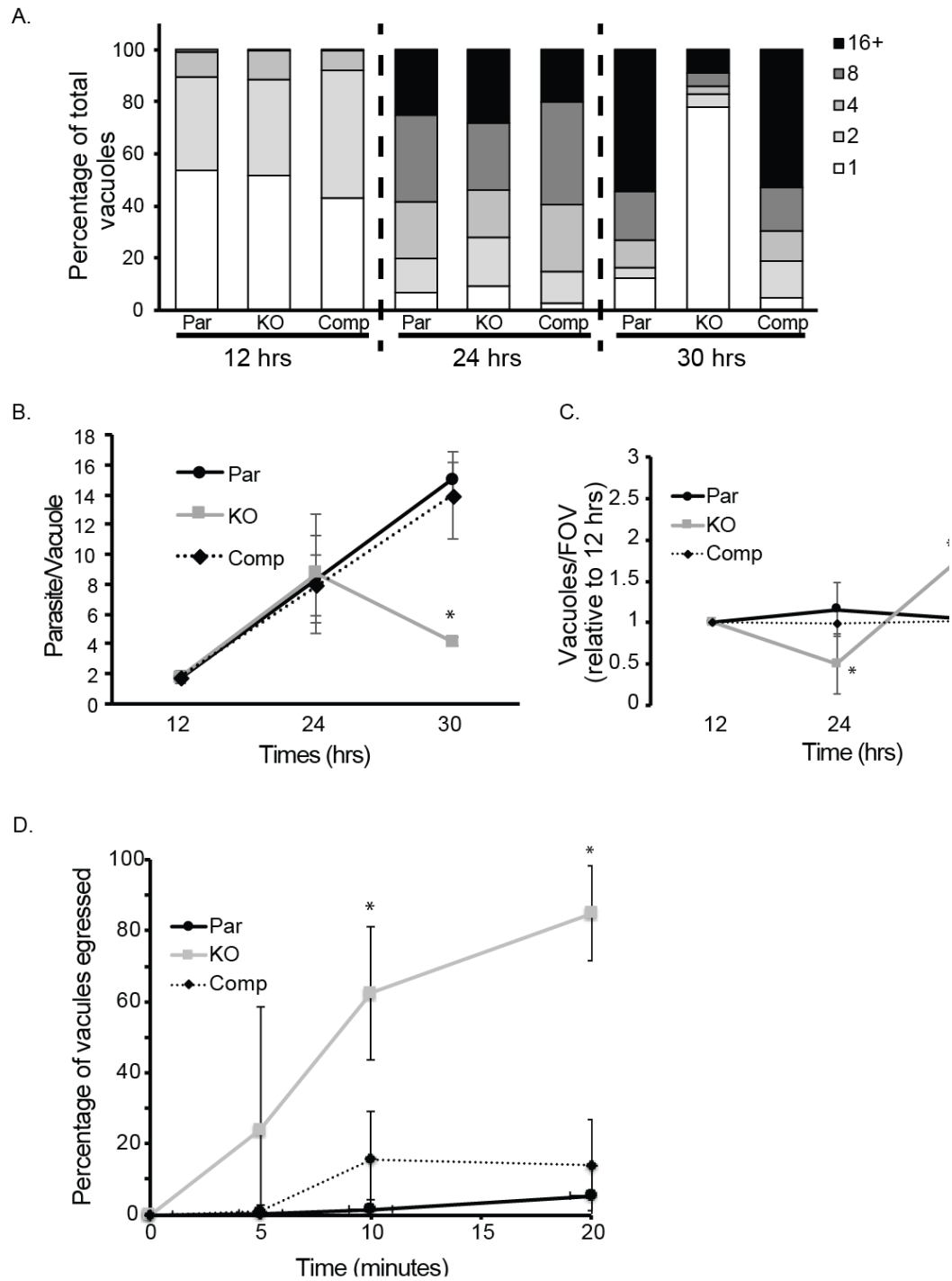


Figure 3.8 Complete knockout of *GRA41* leads to premature egress of parasites.

(A) Extracellular parasites of the parental, knockout and complemented strains were allowed to invade for two hours before removing parasites that remained outside. Invaded parasites were allowed to grow for a total of 12, 24 or 30 hours before fixing and counting the number of parasites per vacuole for a minimum of 100

vacuoles per strain. (B) The average number of parasites per vacuole for the data in (A) was calculated for each strain and graphed as a function of time. (C) The average number of vacuoles per field of view for the data in (A) was calculated for each strain/time point and normalized to the twelve-hour time point. (D) Percentage egress was calculated for each strain following 5, 10 or 20 minute treatment with 5 mM DTT. All data is the average of at least three independent experiments and errors bars represent standard deviation. Asterisk denotes statistical significance based on the results of an unpaired Student's t-test with a p-value of <0.05.

parasite replication. Intracellular parasites from the parental, knockout and complemented strains were manually extracted from host cells, harvested, counted and allowed to invade confluent HFFs in multiple twenty-four well plates for two hours. Each plate was fixed at twelve, twenty-four or thirty hours post-infection and the number of parasites per vacuoles were determined for at least 100 vacuoles per sample (Figure 3.8, above). No statistically significant difference in the average number of parasites per vacuole was seen at twelve or twenty-four hours, suggesting that the knockout parasites were replicating at a normal rate (Figure 3.8A and B, above). However, the knockout parasites showed a more than two-fold decrease in the average number of parasites per vacuole at thirty hours post infection (from 15 ± 1 parasites/vacuole for parental to 4 ± 0.3 parasites/vacuole for knockout, $p < 0.001$, Figure 3.8B, above), while the complemented strain is not significantly different from the parental (14 ± 3 parasites/vacuole, $p > 0.05$). This decrease in the average number of parasite per vacuole from 24 to 30 hours post infection for the knockout strain is due to a decrease in the proportion of large vacuoles, which coincides with an increase in the number of vacuoles containing 1-2 parasites (Figure 3.8A, above). This pattern (i.e. decrease in large vacuoles and increase in small ones) is consistent with egress and reinvasion, and suggests

that natural egress for the *GRA41* knockout strain is occurring between 24 and 30 hours. This contrasts with what is observed with both the parental and complemented parasite strain, which continue to divide within the original vacuoles between 24 and 30 hours (Figure 3.8A, above).

In addition to quantifying the average number of parasites per vacuole, the average number of vacuoles per field of view was also assessed for each strain to see if vacuoles were being lost (due to egress without reinvasion or death) or gained (due to egress with reinvasion). The average number of vacuoles per field of view for both the parental and the complemented strains stayed relatively constant overtime, while the knockout parasites first appeared to lose vacuoles between 12 and 24 hours post infection ($48\pm 13\%$ of the vacuoles twelve hours, $p < 0.05$, Figure 3.8C, above) and then gain vacuoles between 24 and 30 hours post infection ($195\pm 48\%$ of the vacuoles at twelve hours, $p < 0.05$, Figure 3.8C, above). The reduction in number of vacuoles between 12 and 24 hours post infection is consistent with our previous data looking at parasites either shortly after invasion or at twenty-four hours after infection. When looking shortly after invasion, there was only a modest decrease in invasion efficiency for the knockout parasites (Figure 3.7, above). However, there is a pronounced difference in the number of vacuoles present at 24 hours between the strains, which would be explained by losing vacuoles between 12 and 24 hours (Figure 3.6D, above). In conjunction, these results are consistent with an early egress phenotype in the knockout parasites, with the parasites egressing between 12 and 24 hours failing to reinvade and the parasites egressing between 24 and 30 hours reinvading successfully.

Thus, analysis of the lytic cycle indicates that the loss of GRA41 does not impact division rate of the parasites, but does lead to early egress of parasites, which would account for a majority of the decrease in plaquing efficiency reported above.

Interestingly, the original MBD2.1 mutant (Black, Arrizabalaga et al. 2000) as well as the *GRA41* knockout strain (data not shown) appear to also undergo egress at a faster rate than their parental strain after induction with the ionophore A23187. Nonetheless, because of the high efficiency and fast rate of iiEgress the effect is very slight and difficult to statistically validate. Accordingly, I tested the sensitivity of the *GRA41* knockout to a different inducer of egress, the redox reagent DTT, which typically requires that parasites be infected for approximately 36 hours before induction and induces egress with slower kinetics than A23187 (Stommel, Cho et al. 2001). For this purpose, parasites were allowed to infect host cells for 24 hours before inducing egress with 5 mM DTT. The *GRA41* knockout strain does show evidence of significant enhanced egress as compared to the wild-type and complemented strains at both 10 and 20 minutes post-induction (62%±19% versus 2±2% and 15±13% at 10 minutes, 85%±14% versus 5%±9% and 14%±13% at 20 minutes, Figure 3.8D, above, $p < 0.05$), indicating that the *GRA41* knockout strain is sensitive to induction of egress by DTT earlier in the replication phase of the lytic cycle as compared to the parental and complemented strains.

Chapter 4 : Functional Analysis of GRA41

In Chapter 3, I identified the novel dense granule protein, GRA41, as the protein responsible for the resistance to iiDeath in mutant MBD2.1. In this chapter, I aim to elucidate the mechanisms by which GRA41 might be impacting calcium homeostasis by testing calcium levels in the parasite, calcium binding in the recombinant GRA41 protein, identifying GRA41 interactors and looking for additional phenotypes that could explain the resistance to iiDeath.

Ionophore induced death is due to decreased attachment and decreased stimulated microneme secretion

To determine the exact reason why parasites exposed to ionophore for extended periods of time were unable to form plaques in host cells, an ionophore treatment of parental (*RHΔhxcprt*) parasites was conducted followed by an invasion assay. Since the two distinct processes of attachment and invasion are both required for successful entry into a host cell, it was necessary to distinguish which step the ionophore affected. The invasion assay distinguishes between attached and invaded parasites after a short incubation time by selective labeling the parasite surface with antibodies. First, the attached parasites are labeled with antibody directed to a parasite surface antigen without any permeabilization step that would allow the antibody to cross the host cell membrane. The antibody is then washed away before the host cell membrane is permeabilized and all parasites are labeled with an additional antibody, which can be directed to any part of the parasite. Attached parasites are labeled with both antibodies, which can be detected with fluorophore-conjugated secondary antibodies, while invaded

parasites are only labeled with a single antibody. An invasion assay performed after extracellular treatment of the parasites with 1 μ M A23187 for one hour showed that while ionophore-treated parasites showed no defect in invasion (data not shown), they were severely affected in their ability to invade. Compared to DMSO solvent control-treated parasites, ionophore treated parasites exhibited nearly a 70% decrease in the number of attached parasites, indicating that prolonged ionophore treatment leads to a defect in host cell attachment (Figure 4.1A, below). Since attachment has been shown to be mediated by secretion of proteins from the micronemes, which can be stimulated by treatment with ionophore, a micronemal secretion assay was conducted to verify that the defect in attachment was due to a defect in micronemal secretion (Wan, Carruthers et al. 1997, Carruthers and Sibley 1999). To do this, extracellular parental (*RH Δ hxgprt*) parasites were exposed to ionophore or DMSO control for one hour before separating parasites from secreted proteins by centrifugation. Both the DMSO and ionophore pellets were then divided in half and subjected to an additional treatment with either DMSO or ionophore. Subsequent supernatants and pellets were then separated by SDS-PAGE followed by Western Blot in order to visualize micronemal protein MIC2. As expected, the initial treatment with ionophore resulted in increased micronemal secretion as compared to the DMSO control (Figure 4.1B, below). For the parasites subjected to a one hour DMSO treatment, similar results were seen, with ionophore treated parasites showing increased secretion compared to the DMSO treated controls. However, the parasites that had first undergone the ionophore induced death treatment showed no difference in

secretion when treated with ionophore as compared to the DMSO control, showing that secretion of MIC2 is no longer enhanced in response to the induction of calcium fluxes. The resulting pellets from the ionophore induced death treated parasites were also included to show that there is still MIC2 remaining inside the

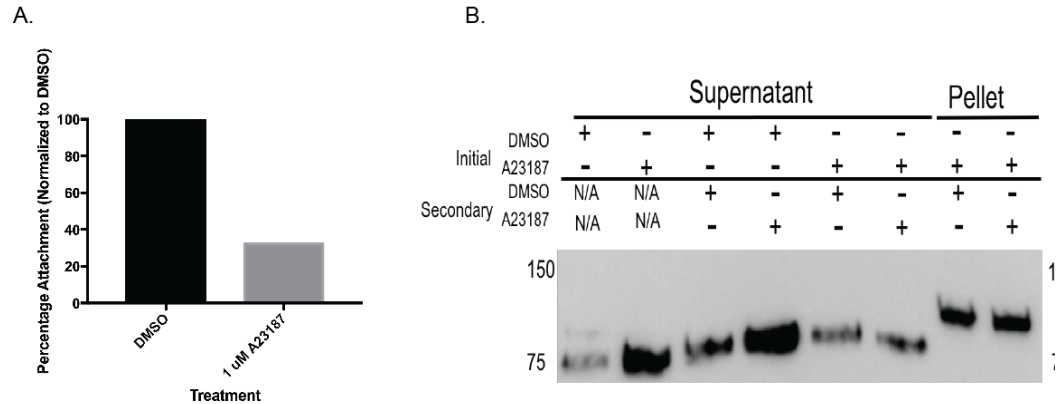


Figure 4.1 Ionophore treatment of extracellular parasites causes a decrease in host cell attachment and microneme secretion.

(A) RH Δ *hxgprt* parasites treated with 1 μ M ionophore A23187 show decreased ability to attach to host cells as compared to DMSO treated control parasites. (B) Western Blot analysis of MIC2 secretion after extracellular treatment of parasites with either DMSO or 1 μ M A23187 for one hour. Supernatants containing secreted proteins were separated by centrifugation before submitting parasites to a second treatment with either DMSO or 1 μ M A23187. Micronemal secretion was assessed by Western blot analysis of the supernatants using a mouse monoclonal antibody directed against MIC2 (Wan et al, 1997).

parasite. Defining the consequences of iiDeath treatment on wild-type parasites can help to clarify the phenotype by which the GRA41 mutant, MBD2.1, was originally isolated. Though A23187 is capable of transporting calcium, it can also transport other divalent cations. These divalent cations are exchanged for protons, meaning this process is also pH-dependent (Reed and Lardy 1972). Here, I have shown that the iiDeath treatment results in parasite death as a result of decreased

attachment and micronemal secretion. Since micronemal secretion (and subsequently attachment) is triggered by a calcium increase in the parasite cytosol, these results suggest that the iDeath phenomenon is a result of A23187's ability to transport calcium, rather than changes in pH or the transport of a different divalent cation. This supports the hypothesis that GRA41 could be impacting parasite sensitivity to iiDeath by a calcium-dependent mechanism.

Complete knockout of *GRA41* leads to dysregulation of parasite calcium

Because GRA41 was initially identified as a result of a forward genetic screen involving altered sensitivity to treatment with calcium ionophore, and its complete knockout led to defects in events known to depend on calcium homeostasis and fluxes, I wanted to compare free cytosolic calcium levels in knockout and complemented strains with the parental (Figure 4.2, below). For this purpose, we collaborated with Silvia Moreno's laboratory at the University of Georgia; all calcium experiments were conducted by a graduate student of Dr. Moreno's, Karla Marquez-Nogueras. To measure free cytosolic calcium within the parasites, extracellular parasites of the parental, *GRA41* knockout and complemented strains were loaded with fluorescent calcium indicator Fura-2 and fluorescence measurements were made before and after adding calcium to the suspension buffer. Compared to the parental strain, the knockout has elevated cytosolic calcium under calcium-free buffer conditions, which is not rescued by complementation with wild-type GRA41 (Figure 4.2, below). This suggests that the elevated free cytosolic calcium might not be a direct consequence of the loss of GRA41. Instead it could be either part of the way the parasites adapt to its loss or

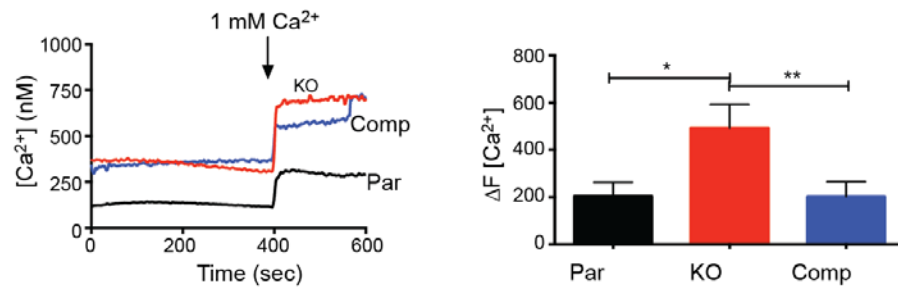


Figure 4.2 *GRA41* knockout parasites exhibit enhanced uptake of extracellular calcium.

Extracellular parasites from the parental, knockout and complemented strains were loaded with Fura-2 AM to monitor calcium levels. The arrows represent the time at which 1 mM Ca^{2+} was spiked in to the medium. Increase in calcium levels after addition of extracellular calcium over basal levels was quantitated for at least three independent replicates, trace shown is the average of three independent experiments. Error bars represent standard deviation. Asterisk denotes statistical significance based on the results of an unpaired Student's t-test with a p-value of <0.05 , double asterisks denotes p value of <0.01 . Calcium measurements conducted by Karla Marquez-Noguera, Moreno Laboratory, University of Georgia.

an unrelated event. However, when the ability of parasites to uptake extracellular calcium was measured by adding 1mM $CaCl_2$ to the buffer, the knockout strain showed a 2.45-fold increase in uptake of extracellular calcium over both the parental and complemented strains (Figure 4.2, above, $p < 0.05$). Thus, these results suggest that the loss of *GRA41* leads to a dysregulation of parasite calcium, which likely has wide-reaching impacts on calcium-dependent events in the lytic cycle.

Complete knockout of *GRA41* disrupts vacuolar morphology

During the lytic cycle analysis described in Aim 1 Results, consistent differences in the organization of parasites within the vacuole and the gross morphology of the vacuole membrane between the knockout and parental strain

were seen, suggesting a role of GRA41 to maintain normal vacuolar morphology. To investigate the possibility that the loss of GRA41 disrupted vacuolar morphology, I visualized the parasites under high power magnification and noted that many of the vacuoles in the knockout strain appeared to be collapsed around the parasites within (Figure 4.3A, below). Quantitation of this “collapsed vacuole” phenotype showed it was significantly more common in the *GRA41* knockout strain as compared to the parental and complemented strains ($43\pm 1\%$ versus $10\pm 6\%$ and $10\pm 4\%$, respectively, $p < 0.05$, Figure 4.3B, below). Furthermore, I noted that the vacuoles in the knockout strain were more likely to have atypical numbers of parasites. Typically, all parasites within the vacuole divide simultaneously into two daughter parasites leading to a doubling of parasite number and a geometric sequence of parasite number within each vacuole (i.e. 2, 4, 8, 16, etc.). Nonetheless, $35\pm 2\%$ of the knockout vacuoles contained a number of parasites that did not follow the normal pattern. This was significantly higher than both the parental and complemented strains, with $12\pm 3\%$ and $7\pm 2\%$ respectively (Figure 4.3C, below, $p < 0.05$). To investigate how this might be occurring, both parental and *GRA41* knockout parasites were stained for acetyl tubulin. The acetylation of tubulin occurs during parasite replication and can be used to visualize the daughter parasites as they are dividing (Varberg, Padgett et al. 2016). Using this method, I was able to image *GRA41* knockout parasites that showed evidence of more than two daughters forming per mother parasites, which would explain the abnormal number of parasites in some vacuoles (Figure 4.3D, below). The formation of

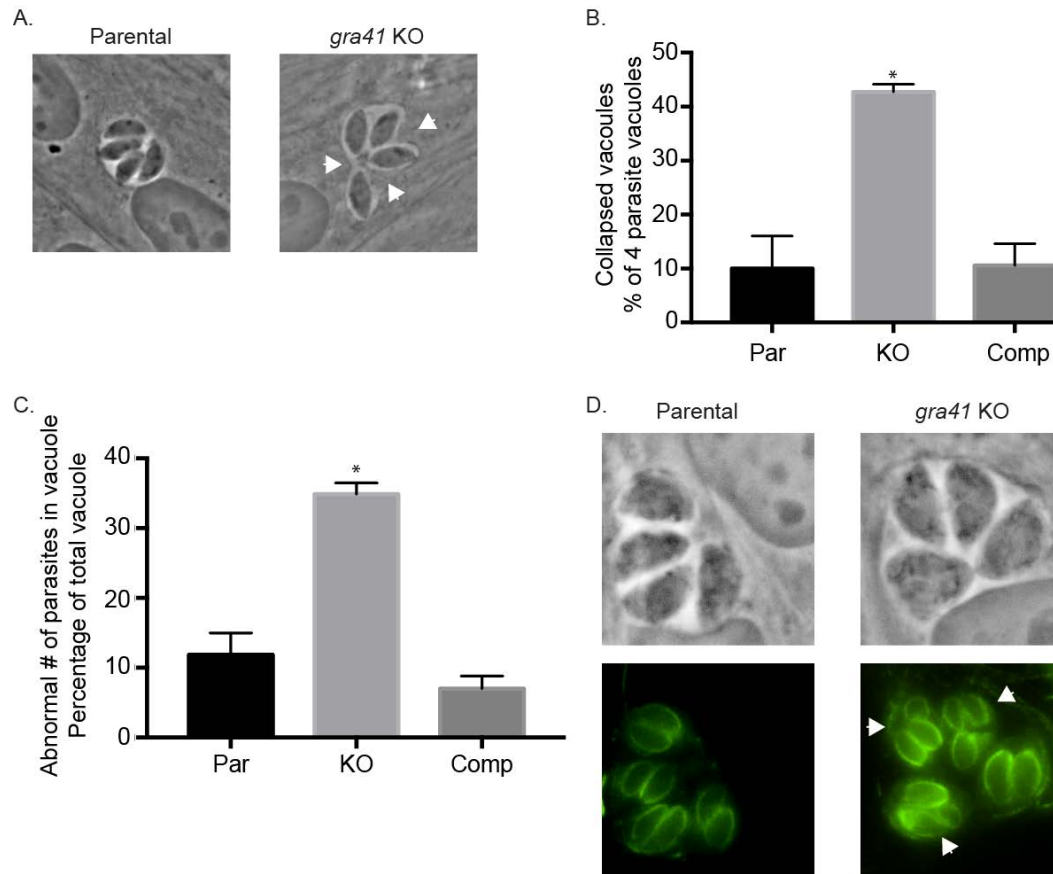


Figure 4.3 *GRA41* knockout parasites have altered vacuole morphology and division pattern.

(A) Intracellular parasites of the parental, knockout and complemented strains were fixed and imaged at 24 hours post infection. White arrowheads indicate the collapsed appearance of a vacuole around the parasites in parasites of the knockout strain. (B) Vacuoles from the parental, knockout and complemented strains containing four parasites each were assessed for the “collapsed vacuole” phenotype. Bars are average of three independent experiments and errors bars represent standard deviation. Asterisk denotes statistical significance based on the results of an unpaired Student’s t-test with a p-value of <0.05. (C) Vacuoles from the parental, knockout and complemented strains were fixed at twenty-four hours post infection. Vacuoles with an abnormal number of parasites (i.e. not 2, 4, 8 or 16) were quantified for each strain. Bars are average of three independent experiments and errors bars represent standard deviation. Asterisk denotes statistical significance based on the results of an unpaired Student’s t-test with a p-value of <0.05. (D) Intracellular parasites of the parental and knockout strains were stained with an antibody against acetylated tubulin to visualize dividing parasites. Arrows

show three daughter parasites for a single mother parasite in the knockout strain. triplet and even quadruplet parasites has been observed in wild-type parasites at low levels (Hu, Mann et al. 2002), suggesting that the knockout of *GRA41* has increased the frequency with which this happens.

Complete knockout of *GRA41* leads to altered structure of the tubulovesicular network

The “collapsed vacuole” and abnormal cell division are both similar to the abnormal vacuole morphology and parasite organization associated with the genetic disruption of *GRA2*, another secreted protein that localizes to the TVN and that is critical for its formation (Mercier, Dubremetz et al. 2002). Accordingly, I examined the structure of the TVN in the *GRA41* knockout strain by transmission electron microscopy (Figure 4.4, below). Host cells were infected with freshly egressed tachyzoites for twenty-four hours prior to fixing and preparing samples for thin sectioning. Thin sectioning and imaging were done with the assistance of Dr. Barry Stein of the Indiana University-Bloomington Electron Microscopy Core Facility. The parental, knockout and complemented strains all showed normal morphology of the PV membrane, but the knockout strain appeared to have fewer tubules within its network and an increase in the small vesicles from which the tubules form (Figure 4.4, below). Additionally, the tubules that do form in the TVN of the knockout strain appeared to be shorter than those of the parental and complemented strains (Figure 4.4, below). Since the *GRA41* knockout showed similar disruption of the tubulovesicular network with the *GRA41* knockout, I tested

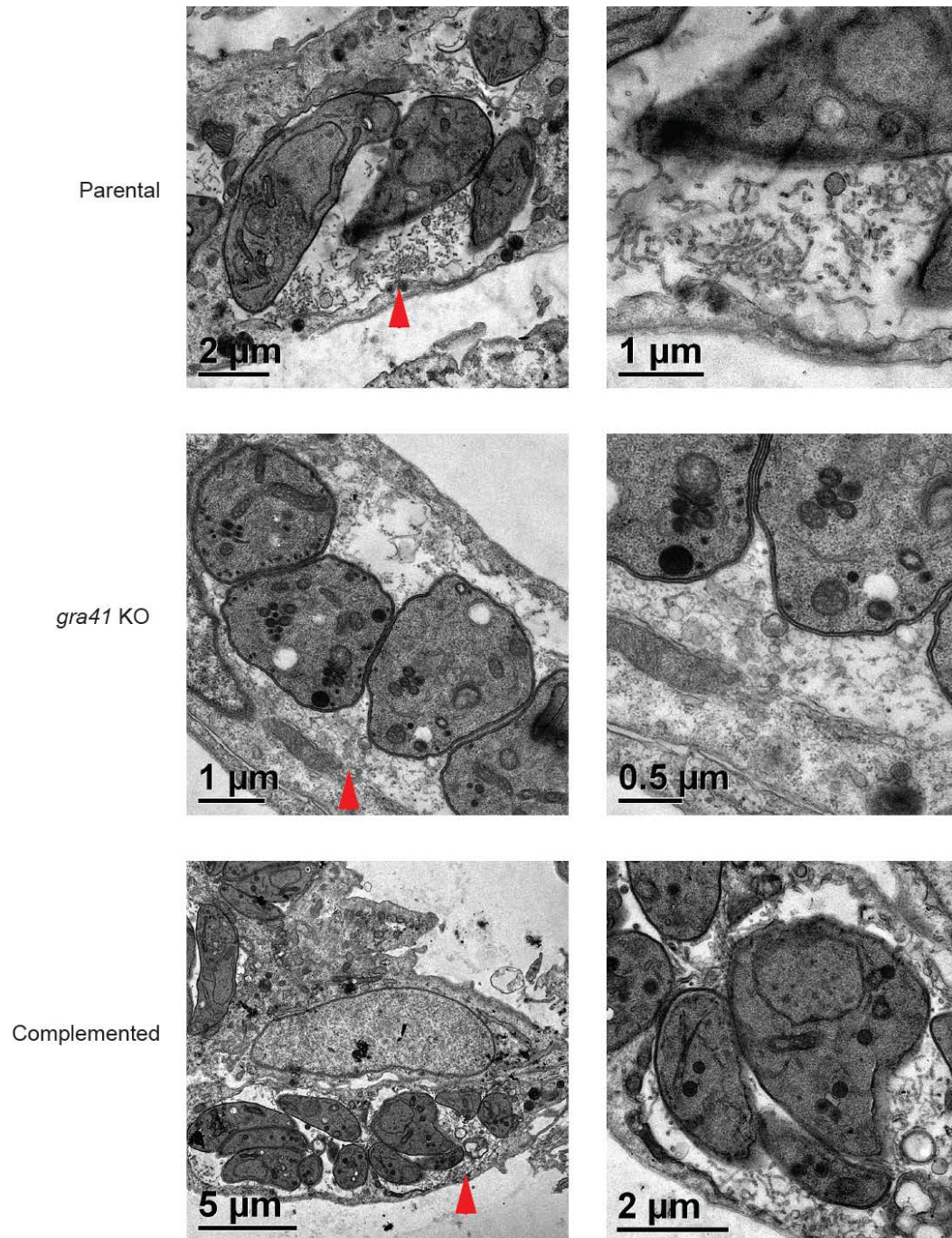


Figure 4.4 *GRA41* knockout parasites show altered morphology and size of tubulovesicular network (TVN) as compared to the parental and complemented strains. Intracellular parasites were fixed at 24 hours post infection and prepared for imaging. Red arrowheads in left panels point at regions were imaged at higher magnification in the respective right panels.

to determine whether the *GRA2* knockout (parental, knockout and complemented strains graciously provided by Dr. Vern Carruthers, University of Michigan) would mirror the resistance to iiDeath treatment of the *GRA41* knockout. In contrast to the *GRA41* knockout, the *GRA2* knockout did not show any increased survival over its parental and complemented strains at either 45 or 60 minutes of treatment (32±10% versus 26±4% and 30±13% at 45 minutes, respectively and 17±17% versus 12±7% and 18±14% at 60 minutes, respectively, $p>0.05$, Figure 4.5, below), suggesting that this phenomenon is restricted to the disruption of *GRA41* and not a general feature of parasites with disrupted tubulovesicular networks.

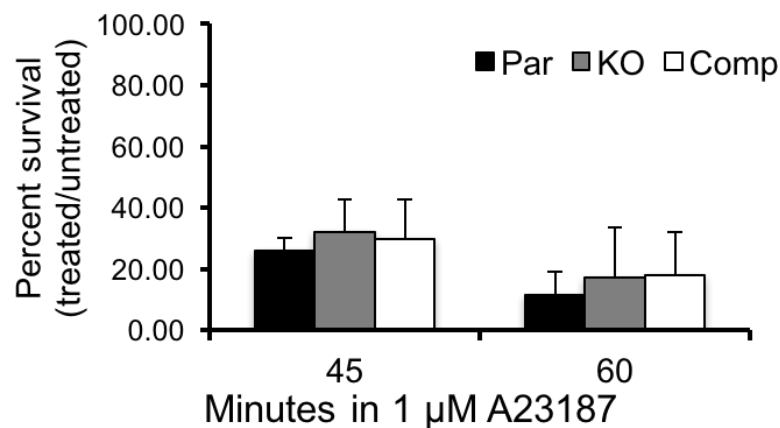


Figure 4.5 Ionophore induced death phenotype of *Gra2* parental, knockout and complemented strains.

Percent survival of parasites treated with 1 μ M A23187 versus DMSO solvent control for 45 or 60 minutes. Average of three independent replicates. Error bars represent standard deviation.

Incubation of recombinant *GRA41* with calcium does not affect protein melting temperature

To address question of whether *GRA41* binds calcium and impacts calcium homeostasis in this way, I isolated recombinant Histidine-tagged Tg*GRA41* from transfected *E. coli* cells with the assistance of Dr. Sanofar Abdeen (Johnson

Laboratory, Indiana University School of Medicine). Purified GRA41 was incubated with varying concentrations of CaCl_2 and subjected to a melt curve analysis using SYPRO Orange Dye. This technique, termed differential scanning fluorimetry, utilizes the capability of SYPRO orange dye to bind to the unfolded hydrophobic regions of denatured proteins. Once bound, the SYPRO orange dye will fluoresce; the intensity of this fluorescence is directly related to the portion of the protein that is unfolded. In this way, the samples can be subjected to a melt curve analysis using a real-time PCR machine and melting temperatures can be calculated. The addition of a ligand to the protein/dye combination will shift the melting

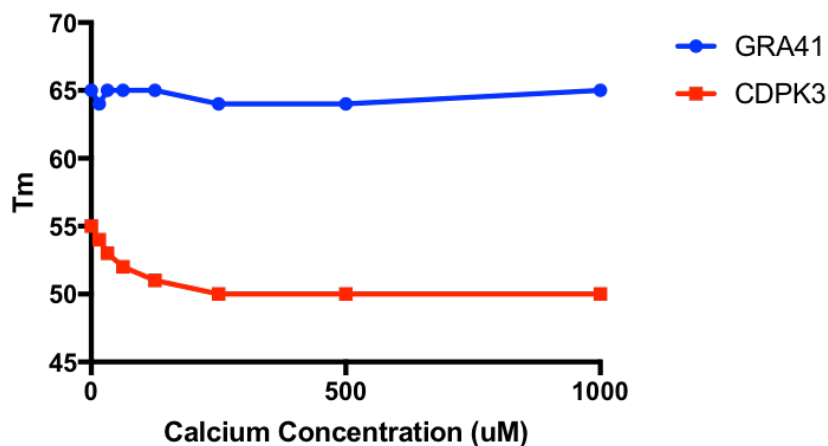


Figure 4.6 Melt curve analysis of GRA41 recombinant protein incubated with calcium

When recombinant GRA41 is incubated with varying concentrations of CaCl_2 there is no apparent difference in the melting temperature of protein incubated in the presence of calcium. The Calcium-Dependent Kinase 3 (CDPK3), shows an inverse relationship between calcium concentration and melting temperature.

temperature, with increasing amounts of ligand causing increasingly larger shifts (Niesen, Berglund et al. 2007). In contrast to recombinant CDPK3, which contains calcium binding EF hand domains, GRA41 does not show any change in melting

temperature when calcium is added to the sample, suggesting that the recombinant protein is not capable of binding calcium. Though this does not rule out the possibility that GRA41 is capable of binding calcium under certain circumstances, it suggests that it does not form a strong interaction with calcium at the concentrations tested that is detectable using this assay.

Attempts to identify interactors of GRA41 by immunoprecipitation yield inconsistent results

To begin to understand the mechanisms by which GRA41 might be functioning, I performed a traditional co-immunoprecipitation using the Type I endogenously HA-tagged strain to identify potential protein interaction partners. Due to its location in the parasitophorous vacuole, intracellular parasites were harvested along with the host cells and parasitophorous vacuoles by scraping and

Gene ID (ToxoDB.org)	Product Description (ToxoDB.org)	Computed Gene Ontology Function (ToxoDB.org)	Expect Value
TGME49_227280	dense granule protein GRA3	None	2.70E-05
TGME49_217460	glutamyl-tRNA synthetase (GlnRS)	ATP binding, glutamine-tRNA ligase activity	1.80E-04
TGME49_219540	tRNA-Ala synthetase	ATP binding, alanine-tRNA ligase activity, nucleic acid binding	2.40E-04
TGME49_299810	cysteine-tRNA synthetase (CysRS)	ATP binding, cysteine-tRNA ligase activity	2.40E-04
TGME49_233460	SAG-related sequence SRS29B	None	2.70E-04
TGME49_291960	rhoptry kinase family protein ROP40 (incomplete catalytic triad)	transferase activity, transferring phosphorus-containing groups	5.70E-04
TGME49_236210	peptidase M16 family protein, putative	catalytic activity, metal ion binding, metalloendopeptidase	6.20E-04

		activity, zinc ion binding	
TGME49_233480	SAG-related sequence SRS29C	None	6.60E-04
TGME49_251500	eukaryotic initiation factor-3, subunit 3, putative	protein binding	9.30E-04
TGME49_308090	roptry protein ROP5	ATP binding, protein kinase activity	0.001
TGME49_309730	thioredoxin reductase	NADP binding, flavin adenine dinucleotide binding, glutathione-disulfide reductase activity, thioredoxin-disulfide reductase activity	0.001
TGME49_219550	dihydrolipoyllysine-residue succinyltransferase component of oxoglutarate dehydrogenase	dihydrolipoyllysine-residue succinyltransferase activity	0.0011
TGME49_290700	hypothetical protein	None	0.0014
TGME49_319340	hypothetical protein	None	0.0015
TGME49_295110	roptry protein ROP7	ATP binding, protein kinase activity	0.0017
TGME49_251540	dense granule protein GRA9	None	0.002
TGME49_309590	roptry protein ROP1	None	0.0051
TGME49_279100	hypothetical protein	None	0.016
TGME49_297650	Ser/Thr phosphatase family protein	acid phosphatase activity, hydrolase activity	0.02
TGME49_226380	hypothetical protein	None	0.022
TGME49_215775	roptry protein ROP8	ATP binding, protein kinase activity	0.027

Table 4.1 Proteins identified following immunoprecipitation of GRA41 from whole cell lysates

Proteins are ranked by expect value, from smallest to largest. resuspending in lysis buffer. The samples were further solubilized by sonication before the lysates were incubated with anti-HA antibody. After the antibody was allowed to bind to the GRA41 HA epitope tag, the entire antibody/antigen complex

was pulled out of the lysate using Protein G-coupled dynabeads, which bind to the anti-HA antibody. The beads were washed and the contents eluted in sample buffer before performing an SDS-PAGE separation and silver stain of the resultant gel. After successful detection of bands at the correct molecular weight for the GRA41 doublet observed by Western Blot analysis, three regions with significant silver staining were excised and sent to the Indiana University Bloomington Mass Spectrometry core facility for protein identification. The resulting protein list was restricted to proteins not found in unrelated pulldowns (LaFavers and Arrizabalaga, unpublished data), those which contained a signal peptide and those which had an expect value of <0.0025 . These proteins are listed from most to least likely in Table 4.1, above. Of these proteins, only two are known dense granule proteins, GRA3 and GRA9. Of the remaining proteins, five are known rhoptry proteins and two are surface antigens. The remaining proteins are a mixture of proteins of hypothetical function and uncharacterized proteins that have conserved functional domains, such as a putative glutamyl-tRNA synthetase. Additional efforts to repeat these results were met with little success, as mass spectrometry analysis of both prior and subsequent GRA41 pulldowns with samples submitted on magnetic beads failed to identify GRA41 as a hit in the data analysis and were disregarded. Due to these difficulties, a yeast two-hybrid approach was taken to identify GRA41 candidate interactors.

GRA41 has several high confidence interactions in yeast two hybrid screen

A yeast two hybrid screen was conducted by Hybrigenics Services using the GRA41 sequence with the signal peptide removed as a protein bait. Resulting

interactors were scored for statistical significance and ranked according to expected values that take into account results from the GRA41 screen along with all other screens against the *T. gondii* prey library. They are then assigned a global predictive biological score from A (interactions with very high confidence) to F (experimentally proven technical artifacts). Included in the table below are prey proteins with a score of A, B (high confidence) and C (good confidence). Prey with scores of D (moderate conference), E (interactions involving highly connected prey domains, likely non-specific), and F were not included. Also removed were common hits from unrelated nuclear proteins used as bait by the Sullivan laboratory and an unrelated mitochondrial protein used as bait by the Arrizabalaga lab against the same database (Garbuz, Harris, Huang, Srivasta, Arrizabalaga, and Sullivan, unpublished data). The remaining hits included 11 proteins, three

ToxoDB.org Gene ID	Global PBS	Product Description (ToxoDB.org)	Signal Peptide	# TM Domains	Predicted Localization (psort)
TGME49_270800	A	GAF domain-containing protein	Yes	0	Nuclear/mitochondrial
TGME49_202680	A	peptidase M16, alpha subunit, putative	Yes	0	Mitochondrial
TGME49_202370	A	T-complex protein 1, epsilon subunit (TCP-1-epsilon), putative	No	0	N/A
TGME49_270250	B	dense granule	Yes	0	Extracellular

		protein GRA1			
TGME49_2517 80	B	heat shock protein	Yes	0	Mitochondrial
TGME49_2204 80	B	hypothetical protein	Yes	0	Nuclear, plasma membrane or extracellular
TGME49_2236 80	B	ubiquitin family protein	No	0	N/A
TGME49_2334 90	C	hypothetical protein	No	0	N/A
TGME49_2858 30	C	hypothetical protein	No	2	N/A
TGME49_2441 10	C	nucleosome assembly protein (nap) protein	No	0	N/A
TGME49_3063 50	C	variable surface lipoprotein	No	0	N/A

Table 4.2 GRA1 Potential Interactors from Yeast Two Hybrid Analysis

Proteins are ranked by global predictive biological score (PBS) from highest confidence interactions to lowest confidence interactions. TM = transmembrane Yeast Two Hybrid Analysis conducted by Hybrigenics Services.

with a score of A, and four each with scores of B and C (Table 4.2, above). Of these, five have predicted signal peptides, suggesting they could be secreted into the parasitophorous vacuole with GRA1. One of the proteins with a signal peptide is the founding member of the dense granule family, GRA1, which is a highly abundant protein secreted into the parasitophorous vacuole. Interestingly, GRA1 has been shown to be capable of binding calcium *in vitro*, though the exact function of this protein is unknown due to the lack of a published knockout (Cesbron-Delauw, Guy et al. 1989). Of the remaining hits containing signal peptides, only one is predicted to be potentially secreted according to Psort, a protein of

hypothetical function with the gene ID TGME49_220480, which lacks sequence homology to any proteins of known function. The remaining proteins are either predicted to be trafficked to other locations within the cell, such as the mitochondrion or nucleus, or do not contain a signal peptide. If these predicted localizations are accurate, it is unlikely that GRA41 would ever encounter these proteins within the parasite.

Using a combination of co-immunoprecipitation and yeast two-hybrid analysis, I have generated a list of potential GRA41 interactors. Future studies should focus on verifying potential interaction partners and using genetic approaches to determine their impact on the phenotypes associated with the loss of GRA41.

Chapter 5 : Characterization of GRA41 During Parasite Differentiation

T. gondii parasites circulating in North American and Europe are composed of many different strains belonging to three distinct clonal lineages. Historically, the majority of human infections have been caused by Type II strains, with a minority of infections caused by either the Type I or Type III strains. Type III strains are common causes of animal infection, while overall rates of infection with the highly virulent Type I strain are low in both humans and animals (Howe and Sibley 1995). Of the three strains, the highly virulent Type I strain, RH, and the moderately virulent Type II strain, Prugniaud (Pru) are commonly used to study parasites in tissue culture and mouse models of infection. The RH strain is highly virulent in mice, with a single parasite capable of causing mortality during the acute phase of the disease (Johnson, McDonald et al. 1979), making it a useful model to investigate the tachyzoite lytic cycle and identify key virulence factors. The Pru strain is capable of spontaneously switching from the rapidly replicating tachyzoite form to the slow-growing, tissue cyst-forming bradyzoite stage under normal culture conditions (Soete, Fortier et al. 1993) or using high pH stress conditions (Soete, Camus et al. 1994). The high switching efficiency of the Pru strain, combined with relatively modest virulence in the mouse model (few mice succumb to the acute stage of infection if doses are kept below 10^5 /mouse, Figure 5.3) makes it ideal for studying the tachyzoite to bradyzoite switch and the chronic stage of the infection *in vivo*.

The initial characterization of TgGRA41 was performed in a derivative of the RH strain of *T. gondii*, allowing for a complete characterization of this protein's role

during the tachyzoite lytic cycle. However, to determine the role of TgGRA41 in the bradyzoite stage of infection, I utilized the Pru strain to facilitate our analysis of this stage. To do this, I endogenously tagged TgGRA41 in the Pru strain as described for the RH strain to determine if TgGRA41 is expressed during the bradyzoite stage of development and to analyze its localization at this time. I then generated a knockout of the TgGRA41 in the Pru strain in order to determine the impact of its loss during bradyzoite development and *in vivo* infection.

TgGRA41 is expressed in a Type II strain and localizes to the wall of bradyzoite tissue cysts

In order to confirm that GRA41 is expressed in tachyzoites and bradyzoites of a Type II strain, sequences encoding a carboxy-terminal (C-terminal) triple-hemagglutinin (HA) tag were introduced into the endogenous locus in the Pru Δ Ku80 Δ hxgprt strain just before the stop codon, using a previously described approach (Fox, Falla et al. 2011). Western blot analysis of protein extract from the endogenously tagged strain revealed a single band migrating at approximately 20-25 kDa, which is approximately the same size as the predicted molecular weight of the tagged protein, 24 kDa (Figure 5.1A, below).

Since the doublet pattern found in Type I parasites (Figure 3.3A, above) was not visible in the Type II strain, I conducted a sequence alignment using Clustal Omega of the predicted protein sequences for Type I and Type II strains (ToxoDB.org) to determine if any polymorphisms could account for the differences in the banding patterns between the two strains (Figure 5.1B, below). Overall, there is high identity between the two sequences (97%), with only 6 amino acids differing

between the two protein sequences. These include a cysteine at position 12 of the Type I sequence that is a tryptophan in the Type II strain, two glutamic acids at positions 124-125 that are glycines in the Type II strain, a serine at position 134

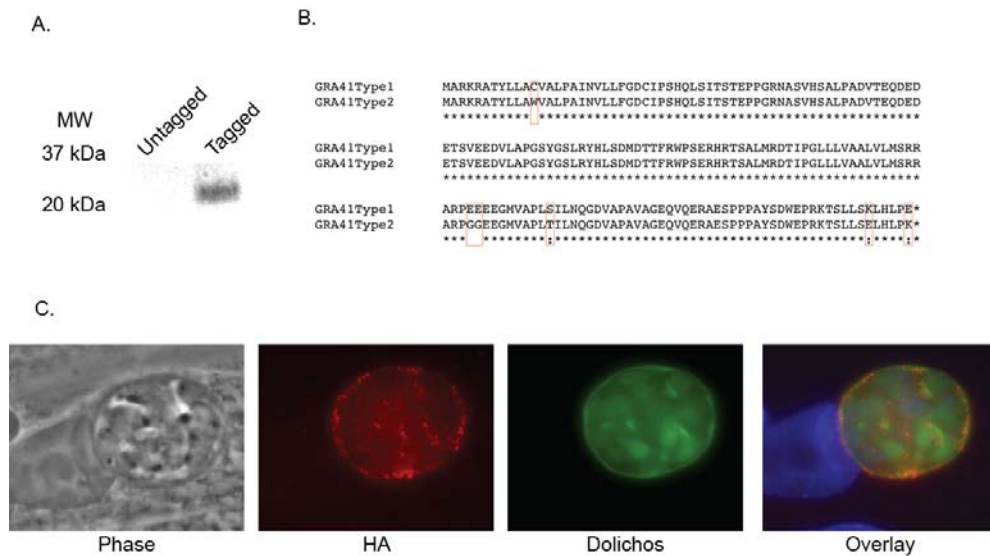


Figure 5.1 GRA41 is expressed in a type II strain and localizes to the wall of bradyzoite tissue cysts

(A) GRA41 was tagged at the endogenous locus with a triple hemagglutinin tag in the Type II strain, Pru Δ Ku80. Western Blot analysis of the tagged line compared to the untagged parental with an antibody directed against the hemagglutinin tag shows a single protein of slightly over 20 kDa in the tagged line only. (B) Clustal Omega alignment of the predicted protein sequences of the Type I and Type II strains with differences between the sequences boxed in red. (C) Immunofluorescence analysis of the GRA41 hemagglutinin tagged line after conversion to bradyzoites (7 days of pH stress). HA = hemagglutinin, *Dolichos* = *Dolichos biflorus* agglutinin, Overlay = merge of HA, *Dolichos* and DAPI (DNA) channels.

that is a threonine in the Type I strain, a lysine at position 174 that is a glutamic acid in the Type II strain and a glutamic acid in the final position 179 that is a lysine in the Type II strain. Many of these are potential candidates for post-translational modifications that could impact the electrophoretic mobility of the protein by SDS-PAGE analysis.

The localization of GRA41 in a bradyzoite tissue cyst was then examined by immunofluorescence microscopy conducted after tachyzoites were converted to bradyzoite cysts by 7 days of pH stress with CO₂ deprivation. GRA41 protein was visualized by probing with an antibody directed against the hemagglutinin tag of the endogenously tagged strain. The cyst wall of the bradyzoite was visualized by staining with Fluorescein-conjugated DBA; individual bradyzoites are also shown in the green channel due to the presence of a GFP-encoding gene under the control of the bradyzoite-specific LDH2 promoter that is stably integrated into the Pru Δ ku80 Δ hxgprt strain (Cleary, Singh et al. 2002). Organelles containing DNA (i.e. nucleus, apicoplast) are stained with DAPI. As expected for a dense granule protein that is localized to the vacuole in tachyzoites, GRA41 is enriched in the cyst wall of the newly formed bradyzoite tissue cyst (Figure 5.1C, above).

Knockout of *GRA41* in a Type II Strain recapitulates resistance to ionophore induced death

To further study the role of GRA41 in the bradyzoite stage of the parasite, I generated a knockout of the gene by replacing the entire coding sequence with the selectable marker hypoxanthine-guanine phosphoribosyltransferase (HXGPRT) through double homologous recombination into the Pru Δ ku80 Δ hxgprt parental strain, hereafter referred to as Pru Δ ku80 (Fox, Falla et al. 2011) (Figure 5.2A, below). Parasites transfected with the knockout vector (pGRA41KO) and stably expressing HXGPRT were selected by resistance to mycophenolic acid and xanthine and cloned by limiting dilution. Clones were imaged live on a Leica inverted DMI6000B microscope to determine whether or not they were expressing

GFP. Since a GFP expression cassette is present within the pGRA41KO vector but is downstream of the 3' flanking region, any GFP positive parasites are likely to be the result of integration of the construct by single homologous recombination rather than double homologous recombination. A single clone was isolated that was GFP negative out of over 150 clones screened, which was then shown to have correct integration of the construct by PCR (Figure 5.2B, below). Based on the nature of the genetic disruption expected from double recombination of the knockout construct (pGRA41KO, (Figure 5.2A, below)) the established clone represents a functional knockout and is unlikely to produce any GRA41 protein. I then assessed whether the complete knockout of *GRA41* in the Pru Δ *ku80* strain recapitulated the iiDeath⁻ phenotype seen in GRA41 truncation mutant MBD 2.1 and the GRA41 Type I knockout.

Pru Δ *ku80* Δ *gra41* showed statistically significant increases in survival as compared to the parental strain after 10 or 30 minutes of treatment with A23187 (87% \pm 5.5% versus 74% \pm 5.2% for the parental strain at ten minutes and 48% \pm 14% versus 28% \pm 13% for the parental strain at thirty minutes, $p < 0.05$, Figure 5.2C, below). Despite the differences in timing of the iiDeath phenotype as compared to the RH strain, which has been shown previously (Lavine, Knoll et al. 2007), the Pru Δ *ku80* Δ *gra41* recapitulates the decrease in sensitivity to ionophore induced death found in the type I knockout, suggesting that Gra41 likely plays a similar role in Type II strains as it does in Type I.

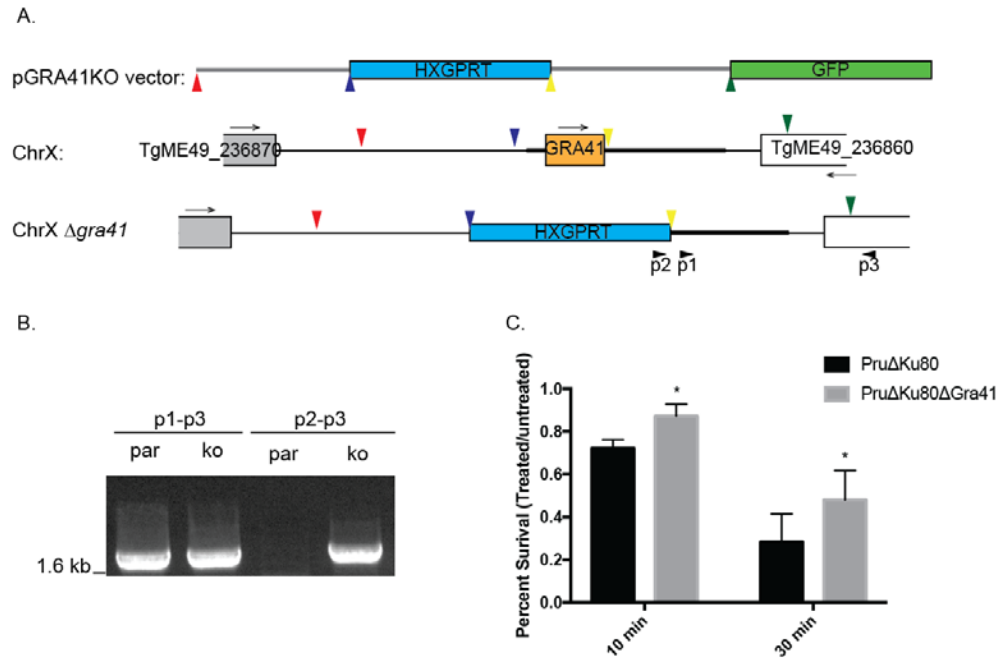


Figure 5.2 Complete knockout of *GRA41* in a Type II Strain recapitulates the iiDeath phenotype seen in Type I Knockout.

(A) Diagram shows strategy used to knockout *GRA41* by double homologous recombination replacing the *GRA41* locus with the HXGPRT selectable marker. Colored arrow heads indicate beginning and end of genomic regions used to drive homologous recombination of pGRA41KO vector with target locus in chromosome X (ChrX). Arrows indicate relative direction of transcription of the three genes depicted and black arrow heads represent primers p1, 2 and 3 used to corroborate integration. (B) PCR analysis of DNA from parental strain (par) and knockout (ko) using either a primer pair expected to produce an amplicon in both parental and knock strains (p1-p2, left panel) or a test primer pair that would produce a product only if the *GRA41* gene were replaced (p2-p3, right panel). (C) Extracellular parasites of the parental and knockout lines were exposed to 1 μ M A23187 for 10 or 30 minutes and survival rate was determined as in Fig. 1. Bars are average of three independent experiments and error bars represent standard deviation. Asterisk denotes statistical significance based on the results of an unpaired Student's t-test with a p-value of <0.05.

Preliminary Data on Impact of *GRA41* Loss on Tissue Cyst Development

Having established that *GRA41* plays a similar role in resistance to ionophore induced death in a type II strain as it did in a type I strain, I then utilized

the type II GRA41 knockout to determine the role GRA41 plays in the tissue cyst stage of the *T. gondii* life cycle. To do this, host cells were infected with parasites for 2-4 hours before using an established pH stress protocol to induced conversion to the bradyzoite stage (Weiss, Laplace et al. 1995). The pH stress media was replaced every two days and the cells were kept in a CO₂ deprivation incubator to ensure high rates of stage switching were achieved. Conversion to bradyzoites was measured utilizing rhodamine-conjugated DBA, which binds to glycosylated proteins in the bradyzoite cyst wall (Scholytyseck, Mehlhorn et al. 1974, Tomita, Bzik et al. 2013). Cells were fixed at four or seven days post infection to look for defects in tissue cyst formation or maintenance. A minimum of 100 vacuoles were scored as either DBA positive or negative. Small clusters of DBA negative vacuoles containing 1-2 parasites that appeared to have remained as tachyzoites, egressed and reinvaded nearby host cells were counted as a single DBA negative vacuole, since these parasites likely came from one original vacuole. Though there was no statistically significant difference in the percentage of DBA positive vacuoles between the parental and knockout strains at four days post infection (73%±16% and 53%±29% respectively, Figure 5.3A, below), there is a significant difference between the two strains at seven days post infection (75%±7% and 20%±12%, respectively, **, p<0.01), suggesting that the knockout parasites form bradyzoite cysts initially, but fail to maintain these bradyzoite cysts. Some of the cysts formed by the knockout parasites had lost cyst wall staining at seven days post infection, while many others had egressed and reinvaded, either as tachyzoites or bradyzoites.

To further investigate bradyzoite formation under *in vivo* conditions, female CBA/J mice were injected by Dr. Arrizabalaga with 10^3 , 10^4 or 10^5 parasites per mouse. Mice were allowed to progress from an acute infection to a chronic infection for 28 days before brains and blood were harvested by myself and Tamila Garbuz. The average number of tissue cysts per brain was measured by fixing and staining brain homogenate with rhodamine-conjugated DBA for visualization by fluorescent microscopy. Successful infection of mice containing no cysts was verified by testing mouse serum against *T. gondii* antigens by dot blot analysis. At a low dose (10^3 parasites/mouse), very few cysts were found in each mouse brain for both the parental and the knockout strain and no differences were seen between the two strains (Figure 5.3B, below). However, at a slightly higher dose (10^4 /mouse), the number of cysts is almost two-fold higher in the knockout as compared to the parental (91 cysts versus 39, $p < 0.1$, Figure 5.3B, below). Due to a relatively small sample size, this difference is not statistically significant for a cutoff of $p < 0.05$, but is trending toward statistical significance. At the highest dose (10^5 /mouse), the knockout strain showed highly variable results, with two of the mice not showing any evidence of cysts and two showing high numbers of cysts as compared to the parental strain (Figure 5.3B, below). It is not clear whether or not the lack of cysts in some of the mice at this dose is due to variability in the counting method (since only a small percentage of the total brain material is imaged), the failure of parasites to reach the brain or that cysts were too small and could not be imaged with the magnification used for counting. When combined with the *in vitro* switching

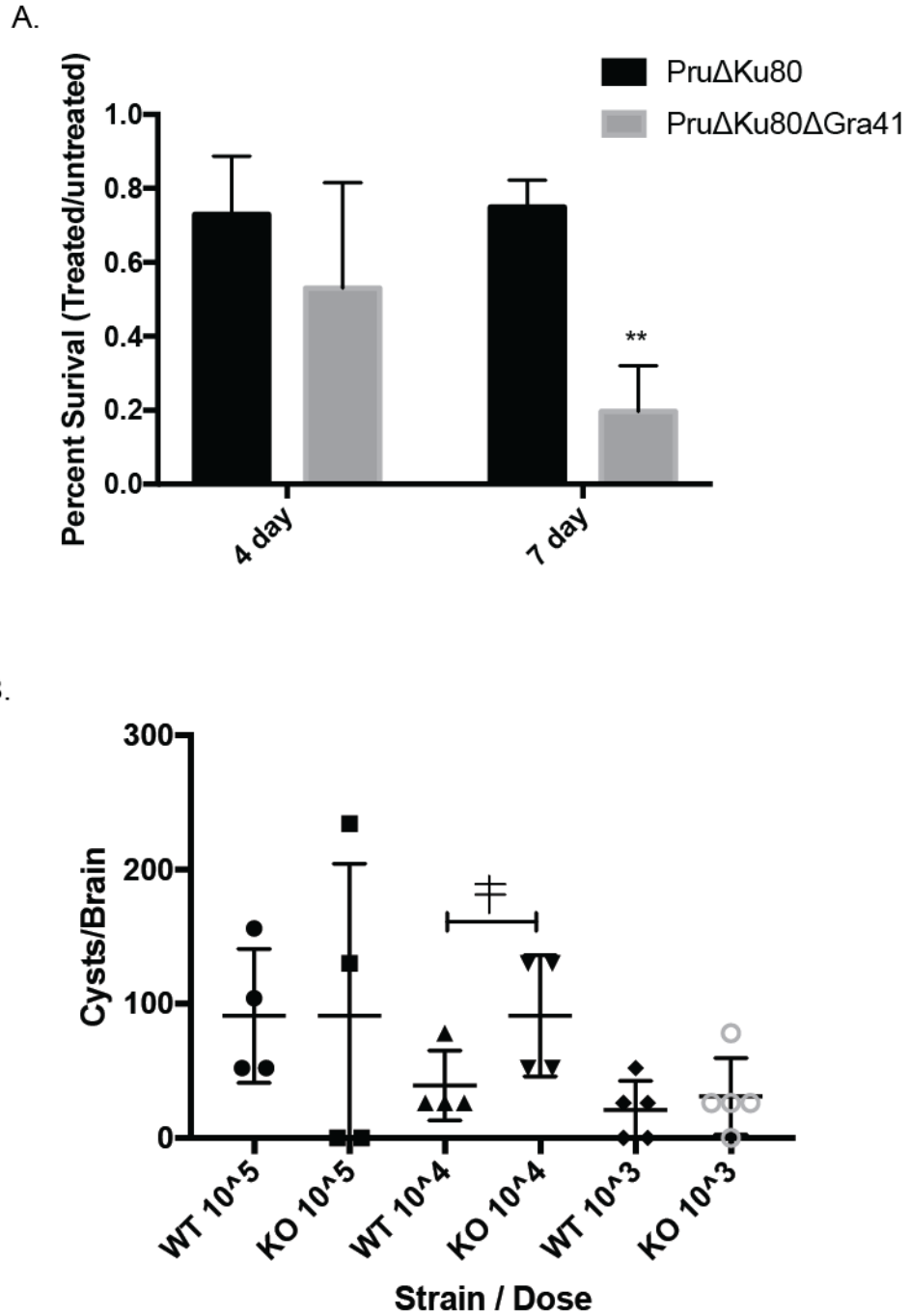


Figure 5.3 Differentiation of Type II Gra41 Knockout
 (A) Parental or GRA41 knockout parasites were allowed to form bradyzoite cysts under pH stress for 4 or 7 days before parasites were fixed and cyst walls were stained using rhodamine-conjugated DBA. Bars are average of three independent experiments and error bars represent standard deviation. Double asterisk denotes statistical significance based on the results of an

unpaired Student's t-test with a p-value of <0.01. (B) Female CBA/J mice were infected with parental (WT) or GRA41 knockout (KO) parasites at the indicated doses and allowed to progress to chronic infection for 28 days before brains were harvested and cysts counted following staining with rhodamine-conjugated DBA. Individual mice are presented as data points in each treatment and error bars represent standard deviation. ‡ denotes statistical significance based on the results of an unpaired Student's t-test with a p-value of <0.1.

data, the *in vivo* cyst formation data suggests that the bradyzoite cysts from the knockout strain may have a defect in maintenance, leading to their reconversion to tachyzoites, which then invade additional host cells and lead to the formation of more cysts. However, without conducting an analysis at multiple time points during bradyzoite infection with additional animals, the exact interpretation remains unclear.

Chapter 6 : Discussion

Calcium-dependent signaling is central to the propagation of parasites of the phylum Apicomplexa, including the causative agent of malaria, *Plasmodium falciparum*, and the opportunistic pathogen *T. gondii*. Calcium-dependent events underlie the motility, invasion, and egress of these parasites and thus calcium homeostasis and fluxes are tightly controlled. Calcium signaling is proposed to be an attractive drug target for controlling these parasitic infections, due to its essential nature and uniqueness from vertebrate calcium-dependent signaling pathway. While many of the effectors of calcium that drive events of the lytic cycle in both *Plasmodium* species and *T. gondii* have been identified, much remains unknown about how these calcium fluxes are regulated. In an effort to address this knowledge gap our lab has used a forward genetics approach to identify genes that influence *T. gondii*'s sensitivity to calcium fluxes, specifically those induced by the calcium ionophore A23187. Surprisingly, I have discovered that a secreted protein, which resides within the parasitophorous vacuole during parasite intracellular growth, influences several calcium related events in both intra and extracellular parasites. These results suggest a role for PV proteins in the regulation of calcium homeostasis, timing of egress, and parasite division. Additionally, preliminary results investigating the impact of this protein on bradyzoite tissue cyst formation suggest this protein is also required for normal cyst maintenance.

The novel dense granule protein GRA41 was first identified through the sequencing of a mutant resistant to extracellular exposure to the ionophore

A23187. Normally, exposure to this calcium ionophore for over thirty minutes renders extracellular parasites non-invasive, which, for this obligate intracellular parasite, results in death. While this phenomenon, known as ionophore induced death (iiDeath), has been known and exploited for decades (Mondragon and Frixione 1996, Black, Arrizabalaga et al. 2000), the underlying mechanism is not well understood. It has been proposed that prolonged exposure to elevated calcium, which normally induces secretion of adhesive molecules required for invasion, exhausts the contents of the secretory organelles that harbor such proteins. Other plausible mechanisms include toxic effects from elevated cytoplasmic calcium levels, and changes to the calcium sensitivity of the molecules and machinery that regulate secretion. I have actually detected that following a one-hour ionophore exposure, the levels of micronemal proteins do not change compared to untreated parasites but the ability to elicit micronemal secretion upon subsequent ionophore exposure is significantly affected (Figure 4.1, above). This observation would indicate that iiDeath is not merely the consequence of the exhaustion of proteins to be secreted, but of an alteration in the sensitivity to calcium, which would lead to a reduction in active secretion. In this context, I hypothesize that the resistance to iiDeath of the parasites lacking GRA41 is due to an altered sensitivity to the ionophore, brought upon by the clear changes in calcium regulation detected in the *GRA41* knock out strain. Indeed, the *gra41* mutant strain (MBD2.1) is over-sensitive to the effects of calcium chelation by BAPTA-AM (Mondragon and Frixione 1996, Black, Arrizabalaga et al. 2000). It is not yet clear whether the altered calcium regulation exhibited by the *GRA41*

knockout strain is due to a direct effect of lack of GRA41 or an indirect consequence of how the parasites adapt to the loss of GRA41. The latter explanation is supported by the observation that the mutant strain has an elevated level of cytosolic calcium that is not corrected by genetic complementation. Nonetheless, lack of GRA41 does seem to affect calcium regulation as the mutant parasites exhibited dysregulated calcium uptake, a phenotype that is reverted by complementation. While I have yet to elucidate the exact mechanism by which the knockout parasites are adapting, I have observed that the premature egress phenotype is very stable during culture, suggesting that the mutant and knockout strains could adapt to this change in egress timing by modifying one of the other steps in the lytic cycle (i.e. increasing attachment) which is also dependent on calcium signaling processes. Though it is difficult to determine the specific function of GRA41, the calcium uptake defect of extracellular parasites suggests that GRA41 is involved in regulating calcium homeostasis. Higher levels of cytosolic calcium and increased rates of calcium uptake by extracellular parasites shows how the parasites respond to the loss of GRA41.

How a protein that resides outside of the parasite but within the parasitophorous vacuole might affect calcium regulation within the cytoplasm of the parasite is puzzling, especially considering that some of the phenotypes related to its deletion, such as *iiDeath* resistance, manifest only once the parasites are extracellular. It is plausible that the protein, which is in the dense granules before secretion, has a role within this organelle that influences calcium homeostasis in extracellular parasites. Nonetheless, there is no evidence that dense granules

accumulate significant amounts of calcium (Bonhomme, Pingret et al. 1993) or are involved in the regulation of calcium homeostasis or fluxes. It is also conceivable that GRA41, while in the PV, directly or indirectly influences the physiology of the vacuole, which in turns affects that of the parasite. In such a model, the absence of GRA41 would alter the physiology of the intracellular parasite and, once outside, these parasites would react differently to external stimuli such as the calcium ionophore.

Though the PV lumen has long been considered physiologically at equilibrium with the host cell through a nonselective pore (Schwab, Beckers et al. 1994), whose components were recently identified (Gold, Kaplan et al. 2015), several studies indicate that ionic concentration of the PV can vary in respect to that of the host cytoplasm during intracellular growth. For instance, measurements of calcium levels using non-ratiometric indicators in the PV have shown that calcium is concentrated in the PV relative to the host cell cytoplasm and the frequency of this calcium sequestration increases as egress approaches (Pingret, Millot et al. 1996). Interestingly, one of the most abundant PV proteins, GRA1, has been shown to bind calcium (Cesbron-Delauw, Guy et al. 1989), which suggests a potential mechanism for this calcium sequestration. The calcium concentration of the *Plasmodium* PV has been determined through the use of ratiometric indicators to be approximately 40 μ M, many fold higher than the 20 nM that would be expected if the PV calcium levels were in equilibrium with the host red blood cell's cytosol (Murphy, Berkowitz et al. 1987, Gazarini, Thomas et al. 2003). Additionally, the same study showed that depletion of calcium in the *Plasmodium*

PV leads to a depletion of intracellular calcium stores, which suggests that the parasite depends on the sequestration of calcium in the PV to maintain its intracellular pools of calcium (Gazarini, Thomas et al. 2003). It is possible that similar mechanisms are regulating calcium levels within the *T. gondii* PV. Interestingly, calcium is not the only ion which the parasite regulates the concentration of within the PV; it has recently been shown that the pH of the vacuole decreases as egress approaches and this increased acidification is associated with enhanced parasite motility and protein secretion (Roiko, Svezhova et al. 2014). While it is possible that one or more dense granule proteins that *T. gondii* secretes into its vacuole are responsible for the sequestration of ions as egress approaches, it is unlikely that this is occurring in *Plasmodium* species, since the dense granule proteins described to date are restricted to the tissue-cyst forming coccidia and are not found in other apicomplexans such as *Plasmodium* (Mercier and Cesbron-Delauw 2015). Therefore, it is possible that these two related organisms have evolved different strategies to utilize calcium signaling within the context of the calcium-poor cytosol of their host cells.

It is unlikely that GRA41 binds calcium directly, since bioinformatic analysis fails to identify any conserved calcium binding domains (SMART, NCBI, Prosite, Interpro) and recombinant GRA41 protein fails to bind calcium *in vitro* (Figure 4.6, above). Rather, I hypothesize that GRA41 might influence physiological calcium homeostasis by its localization and functional role within the tubulovesicular network (TVN). Loss of GRA41 leads to altered morphology of the TVN, which interestingly has been proposed to play a role in calcium storage based on electron

microscopy studies (Bonhomme, Pingret et al. 1993). Nonetheless, other dense granule proteins that localize to the membranes of the TVN are also critical for its formation (Mercier, Dubremetz et al. 2002), but do not seem to appear to affect the same of processes influenced by GRA41. The loss of the TVN in parasites lacking GRA2 leads to a variety of phenotypes, including the formation of vacuoles containing poorly organized parasites that egress erratically (Muniz-Hernandez, Carmen et al. 2011), altered presentation of antigens to the host immune system (Lopez, Bittame et al. 2015), decreased ingestion of host cytosolic proteins (Dou, McGovern et al. 2014) and decreased virulence in mice (Mercier, Howe et al. 1998). However, I have shown that the loss of GRA2 does not phenocopy the iiDeath resistance of the *GRA41* knockout and forward genetic mutant, suggesting that the disruption of the TVN might not be the underlying reason for the iiDeath resistance of *GRA41*(Figure 4.5, above). Rather, it appears that the iiDeath resistance of the *GRA41* knockout strain is a direct effect of GRA41 by a novel mechanism that has yet to be completely discerned. Nonetheless, there remains the possibility that although the TVN is structurally affected in both the *GRA41* and *GRA2* knockout strains, the nature, level and the functional consequences of that effect might be different between the two mutant strains. For example, the loss of GRA41 might prevent the formation of specific protein complexes within the PV which are required for normal egress timing, which might explain why the loss of GRA2 leads to erratic egress that occurs with normal timing.

At the current time, it is unclear which of the pleiotropic effects of GRA41 loss is the primary impact of its loss and which are simply downstream defects.

However, one of the most severe and distinct phenotypes of the *GRA41* knockout strain is a premature egress from the host cell. Natural egress from host cell can be an active process dependent on calcium fluxes (Moudy, Manning et al. 2001). Two alternative hypotheses to explain the premature egress are 1) that the altered TVN, which might normally act as a mechanical barrier, allows for early exit and 2) that the dysregulation of calcium homeostasis results in changes in the timing of egress. The fact that other mutant parasites lacking a normal TVN, such as the *GRA2* knockout, don't have a premature egress phenotype would argue against a model in which the altered TVN, caused by *gra41* disruption, allows for early egress. To further separate these two phenotypes, complementation studies with modified (i.e. truncated, mutated) forms of *GRA41* in the knockout background should be performed to determine if these two phenotypes can be functionally linked to domains or residues within *GRA41*. Additionally, the only other dense granule protein whose loss leads to an early egress phenotype similar to the *GRA41* knockout is *GRA22*. However, the *GRA22* knockout does not exhibit any obvious defect in TVN formation (Okada, Marmansari et al. 2013), suggesting that *GRA41* plays a structural role within the TVN that is independent from its role in egress and, by inference, calcium-dependent signaling processes within the parasite. It remains unclear whether or not these two proteins are interacting together directly or within the same pathway to influence the timing of egress. Though preliminary interaction studies failed to identify *GRA22* as a potential interactor as *GRA41*, future studies to expand and refine this list of *GRA41* interactors and to create a strain lacking both *GRA22* and *GRA41* would address

some of these questions. Considering that tight control of calcium levels is needed for egress, it is plausible that the early egress phenotype of the *GRA41* knockout is related to the dysregulation of calcium seen in this strain. Interestingly, the MBD2.1 mutant, as well as the *GRA41* knockout, show a slight but consistent increase in the rate of calcium dependent iiEgress ((Black, Arrizabalaga et al. 2000) and unpublished data, LaFavers and Arrizabalaga). Additional support for a connection between early egress and calcium dysregulation in the mutants, is the fact that the *GRA41* knockout is much more sensitive to DTT-induced egress than the parental strain. The redox reagent DTT is proposed to induce egress by activating NTPases located in the PV since it is capable of activating isolated enzyme (Bermudes, Peck et al. 1994). Treatment with DTT has also been shown to lead to calcium fluxes within the parasite, resulting in induced egress, which can be blocked by chelating calcium, indicating that DTT-induced egress is also calcium dependent (Stommel, Ely et al. 1997, Borges-Pereira, Budu et al. 2015). Unlike calcium ionophores such as A23187, DTT is not capable of inducing egress at early stages of parasite vacuole formation and requires longer growth times (~36 hours) for vacuoles to consistently egress. This suggests that DTT-induced egress might be dependent on processes preceding natural egress and is therefore a more accurate model for what is happening in natural uninduced egress (Stommel, Cho et al. 2001). In this context, the ability of the *GRA41* knockout strain to undergo DTT-induced egress at 24 hours is consistent with its early egress phenotype. The formation of more than two daughter parasites in the dividing *GRA41* knockout strain could also occur as a result of calcium dysregulation rather than simply being

an additional function of GRA41. Knockdown of the calcium-dependent kinase CDPK7 has previously been shown to disrupt normal division (Morlon-Guyot, Berry et al. 2014). Additionally, experiments to identify novel proteins in the inner membrane complex (IMC) of the parasite, which serves as the scaffold for daughter cell formation (Harding and Meissner 2014), identified a protein (ISC6, TgGT1_267620, ToxoDB.org), that localizes to the IMC and contains a C2 calcium binding domain (Chen, Moon et al. 2017), which could suggest a link between calcium and daughter parasite formation in *T. gondii*.

Of note is the fact that *GRA41* is not annotated as a protein encoding gene in the latest version of the *T. gondii* genome database. This locus was denoted as a gene in earlier annotations with both transcriptomic and proteomic corroborating evidence. As I have shown there is clearly a protein encoding locus in that genomic region; underscoring the limitation of genome annotations. One of the drawbacks of *GRA41* not being denoted as a protein in the current annotated genome is that it is not considered when analyzing datasets that rely on the annotation. In the many gene expression studies, mappings of post-translational modifications, and sequencing of mutant strains that have been undertaken in the last few years, *GRA41* has not been included, significantly reducing our ability to understand its function. For example, the presence of certain post-translational modifications could provide clues to how *GRA41* is associated with the TVN membrane. Though *GRA41* lacks an amphipathic alpha helix (Helical Wheel Predictions, RZ Lab) like those found in other TVN-localized proteins such as *GRA2* (Mercier, Cesbron-Delauw et al. 1998), it does contain a predicted palmitoylation site at Cys26 (CSS-

Palm, Cuckoo Workgroup) that could explain membrane association. Though the palmitoylome for *T. gondii* has been published (Foe, Child et al. 2015), GRA41 was not included in the database at the time and any potential palmitoylation modifications were not mapped. As a result, future directions for the study of GRA41 would include mapping post-translational modifications and determining how they impact protein localization and function by mutational analysis.

In this context, the difference in electrophoretic mobility between the Type I and Type II GRA41 proteins (i.e. migrating as a doublet in Type I and a singlet in Type II strains) combined with the results of an alignment between the two proteins could help to identify residues that are differentially modified between the two strains. Though the modification responsible for the difference in electrophoretic mobility is likely to not be essential for overall protein function, it is possible that it could lead to subtle differences in protein function between the two strains. Such differences could prove informative for both the study of GRA41 and differences between Type I and Type II strains. Many of the amino acids which are different between the Type I and Type II GRA41 amino acid sequences could be responsible for the observed mobility difference. For example, the cysteine found at position twelve in the Type I strain could participate in the formation of a disulfide bond, which has been shown to lead to the production of a protein doublet by SDS-PAGE analysis (Ruiz, Chng et al. 2010). This cysteine is also predicted as a possible palmitoylation site by CSS-Palm, which would be lost if the amino acid at this location were a tryptophan, as it is in the Type II strain (Ren, Wen et al. 2008). The glutamic acid residues at positions 124, 125 and 179 may also be modified,

such as in the addition of a CO₂ molecule to form gamma-carboxyglutamic acid. The resulting modified amino acid has two negatively charged groups which have been found to be important in coordinating divalent cations, such as calcium, in blood clotting factors (Furie, Bouchard et al. 1999). Though serine residues are capable of receiving many types of modifications, including phosphorylation and glycosylation, threonine is also capable of accepting these types of modifications, making the conversion of the serine to threonine at position 134 a somewhat less likely candidate for the differences in protein migration observed (Blom, Sicheritz-Ponten et al. 2004). Finally, lysines such as the one found at position 174 can be modified by as many as 12 different post-translational modifications, including acetylation, methylation and ubiquitination (Liu, Wang et al. 2014).

The discovery of GRA41 as a novel dense granule protein with a role in calcium-dependent events helps to both answer and create new questions about the role of the PV in these signaling processes. This work demonstrates that the parasite is dependent on a dense granule protein for normal calcium homeostasis, but it is still unclear how and if the parasite might regulate PV calcium levels independent of the host cell cytosol in the presence of a nonselective PVM pore (Schwab, Beckers et al. 1994). The explanation for this might be the existence of additional calcium binding proteins that, in addition to GRA1 (Cesbron-Delauw, Guy et al. 1989), could bind and sequester calcium within the PV. Future efforts to directly measure calcium concentration in the PV of *GRA41* mutant strains might shed light on the specific function of this protein.

The localization of GRA41 to the TVN suggests that this membranous structure may also play a direct or indirect role in the physiological regulation of

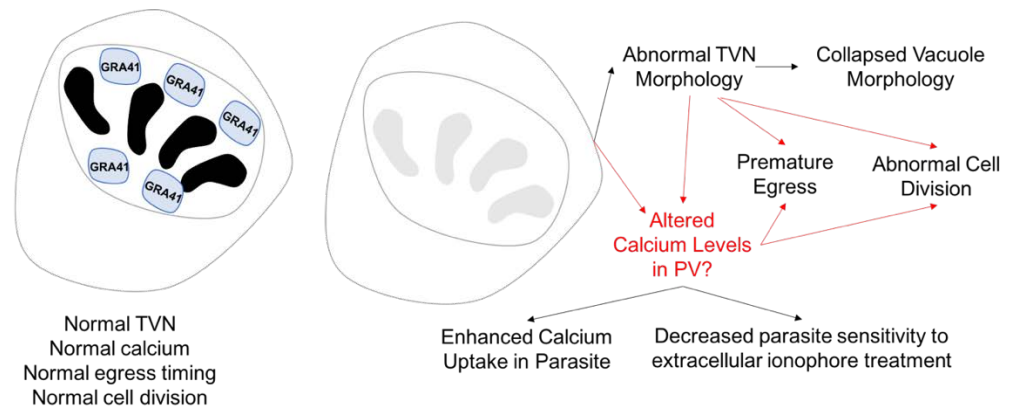


Figure 6.1 Proposed model for phenotypes associated with Loss of GRA41 in Type I Strain

Host cell containing a parasitophorous vacuole with four parasites (black) and GRA41 present in the vacuole (left) shows wild-type phenotypes for TVN structure, calcium levels/uptake, egress timing and cell division. When GRA41 is lost (vacuole on right, grey parasites) a variety of phenotypes are observed. The model proposes possible links between the phenotypes. Links with more than one possibility and unconfirmed phenotypes are labeled in red.

the parasite, pointing to a novel function for this poorly understood element of intracellular parasite development. Thus, in conjunction with previous knowledge, our results underscore the critical importance of the parasitophorous vacuole and its contents in the life cycle of *T. gondii* and, likely, of related parasites. To begin to address the question of how GRA41 performs its functions, I used two different approaches to create a list of potential interactors of GRA41. The co-immunoprecipitation approach has the benefit of assessing interactions as they occur naturally, but it has many drawbacks. Co-immunoprecipitation protocols must be optimized for each protein individually, which can be time and labor intensive and still may not yield reproducible results. This is because it is difficult

to capture transient or weak interactions, especially when strong detergents and sonication are necessary to fully solubilize a target protein such as GRA41, which has been shown to partition as a membrane protein (Figure 3.4, above). A single successful co-immunoprecipitation was conducted on GRA41 using the strain which has GRA41 endogenously tagged with HA and harvesting intracellular parasites, which identified several potential interactors. Of these, some were previously characterized dense granule and rhoptry proteins, while others are proteins of hypothetical function that contain a signal peptide (characteristics common to dense granule proteins). Two of these proteins that are most likely to be *bona fide* interactors are GRA3 and GRA9, both of which at least partially localized to the tubulovesicular network where GRA41 resides (Adjogble, Mercier et al. 2004, Kim, Ahn et al. 2008). The large number of rhoptry proteins, which all traffic to the membrane of the parasitophorous vacuole (Soldati, Lassen et al. 1998, El Hajj, Lebrun et al. 2007, Peixoto, Chen et al. 2010), are also potentially *bona fide* interactors, since the tubulovesicular network can come into close contact with the PVM. If these interactors are real, they could suggest a possible function of GRA41 wherein it helps form the links between the TVN and the PVM. If these links are required for the correct morphology of the TVN, they could explain why loss of GRA41 leads to disruption of the TVN. It is important to note that none of these interactions have been validated by targeted co-immunoprecipitations, which would be necessary to demonstrate that they are true interactors.

Using the yeast two hybrid approach allows us to continue our search for interactors while avoiding some of the pitfalls of the co-immunoprecipitation

approach. When samples do not need to be lysed and solubilized, there is no concern that weak interactions are being missed. Since the yeast two-hybrid approach takes place in a heterologous system, it will only give direct interactors, rather than proteins that are part of the same complex as the target protein but do not bind it directly. Additionally, because the prey fragments used in the library are often smaller than the entire protein, it is possible to determine what region of the prey protein that the bait protein is binding. Using this technique has generated a list of 11 high confidence potential interactors for GRA41. Of these, probably the most intriguing is GRA1, which is a dense granule protein that localizes to both the lumen of the PV as well as the TVN. In addition to partially sharing localization with GRA41, GRA1 also contains a motif that has been shown to bind calcium (Cesbron-Delauw, Guy et al. 1989). It is possible that GRA1 acts to sequester calcium within the vacuole and a potential interaction with GRA41 would allow it to associate with the TVN. Of the remainder of the list, only a single protein of hypothetical function is predicted to be secreted by Psort (Horton, Park et al. 2007), though many of the remaining proteins do have signal peptides. Unfortunately, none of the high confidence proteins on the yeast two-hybrid list overlap with the high confidence proteins from the co-immunoprecipitation, likely due to the differences and drawbacks of each approach. Since interactions of lower confidence for both data sets were excluded from the analysis, it is possible that are some genuine interactors that show up on both lists but are not listed as high confidence due to low abundance of the potential interactor. The yeast two-hybrid approach is likely to capture interactions that are possible based on protein

structure, but may not occur within the parasite because the proteins are localized to different areas within the cell. They are also incapable of detecting indirect interactions with multiple components of a protein complex. The co-immunoprecipitation approach is limited by the optimization of the solubilization and pull-down of the target antigen, but is more likely to be able to pull down large, multi-protein complexes. To validate these potential interactors, it will be necessary to show co-localization, which may require immunoelectron microscopy to potential interactions between the PVM-localized rhoptries and the TVN-localized GRA41. A proximity-labeling approach, such as BioID (Roux, Kim et al. 2013) or APEX2 (Lam, Martell et al. 2015), could also help to verify transient or weak interactions that show up in the yeast two-hybrid screen but are not seen using a traditional co-immunoprecipitation approach.

A complete knockout of GRA41 in a Type II strain recapitulates the resistance to iiDeath seen in both the Type I knockout and forward genetic mutant, suggesting that the overall role in calcium processes is conserved between the two strains. However, no significant defect in plaque formation was detected for the knockout strain and additional phenotypes found in the Type I knockout strain were not tested, so it remains unclear the exact function GRA41 might play in a Type II strain. Determining whether or not the Type II knockout recapitulates all of the phenotypes of the Type I knockout is particularly interesting in light of the differences in electrophoretic mobility for the tagged proteins described above, making it likely that GRA41 is differentially modified in the two different strains.

The most important question that generating a Type II knockout allows us to answer is whether or not the loss of GRA41 plays any role in tissue cyst formation or maintenance and what role it plays during *in vivo* infection. Here I show preliminary data that the knockout of GRA41 shows a significant decrease in the percentage of vacuoles with an intact cyst wall at 7 days when compared to the parental strain. Since this phenotype is not seen at four days, it suggests that the loss of GRA41 does not impair the parasite's ability to form a cyst wall, but that the cyst wall is not able to be maintained, even in the presence of continued pH stress. It is unclear whether or not this failure to maintain the cyst wall is due to defects in calcium signaling as seen in the Type I strain or structural defects in the cyst wall. A pilot *in vivo* experiment shows that the loss of GRA41 shows highly variable phenotypes according to the dose used to infect mice. At a low dose, cysts counts are very low in both the parental and knockout-infected mice and no difference is seen between the two groups. However, at a higher dose, there is a 2-fold increase in the number of cysts/mouse brain. This increase is also seen in the cyst-containing brains of the mice that received the highest dose of knockout parasites, though many of the brains in this group have no detectable cysts, so the average number of cysts is equivalent in the parental and knockout strains. Follow-up mouse experiments would need to address the issue of acute virulence by increasing the highest dose to one that is lethal in at least some of the mice. This would allow us to determine the impact that GRA41 has on virulence during the acute infection. Given the high variability in the tissue cyst count data from the pilot experiment, follow-up experiments should increase the number of animals

assessed to get a more accurate representation of total cyst numbers. Since the preliminary results suggest that the knockout strain could have a defect in cyst maintenance, which would lead to overall higher cyst counts due to the reactivation of cysts to tachyzoites, followed by reinvasion and conversion back to bradyzoite cysts, additional experiments examining cyst counts for mice infected with the parental and knockout strains at later time points in the chronic infection might help support this hypothesis. It is possible that some of the cysts of the knockout strain are not able to be visualized with the current protocols due to small size, and it is expected that looking at later time points might allow cysts to increase in size and/or number. Overall, these results suggest that GRA41 plays an important role in the bradyzoite stage of the life cycle and that differences between the Type I and Type II proteins could provide important information about the role of specific residues and potential posttranslational modifications in phenotypes already characterized in Type I tachyzoites. Additionally, since very little is known about the calcium regulation of bradyzoite formation, maintenance and reactivation, this knockout could play a key role in elucidating the role of calcium in these processes.

Chapter 7 : Conclusion and Future Directions

Conclusion

Calcium-dependent signaling processes are critical for multiple steps of the parasite's lytic cycle and represent an appealing target for drug discovery (Arrizabalaga and Boothroyd 2004). Former members of the Arrizabalaga laboratory have used a forward genetic approach to identify and characterize some of the key players in these signaling events (Black, Arrizabalaga et al. 2000, Garrison, Treeck et al. 2012). Here I describe the characterization of a previously generated mutant, MBD2.1, that is capable of surviving prolonged extracellular treatment with a calcium ionophore, which renders wild-type parasites unable to attach to host cells. I show that the mutation responsible for this phenotype is the introduction of a premature stop codon at serine 92 of the protein of hypothetical function, TgGT1_069070. Endogenous tagging at this locus reveals that the encoded protein is secreted from the parasite organelle known as the dense granules into the parasitophorous vacuole in which the parasite resides and divides. Once in the vacuole, it traffics to the TVN. Its secretion from the dense granule leads to its designation as a GRA protein and given the current published GRA proteins in the field, it is specifically designated as GRA41.

A complete knockout of the locus encoding GRA41 leads to a recapitulation of the resistance of extracellular ionophore treatment, while also showing a defect in the efficiency of plaquing. This defect is rescued by complementing the knockout strain with a wild-type copy of GRA41 and is demonstrated to be largely due to premature egress of parasites from host cells. The GRA41 knockout strain also

exhibits increased uptake of calcium when extracellular, which was restored to normal levels in the complemented strain. A morphological analysis of the knockout strain revealed an improperly formed TVN and evidence of atypical cell division. A knockout parasite strain with similar TVN disruption (Travier, Mondragon et al. 2008) does not exhibit resistance to iiDeath treatment. Current efforts to identify protein interaction partners have resulted in a list of unverified potential interactors obtained by co-immunoprecipitation and yeast two-hybrid analysis.

Studies to investigate the function of GRA41 in the bradyzoite life stage were conducted in the Type II Pru strain. Endogenous tagging of the Type II GRA41 protein revealed that it localizes primarily to the tissue cyst wall and has a unique electrophoretic migration pattern as compared to the Type I Gra41 protein. The loss of GRA41 in the Type II strain recapitulated the resistance to ionophore induced death seen in the original mutant and Type I knockout strain. This strain also shows reduced tissue cyst wall staining of vacuoles following seven days of bradyzoite differentiation by pH stress, though this difference is not seen after four days of differentiation. A pilot study of chronic mouse infection with the Type II knockout strain showed highly variable cyst counts at the highest dose and very low cyst counts at the lowest dose, while the middle dose showed adequate cyst counts in both the parental and the knockout with somewhat less variability than was seen at the top dose. At this middle dose, the knockout strain was shown to have an approximately two-fold higher cyst burden as compared to the parental strain.

Overall, the forward genetic approach to identifying novel regulators of calcium signaling processes has provided unexpected and intriguing results in the identification of a novel dense granule protein that plays a role in calcium sensitivity/uptake, the timing of egress and vacuolar morphology. Though the exact mechanism by which this protein performs these important functions remains unclear, these results provide many tantalizing clues and avenues for possible future work in this area. An original goal of this work was to identify novel potential drug targets to be able to develop inhibitors against for treatment of clinical toxoplasmosis. Since GRA41 lacks homologues even among most other apicomplexans, its uniqueness could be advantageous in developing specific inhibitors that would not target host processes. However, the loss of GRA41 is not lethal and, in fact, exhibits what could be considered a gain of function phenotype in its premature egress from host cells and ability to withstand extended calcium ionophore treatment. This suggests that a more viable strategy to target GRA41 for drug treatment could be to increase either its amount or stability. To test whether or not this might be a viable strategy, we could generate a line which overexpresses GRA41 under the promoter of a more highly expressed gene (i.e. tubulin) and determine what impact this has on parasite growth.

After the initial identification and characterization of GRA41 from the forward genetic approach, it is clear that the forward genetic approach has come with some important advantages and limitations. This approach has allowed us to identify a novel protein involved in calcium-dependent signaling processes that would have easily been overlooked with a reverse genetic approach, due to its lack of

conserved domains. Additionally, the calcium-related phenotype by which the mutant was isolated gave important clues to GRA41's function. However, this approach has a few key limitations. Specifically, the use of iiEgress/iiDeath phenotypes for forward genetic selection has oftentimes resulted in the generation of mutants in the calcium-dependent protein kinase 3 (TgCDPK3, (Garrison, Treeck et al. 2012)), suggesting that this selection needs to be refined in order to identify novel proteins involved in these processes. For example, the knockout of GRA41 results in enhanced natural and DTT-induced egress, though the timing of ionophore-induced egress is very similar to wild-type parasites. To identify more proteins that might play a role in the timing of natural egress, the screen could be modified by using DTT as the inducer of the egress rather than the calcium ionophore. By isolating parasites that have delayed (i.e. do not egress following DTT treatment at 35 hours post infection) or early (i.e. do egress following egress treatment before 35 hours post infection) DTT-induced egress, it would be possible to identify proteins that play a role in the timing of natural (uninduced) egress.

Future Directions

Does the loss of GRA41 impact calcium levels within the parasitophorous vacuole?

Though this work has shown that the loss of GRA41 in a Type I strain leads to enhanced calcium uptake in extracellular tachyzoites, it is unclear how a secreted protein demonstrates many of its calcium-related phenotypes (decreased sensitivity to ionophore treatment, enhanced calcium uptake) when the parasite is extracellular. I hypothesize that the calcium levels within the parasitophorous

vacuole of parasites without GRA41 are higher than those seen in wild-type parasites and that this impacts how the parasites within these vacuoles respond to calcium. This is consistent with the premature egress seen in the GRA41 knockout, since calcium is an important trigger of parasite egress. However, I do not have any direct evidence that the calcium levels within the PV are different between the strains. To address this, I could load host cells containing parasites with chemical calcium indicators that have been shown to traffic to the PV once inside the host cell and use previously described methods to measure the calcium concentration within the vacuoles (Pingret, Millot et al. 1996). This will help to address an important question about how a secreted protein can play a role in the calcium homeostasis within the parasite.

How does GRA41 localize to the tubulovesicular network?

The localization of GRA41 to a membranous network is unexpected, since there is no strong prediction for a transmembrane domain within this protein. Attempts to identify an amphipathic alpha helix, such as the one responsible for localizing GRA2 to the TVN (Mercier, Cesbron-Delauw et al. 1998), have also been unsuccessful. This makes it likely that the localization of GRA41 to this membranous network is due to either a post-translational modification or its interaction with another protein. To address the first possibility, and also provide additional insight into other aspects of GRA41's biology, I propose to conduct a proteomic analysis to identify post-translational modifications of GRA41. Though many proteomic data sets currently exist in the online *T. gondii* genome database, GRA41 has not been annotated in any strain of the genome since v7.2 in 2012, so

any data sets created after this time did not include GRA41. The only known post-translational modification of GRA41 are multiple phosphorylation marks from a phosphoproteome analysis published before this time (Treeck, Sanders et al. 2011). The identification of post-translational modifications on GRA41 will help to suggest potential modifications that could allow association with a membrane (i.e. lipidation) or which may regulate its function. These residues could then be mutated to see if they have any impact on the protein's localization or function.

What parts of the protein are necessary for the different functions of GRA41?

Since GRA41 does not have any domains of known/predicted function, this has made it difficult to ascribe specific functions to domains of the protein. However, the identification of domains with specific functions within the protein can help to understand the mechanisms by which GRA41 impacts vacuolar morphology and calcium-dependent signaling processes. Previous attempts have been made to generate a series of truncation mutants, but these resulted in proteins with low or no expression within the parasite, making it difficult to characterize their localization or potential phenotypes associated with these truncations. Instead, I would take a complementation approach using the previously generated knockout of GRA41. I currently have designed a complementation construct consisting of GRA41 5' and 3' targeting regions flanking a GRA41 coding sequence tagged with a triple HA tag. This construct could be modified by scrambling the amino acid sequences of alpha helices, mutating residues predicted/demonstrated to be post-translationally modified or deleting short sequences from the protein. These could then be incorporated into

the knockout strain to assess their localization and ability to complement the various phenotypes associated with the loss of GRA41.

What are the protein interaction partners of GRA41? Can any of these explain the phenotypes associated with its loss?

Preliminary attempts to define the GRA41 interactome have generated an initial list that will be expanded upon and validated. For this, I propose to take two complementary approaches. Due to difficulties encountered with the traditional co-immunoprecipitation approach, I would instead look to a proximity-based labeling approach to identify potential interactors. In this context, APEX2 is an ascorbate peroxidase that has been used to label compartments for electron microscopy imaging and also to label proximal proteins with a biotin-phenol radical. It was recently modified to have high catalytic activity, and can now be used even with proteins that have low or medium endogenous expression without the requirement of overexpression (Lam, Martell et al. 2015). A fusion between GRA41 and APEX will be generated at the endogenous locus, similar to the addition of the endogenous HA tag. In the presence of biotin phenol and hydrogen peroxide, this fusion protein will add biotin groups to proteins within a 20-nm radius of the fusion protein. These proteins can then be isolated using streptavidin-conjugated agarose or magnetic beads and identified by mass spectrometry. Since the labeling occurs in live parasites, this method is less likely to capture false positive from interactors not found within the same location as the protein of interest. It is also capable of detecting weak or transient interactions and there are no limits on the types of lysis and wash buffers used, since it is not necessary to preserve

protein interactions. This method will be used to complement the data generated from the co-immunoprecipitation and yeast two-hybrid analysis to prioritize candidate proteins.

Candidate interactors identified in the current data and any additional data sets generated from the APEX labeling experiments will be validated by verifying colocalization with GRA41 when parasites are intracellular and extracellular (using antibodies if available or by generating lines with the potential interactor tagged if an antibody is not available). If colocalization is observed, reciprocal co-immunoprecipitations will be performed in a strain tagged with both GRA41 and the potential interactor. To account for the possibility that these interactions are transient, proteins will first be cross-linked chemically using a reversible cross-linker such as those of the N-hydroxysuccinimide class of crosslinkers to preserve these interactions. An antibody will be used to pull down one of the proteins before the crosslinking is reversed. A Western Blot analysis will be performed to detect each protein in the elution fraction. If each pulldown shows both proteins are coming down when one of them is the target, I will conclude they are interactors. In the case of proteins with known functions, verification of these interactions could provide important mechanistic insight into how GRA41 performs its functions. For proteins whose function is not currently not known, this approach could help to identify other novel PV proteins with similar roles to GRA41. These would then be genetically disrupted to see if they share similar phenotypes to the knockout of GRA41 or if they perform altogether different functions. In addition to investigating the proteins found in this list, I also propose to look specifically at GRA22, since it

has been shown previously to have a premature egress phenotype, by generating a single knockout of GRA22 and a double knockout of GRA41 and GRA22 for phenotypic analysis.

Are there differences between the Type I and Type II GRA41 proteins that could provide insight into protein function or parasite biology?

As I have already shown, though both the Type I and Type II GRA41 proteins are secreted proteins, they demonstrate an important difference in electrophoretic mobility. The Type I GRA41 protein runs as a doublet on an SDS-PAGE gel while the Type II protein runs as a single band. Further investigation reveals that there are six amino acid changes between the two protein sequences which could be responsible for the differences observed if any of them are shown to be post-translationally modified within the Type I strain. The Type I and Type II strains differ greatly in the *in vivo* virulence and polymorphisms within dense granule and rhoptry proteins have been previously shown to be important mediators of these virulence differences. I propose to test if the polymorphisms between the Type I and Type II strains are important to GRA41 function by conducting complementation studies in the knockout strains to determine whether or not the Type II protein is capable of rescuing the Type I knockout's phenotypes and vice versa. A failure of the Type II protein to rescue the Type I knockout's phenotypes could help to narrow down key residues associated with certain residues and areas of the protein. The specific residues that differ between the two strains could be mutated to determine which, if any, impact the rescue of phenotype. There are also additional phenotypes of the Type I knockout that have

not yet been assessed in the Type II knockout. Verifying whether or not the Type II knockout retains the premature egress, TVN disruption and calcium uptake phenotypes of the Type II knockout could prove very informative in identifying key residues/domains involved in these various phenotypes.

The exact localization of the Type II protein remains unclear. Though it has been shown to be secreted into the parasitophorous vacuole and localizes to the tissue cyst wall, it is unclear if it localizes to the TVN of the vacuole or if it is found free in the lumen of the PV. Preliminary studies to determine if the Type II GRA41 protein exists as a soluble or membrane-associated protein should first be conducted. As expected for a TVN-associated protein, Type I GRA41 is found within the membrane-associated fraction following partitioning with TX-114. If the Type II protein does not have the same pattern, this may suggest that it has a different localization within the vacuole than the Type I protein, which can be verified by immunoelectron microscopy as was done for the Type I protein. Additionally, very little is known about the TVN in cysts; if GRA41 continues to localize to the TVN of Type II parasites, immunoelectron microscopy of bradyzoite cysts expressing a tagged GRA41 could be informative in studying the TVN of cysts.

Does the knockout of GRA41 in a Type II strain lead to a defect in bradyzoite cyst maintenance?

Our preliminary data supports a hypothesis that the loss of GRA41 in a Type II strain leads to a defect in the maintenance of bradyzoite cysts, both *in vitro* and *in vivo*. However, there is much additional work to be done to test this hypothesis.

Most importantly, the generation of a complemented strain or an independently-derived knockout is necessary to verify that the associated phenotypes are directly due to the loss of GRA41. Preliminary attempts to generate such a strain resulted in a population with a very low rate of successful incorporation and expression of the complementation plasmid within the transfected population (<1%) and an inability to isolate a positive clone. This was also seen when generating the Type II knockout strain, and in this case, the addition of a GFP marker outside of the homology arms that allow for incorporation into the target locus helped to eliminate clones that had integrated the knockout plasmid randomly. Hundreds of clones could be rapidly screened by live fluorescence imaging, rather than the methodical screening of dozens of clones that is done by traditional immunofluorescence analysis. Since the complementation construct has also been targeted to the endogenous locus encoding GRA41, a similar approach could be used to quickly screen for parasites that incorporated the plasmid in the correct location.

Additional work will also aim to further refine and characterize the phenotypes associated with loss of GRA41 in a Type II strain. Given the observed differences in sequence and electrophoretic mobility (and likely post-translational modification), it is important to ask whether or not all of the phenotypes observed in the Type I knockout are also found in the Type II knockout. In addition to this, looking at bradyzoite formation both with a complemented strain and at additional, later time points, will help to further clarify the role of GRA41 in cyst maintenance. Based on the pilot *in vivo* study, future efforts to look at the impact of GRA41 on cyst burden are warranted. Since I suspect that GRA41 might play a role in cyst

maintenance *in vivo* as well, additional time points harvested later during chronic infection can help elucidate how the infection is progressing over time. Additionally, none of the doses utilized in the pilot study led directly to any mouse death during the acute infection, so a trial of a higher dose of parasites will be used to determine if GRA41 plays a role in virulence in the mouse model.

Chapter 8 : References

Adjogble, K. D., C. Mercier, J. F. Dubremetz, C. Hucke, C. R. Mackenzie, M. F. Cesbron-Delauw and W. Daubener (2004). "GRA9, a new *Toxoplasma gondii* dense granule protein associated with the intravacuolar network of tubular membranes." Int J Parasitol **34**(11): 1255-1264.

Alexander, D. L., S. Arastu-Kapur, J. F. Dubremetz and J. C. Boothroyd (2006). "Plasmodium falciparum AMA1 binds a rhoptry neck protein homologous to TgRON4, a component of the moving junction in *Toxoplasma gondii*." Eukaryot Cell **5**(7): 1169-1173.

Alexander, D. L., J. Mital, G. E. Ward, P. Bradley and J. C. Boothroyd (2005). "Identification of the moving junction complex of *Toxoplasma gondii*: a collaboration between distinct secretory organelles." PLoS Pathog **1**(2): e17.

Arrizabalaga, G. and J. C. Boothroyd (2004). "Role of calcium during *Toxoplasma gondii* invasion and egress." Int J Parasitol **34**(3): 361-368.

Arrizabalaga, G., F. Ruiz, S. Moreno and J. C. Boothroyd (2004). "Ionophore-resistant mutant of *Toxoplasma gondii* reveals involvement of a sodium/hydrogen exchanger in calcium regulation." J Cell Biol **165**(5): 653-662.

Asai, T., W. J. O'Sullivan and M. Tatibana (1983). "A potent nucleoside triphosphate hydrolase from the parasitic protozoan *Toxoplasma gondii*. Purification, some properties, and activation by thiol compounds." J Biol Chem **258**(11): 6816-6822.

Bartel, P., C. T. Chien, R. Sternglanz and S. Fields (1993). "Elimination of false positives that arise in using the two-hybrid system." Biotechniques **14**(6): 920-924.

Beck, J. R., A. L. Chen, E. W. Kim and P. J. Bradley (2014). "RON5 is critical for organization and function of the Toxoplasma moving junction complex." PLoS Pathog **10**(3): e1004025.

Beis, J. M., J. M. Andre, A. M. Datie and B. Bruggerolle (2002). "Eye movements and verbal reports in neglect patients during a letter reading task." NeuroRehabilitation **17**(2): 145-151.

Benmerzouga, I., L. A. Checkley, M. T. Ferdig, G. Arrizabalaga, R. C. Wek and W. J. Sullivan, Jr. (2015). "Guanabenz repurposed as an antiparasitic with activity against acute and latent toxoplasmosis." Antimicrob Agents Chemother **59**(11): 6939-6945.

Bermudes, D., K. R. Peck, M. A. Afifi, C. J. Beckers and K. A. Joiner (1994). "Tandemly repeated genes encode nucleoside triphosphate hydrolase isoforms secreted into the parasitophorous vacuole of Toxoplasma gondii." J Biol Chem **269**(46): 29252-29260.

Birch-Andersen, A., D. J. Ferguson and R. D. Pontefract (1976). "A technique for obtaining thin sections of coccidian oocysts." Acta Pathol Microbiol Scand B **84**(4): 235-239.

Black, M. W., G. Arrizabalaga and J. C. Boothroyd (2000). "Ionophore-resistant mutants of Toxoplasma gondii reveal host cell permeabilization as an early event in egress." Mol Cell Biol **20**(24): 9399-9408.

Black, M. W. and J. C. Boothroyd (2000). "Lytic cycle of *Toxoplasma gondii*." Microbiol Mol Biol Rev **64**(3): 607-623.

Blom, N., T. Sicheritz-Ponten, R. Gupta, S. Gammeltoft and S. Brunak (2004). "Prediction of post-translational glycosylation and phosphorylation of proteins from the amino acid sequence." Proteomics **4**(6): 1633-1649.

Bonhomme, A., L. Pingret, P. Bonhomme, J. Michel, G. Balossier, M. Lhotel, M. Pluot and J. M. Pinon (1993). "Subcellular calcium localization in *Toxoplasma gondii* by electron microscopy and by X-ray and electron energy loss spectroscopies." Microsc Res Tech **25**(4): 276-285.

Boothroyd, J. C. and J. F. Dubremetz (2008). "Kiss and spit: the dual roles of *Toxoplasma* rhoptries." Nat Rev Microbiol **6**(1): 79-88.

Borges-Pereira, L., A. Budu, C. A. McKnight, C. A. Moore, S. A. Vella, M. A. Hortua Triana, J. Liu, C. R. Garcia, D. A. Pace and S. N. Moreno (2015). "Calcium Signaling throughout the *Toxoplasma gondii* Lytic Cycle: A STUDY USING GENETICALLY ENCODED CALCIUM INDICATORS." J Biol Chem **290**(45): 26914-26926.

Bougdour, A., E. Durandau, M. P. Brenier-Pinchart, P. Ortet, M. Barakat, S. Kieffer, A. Curt-Varesano, R. L. Curt-Bertini, O. Bastien, Y. Coute, H. Pelloux and M. A. Hakimi (2013). "Host cell subversion by *Toxoplasma* GRA16, an exported dense granule protein that targets the host cell nucleus and alters gene expression." Cell Host Microbe **13**(4): 489-500.

Braun, L., M. P. Brenier-Pinchart, M. Yogavel, A. Curt-Varesano, R. L. Curt-Bertini, T. Hussain, S. Kieffer-Jaquinod, Y. Coute, H. Pelloux, I. Tardieux, A.

Sharma, H. Belrhali, A. Bougdour and M. A. Hakimi (2013). "A *Toxoplasma dense* granule protein, GRA24, modulates the early immune response to infection by promoting a direct and sustained host p38 MAPK activation." J Exp Med **210**(10): 2071-2086.

Brugerolle, G., G. Bricheux, H. Philippe and G. Coffea (2002). "Collodictyon triciliatum and *Diphyllia rotans* (=Aulacomonas submarina) form a new family of flagellates (Collodictyonidae) with tubular mitochondrial cristae that is phylogenetically distant from other flagellate groups." Protist **153**(1): 59-70.

Bullen, H. E., C. J. Tonkin, R. A. O'Donnell, W. H. Tham, A. T. Papenfuss, S. Gould, A. F. Cowman, B. S. Crabb and P. R. Gilson (2009). "A novel family of Apicomplexan glideosome-associated proteins with an inner membrane-anchoring role." J Biol Chem **284**(37): 25353-25363.

Caffaro, C. E., A. A. Koshy, L. Liu, G. M. Zeiner, C. B. Hirschberg and J. C. Boothroyd (2013). "A nucleotide sugar transporter involved in glycosylation of the *Toxoplasma* tissue cyst wall is required for efficient persistence of bradyzoites." PLoS Pathog **9**(5): e1003331.

Caldas, L. A., W. de Souza and M. Attias (2010). "Microscopic analysis of calcium ionophore activated egress of *Toxoplasma gondii* from the host cell." Vet Parasitol **167**(1): 8-18.

Carruthers, V. B., O. K. Giddings and L. D. Sibley (1999). "Secretion of micronemal proteins is associated with *Toxoplasma* invasion of host cells." Cell Microbiol **1**(3): 225-235.

Carruthers, V. B. and L. D. Sibley (1997). "Sequential protein secretion from three distinct organelles of *Toxoplasma gondii* accompanies invasion of human fibroblasts." Eur J Cell Biol **73**(2): 114-123.

Carruthers, V. B. and L. D. Sibley (1999). "Mobilization of intracellular calcium stimulates microneme discharge in *Toxoplasma gondii*." Mol Microbiol **31**(2): 421-428.

Cerede, O., J. F. Dubremetz, M. Soete, D. Deslee, H. Vial, D. Bout and M. Lebrun (2005). "Synergistic role of micronemal proteins in *Toxoplasma gondii* virulence." J Exp Med **201**(3): 453-463.

Cesbron-Delauw, M. F., B. Guy, G. Torpier, R. J. Pierce, G. Lenzen, J. Y. Cesbron, H. Charif, P. Lepage, F. Darcy, J. P. Lecocq and et al. (1989). "Molecular characterization of a 23-kilodalton major antigen secreted by *Toxoplasma gondii*." Proc Natl Acad Sci U S A **86**(19): 7537-7541.

Chaturvedi, S., H. Qi, D. Coleman, A. Rodriguez, P. I. Hanson, B. Striepen, D. S. Roos and K. A. Joiner (1999). "Constitutive calcium-independent release of *Toxoplasma gondii* dense granules occurs through the NSF/SNAP/SNARE/Rab machinery." J Biol Chem **274**(4): 2424-2431.

Chen, A. L., A. S. Moon, H. N. Bell, A. S. Huang, A. A. Vashisht, J. Y. Toh, A. H. Lin, S. M. Nadipuram, E. W. Kim, C. P. Choi, J. A. Wohlschlegel and P. J. Bradley (2017). "Novel insights into the composition and function of the *Toxoplasma* IMC sutures." Cell Microbiol **19**(4).

Cleary, M. D., U. Singh, I. J. Blader, J. L. Brewer and J. C. Boothroyd (2002). "*Toxoplasma gondii* asexual development: identification of developmentally

regulated genes and distinct patterns of gene expression." Eukaryot Cell **1**(3): 329-340.

Cochereau-Massin, I., P. LeHoang, M. Lautier-Frau, E. Zerdoun, L. Zazoun, M. Robinet, P. Marcel, B. Girard, C. Katlama, C. Leport and et al. (1992). "Ocular toxoplasmosis in human immunodeficiency virus-infected patients." Am J Ophthalmol **114**(2): 130-135.

Del Carmen, M. G., M. Mondragon, S. Gonzalez and R. Mondragon (2009). "Induction and regulation of conoid extrusion in *Toxoplasma gondii*." Cell Microbiol **11**(6): 967-982.

Docampo, R., W. de Souza, K. Miranda, P. Rohloff and S. N. Moreno (2005). "Acidocalcisomes - conserved from bacteria to man." Nat Rev Microbiol **3**(3): 251-261.

Donald, R. G., D. Carter, B. Ullman and D. S. Roos (1996). "Insertional tagging, cloning, and expression of the *Toxoplasma gondii* hypoxanthine-xanthine-guanine phosphoribosyltransferase gene. Use as a selectable marker for stable transformation." J Biol Chem **271**(24): 14010-14019.

Dou, Z. and V. B. Carruthers (2011). "Cathepsin proteases in *Toxoplasma gondii*." Adv Exp Med Biol **712**: 49-61.

Dou, Z., O. L. McGovern, M. Di Cristina and V. B. Carruthers (2014). "*Toxoplasma gondii* ingests and digests host cytosolic proteins." MBio **5**(4): e01188-01114.

Dubey, J. P. (2006). "Comparative infectivity of oocysts and bradyzoites of *Toxoplasma gondii* for intermediate (mice) and definitive (cats) hosts." Vet Parasitol **140**(1-2): 69-75.

Dunn, J. D., S. Ravindran, S. K. Kim and J. C. Boothroyd (2008). "The *Toxoplasma gondii* dense granule protein GRA7 is phosphorylated upon invasion and forms an unexpected association with the rhoptry proteins ROP2 and ROP4." Infect Immun **76**(12): 5853-5861.

El Hajj, H., M. Lebrun, S. T. Arold, H. Vial, G. Labesse and J. F. Dubremetz (2007). "ROP18 is a rhoptry kinase controlling the intracellular proliferation of *Toxoplasma gondii*." PLoS Pathog **3**(2): e14.

El Hajj, H., M. Lebrun, M. N. Fourmaux, H. Vial and J. F. Dubremetz (2007). "Inverted topology of the *Toxoplasma gondii* ROP5 rhoptry protein provides new insights into the association of the ROP2 protein family with the parasitophorous vacuole membrane." Cell Microbiol **9**(1): 54-64.

Etheridge, R. D., A. Alaganan, K. Tang, H. J. Lou, B. E. Turk and L. D. Sibley (2014). "The *Toxoplasma* pseudokinase ROP5 forms complexes with ROP18 and ROP17 kinases that synergize to control acute virulence in mice." Cell Host Microbe **15**(5): 537-550.

Fentress, S. J. and L. D. Sibley (2011). "The secreted kinase ROP18 defends *Toxoplasma*'s border." Bioessays **33**(9): 693-700.

Ferguson, D. J. and W. M. Hutchison (1987). "The host-parasite relationship of *Toxoplasma gondii* in the brains of chronically infected mice." Virchows Arch A Pathol Anat Histopathol **411**(1): 39-43.

Fischer, H. G., S. Stachelhaus, M. Sahm, H. E. Meyer and G. Reichmann (1998). "GRA7, an excretory 29 kDa *Toxoplasma gondii* dense granule antigen released by infected host cells." Mol Biochem Parasitol **91**(2): 251-262.

Foe, I. T., M. A. Child, J. D. Majmudar, S. Krishnamurthy, W. A. van der Linden, G. E. Ward, B. R. Martin and M. Bogyo (2015). "Global Analysis of Palmitoylated Proteins in *Toxoplasma gondii*." Cell Host Microbe **18**(4): 501-511.

Formstecher, E., S. Aresta, V. Collura, A. Hamburger, A. Meil, A. Trehin, C. Reverdy, V. Betin, S. Maire, C. Brun, B. Jacq, M. Arpin, Y. Bellaiche, S. Bellusci, P. Benaroch, M. Bornens, R. Chanet, P. Chavrier, O. Delattre, V. Doye, R. Fehon, G. Faye, T. Galli, J. A. Girault, B. Goud, J. de Gunzburg, L. Johannes, M. P. Junier, V. Mirouse, A. Mukherjee, D. Papadopoulo, F. Perez, A. Plessis, C. Rosse, S. Saule, D. Stoppa-Lyonnet, A. Vincent, M. White, P. Legrain, J. Wojcik, J. Camonis and L. Daviet (2005). "Protein interaction mapping: a *Drosophila* case study." Genome Res **15**(3): 376-384.

Fox, B. A., A. Falla, L. M. Rommereim, T. Tomita, J. P. Gigley, C. Mercier, M. F. Cesbron-Delauw, L. M. Weiss and D. J. Bzik (2011). "Type II *Toxoplasma gondii* KU80 knockout strains enable functional analysis of genes required for cyst development and latent infection." Eukaryot Cell **10**(9): 1193-1206.

Francia, M. E., S. Wicher, D. A. Pace, J. Sullivan, S. N. Moreno and G. Arrizabalaga (2011). "A *Toxoplasma gondii* protein with homology to intracellular type Na(+)/H(+) exchangers is important for osmoregulation and invasion." Exp Cell Res **317**(10): 1382-1396.

Frenal, K., V. Polonais, J. B. Marq, R. Stratmann, J. Limenitakis and D. Soldati-Favre (2010). "Functional dissection of the apicomplexan glideosome molecular architecture." Cell Host Microbe **8**(4): 343-357.

Frenkel, J. K., J. P. Dubey and N. L. Miller (1970). "Toxoplasma gondii in cats: fecal stages identified as coccidian oocysts." Science **167**(3919): 893-896.

Fromont-Racine, M., J. C. Rain and P. Legrain (1997). "Toward a functional analysis of the yeast genome through exhaustive two-hybrid screens." Nat Genet **16**(3): 277-282.

Fruth, I. A. and G. Arrizabalaga (2007). "Toxoplasma gondii: induction of egress by the potassium ionophore nigericin." Int J Parasitol **37**(14): 1559-1567.

Fukasawa, Y., T. Oda, K. Tomii and K. Imai (2017). "Origin and Evolutionary Alteration of the Mitochondrial Import System in Eukaryotic Lineages." Mol Biol Evol **34**(7): 1574-1586.

Furie, B., B. A. Bouchard and B. C. Furie (1999). "Vitamin K-dependent biosynthesis of gamma-carboxyglutamic acid." Blood **93**(6): 1798-1808.

Gaji, R. Y., D. E. Johnson, M. Treeck, M. Wang, A. Hudmon and G. Arrizabalaga (2015). "Phosphorylation of a Myosin Motor by TgCDPK3 Facilitates Rapid Initiation of Motility during Toxoplasma gondii egress." PLoS Pathog **11**(11): e1005268.

Gajria, B., A. Bahl, J. Brestelli, J. Dommer, S. Fischer, X. Gao, M. Heiges, J. Iodice, J. C. Kissinger, A. J. Mackey, D. F. Pinney, D. S. Roos, C. J. Stoeckert, Jr., H. Wang and B. P. Brunk (2008). "ToxoDB: an integrated Toxoplasma gondii database resource." Nucleic Acids Res **36**(Database issue): D553-556.

Garcia-Reguet, N., M. Lebrun, M. N. Fourmaux, O. Mercereau-Puijalon, T. Mann, C. J. Beckers, B. Samyn, J. Van Beeumen, D. Bout and J. F. Dubremetz (2000). "The microneme protein MIC3 of *Toxoplasma gondii* is a secretory adhesin that binds to both the surface of the host cells and the surface of the parasite." Cell Microbiol **2**(4): 353-364.

Garrison, E., M. Treeck, E. Ehret, H. Butz, T. Garbuz, B. P. Oswald, M. Settles, J. Boothroyd and G. Arrizabalaga (2012). "A forward genetic screen reveals that calcium-dependent protein kinase 3 regulates egress in *Toxoplasma*." PLoS Pathog **8**(11): e1003049.

Gazarini, M. L., A. P. Thomas, T. Pozzan and C. R. Garcia (2003). "Calcium signaling in a low calcium environment: how the intracellular malaria parasite solves the problem." J Cell Biol **161**(1): 103-110.

Gilbert, R. E. and M. R. Stanford (2000). "Is ocular toxoplasmosis caused by prenatal or postnatal infection?" Br J Ophthalmol **84**(2): 224-226.

Gold, D. A., A. D. Kaplan, A. Lis, G. C. Bett, E. E. Rosowski, K. M. Cirelli, A. Bougdour, S. M. Sidik, J. R. Beck, S. Lourido, P. F. Egea, P. J. Bradley, M. A. Hakimi, R. L. Rasmusson and J. P. Saeij (2015). "The *Toxoplasma* Dense Granule Proteins GRA17 and GRA23 Mediate the Movement of Small Molecules between the Host and the Parasitophorous Vacuole." Cell Host Microbe **17**(5): 642-652.

Gould, S. B., R. F. Waller and G. I. McFadden (2008). "Plastid evolution." Annu Rev Plant Biol **59**: 491-517.

Gray, M. W. (2017). "Lynn Margulis and the endosymbiont hypothesis: 50 years later." Mol Biol Cell **28**(10): 1285-1287.

Greenway, M. R. F., K. A. Sacco and M. C. Burton (2017). "In Deep: Cerebral Toxoplasmosis." Am J Med **130**(7): 802-804.

Haller, T., H. Volkl, P. Deetjen and P. Dietl (1996). "The lysosomal Ca²⁺ pool in MDCK cells can be released by ins(1,4,5)P₃-dependent hormones or thapsigargin but does not activate store-operated Ca²⁺ entry." Biochem J **319 (Pt 3)**: 909-912.

Harding, C. R. and M. Meissner (2014). "The inner membrane complex through development of *Toxoplasma gondii* and *Plasmodium*." Cell Microbiol **16**(5): 632-641.

Hoppe, H. C. and K. A. Joiner (2000). "Cytoplasmic tail motifs mediate endoplasmic reticulum localization and export of transmembrane reporters in the protozoan parasite *Toxoplasma gondii*." Cell Microbiol **2**(6): 569-578.

Horton, P., K. J. Park, T. Obayashi, N. Fujita, H. Harada, C. J. Adams-Collier and K. Nakai (2007). "WoLF PSORT: protein localization predictor." Nucleic Acids Res **35**(Web Server issue): W585-587.

Howe, D. K. and L. D. Sibley (1995). "*Toxoplasma gondii* comprises three clonal lineages: correlation of parasite genotype with human disease." J Infect Dis **172**(6): 1561-1566.

Hu, K., T. Mann, B. Striepen, C. J. Beckers, D. S. Roos and J. M. Murray (2002). "Daughter cell assembly in the protozoan parasite *Toxoplasma gondii*." Mol Biol Cell **13**(2): 593-606.

Hu, K., D. S. Roos and J. M. Murray (2002). "A novel polymer of tubulin forms the conoid of *Toxoplasma gondii*." J Cell Biol **156**(6): 1039-1050.

Huynh, M. H. and V. B. Carruthers (2006). "Toxoplasma MIC2 is a major determinant of invasion and virulence." PLoS Pathog **2**(8): e84.

Huynh, M. H. and V. B. Carruthers (2009). "Tagging of endogenous genes in a *Toxoplasma gondii* strain lacking Ku80." Eukaryot Cell **8**(4): 530-539.

Huynh, M. H., K. E. Rabenau, J. M. Harper, W. L. Beatty, L. D. Sibley and V. B. Carruthers (2003). "Rapid invasion of host cells by *Toxoplasma* requires secretion of the MIC2-M2AP adhesive protein complex." EMBO J **22**(9): 2082-2090.

Israelski, D. M. and J. S. Remington (1993). "Toxoplasmosis in patients with cancer." Clin Infect Dis **17 Suppl 2**: S423-435.

Jacobs, D., J. F. Dubremetz, A. Loyens, F. Bosman and E. Saman (1998). "Identification and heterologous expression of a new dense granule protein (GRA7) from *Toxoplasma gondii*." Mol Biochem Parasitol **91**(2): 237-249.

Jewell, M. L., J. K. Frenkel, K. M. Johnson, V. Reed and A. Ruiz (1972). "Development of *Toxoplasma* oocysts in neotropical felidae." Am J Trop Med Hyg **21**(5): 512-517.

Johnson, A. M., P. J. McDonald and S. H. Neoh (1979). "Kinetics of the growth of *Toxoplasma gondii* (RH strain) in mice." Int J Parasitol **9**(1): 55-56.

Jones, J., A. Lopez and M. Wilson (2003). "Congenital toxoplasmosis." Am Fam Physician **67**(10): 2131-2138.

Karimi, G., A. Mardan and M. Zadsar (2014). "Toxoplasma and blood transfusion." Iran J Parasitol **9**(4): 597-598.

Karsten, V., H. Qi, C. J. Beckers, A. Reddy, J. F. Dubremetz, P. Webster and K. A. Joiner (1998). "The protozoan parasite *Toxoplasma gondii* targets proteins to dense granules and the vacuolar space using both conserved and unusual mechanisms." J Cell Biol **141**(6): 1323-1333.

Kasper, L. H., M. S. Bradley and E. R. Pfefferkorn (1984). "Identification of stage-specific sporozoite antigens of *Toxoplasma gondii* by monoclonal antibodies." J Immunol **132**(1): 443-449.

Kim, J. Y., H. J. Ahn, K. J. Ryu and H. W. Nam (2008). "Interaction between parasitophorous vacuolar membrane-associated GRA3 and calcium modulating ligand of host cell endoplasmic reticulum in the parasitism of *Toxoplasma gondii*." Korean J Parasitol **46**(4): 209-216.

Kim, K., D. Soldati and J. C. Boothroyd (1993). "Gene replacement in *Toxoplasma gondii* with chloramphenicol acetyltransferase as selectable marker." Science **262**(5135): 911-914.

Lam, S. S., J. D. Martell, K. J. Kamer, T. J. Deerinck, M. H. Ellisman, V. K. Mootha and A. Y. Ting (2015). "Directed evolution of APEX2 for electron microscopy and proximity labeling." Nat Methods **12**(1): 51-54.

Landrith, T. A., T. H. Harris and E. H. Wilson (2015). "Characteristics and critical function of CD8+ T cells in the *Toxoplasma*-infected brain." Semin Immunopathol **37**(3): 261-270.

Lau, Y. L., W. C. Lee, R. Gudimella, G. Zhang, X. T. Ching, R. Razali, F. Aziz, A. Anwar and M. Y. Fong (2016). "Deciphering the Draft Genome of *Toxoplasma gondii* RH Strain." PLoS One **11**(6): e0157901.

Lavine, M. D., L. J. Knoll, P. J. Rooney and G. Arrizabalaga (2007). "A *Toxoplasma gondii* mutant defective in responding to calcium fluxes shows reduced in vivo pathogenicity." *Mol Biochem Parasitol* **155**(2): 113-122.

Leander, B. S., O. N. Kuvardina, V. V. Aleshin, A. P. Mylnikov and P. J. Keeling (2003). "Molecular phylogeny and surface morphology of *Colpodella edax* (Alveolata): insights into the phagotrophic ancestry of apicomplexans." *J Eukaryot Microbiol* **50**(5): 334-340.

Lebrun, M., A. Michelin, H. El Hajj, J. Poncet, P. J. Bradley, H. Vial and J. F. Dubremetz (2005). "The rhoptry neck protein RON4 re-localizes at the moving junction during *Toxoplasma gondii* invasion." *Cell Microbiol* **7**(12): 1823-1833.

Lecordier, L., C. Mercier, L. D. Sibley and M. F. Cesbron-Delauw (1999). "Transmembrane insertion of the *Toxoplasma gondii* GRA5 protein occurs after soluble secretion into the host cell." *Mol Biol Cell* **10**(4): 1277-1287.

Lelu, M., I. Villena, M. L. Darde, D. Aubert, R. Geers, E. Dupuis, F. Marnef, M. L. Poulle, C. Gotteland, A. Dumetre and E. Gilot-Fromont (2012). "Quantitative estimation of the viability of *Toxoplasma gondii* oocysts in soil." *Appl Environ Microbiol* **78**(15): 5127-5132.

Liu, J., D. Pace, Z. Dou, T. P. King, D. Guidot, Z. H. Li, V. B. Carruthers and S. N. Moreno (2014). "A vacuolar-H(+) -pyrophosphatase (TgVP1) is required for microneme secretion, host cell invasion, and extracellular survival of *Toxoplasma gondii*." *Mol Microbiol* **93**(4): 698-712.

Liu, Z., Y. Wang, T. Gao, Z. Pan, H. Cheng, Q. Yang, Z. Cheng, A. Guo, J. Ren and Y. Xue (2014). "CPLM: a database of protein lysine modifications." Nucleic Acids Res **42**(Database issue): D531-536.

Lopez, J., A. Bittame, C. Massera, V. Vasseur, G. Effantin, A. Valat, C. Buillon, S. Allart, B. A. Fox, L. M. Rommereim, D. J. Bzik, G. Schoehn, W. Weissenhorn, J. F. Dubremetz, J. Gagnon, C. Mercier, M. F. Cesbron-Delauw and N. Blanchard (2015). "Intravacuolar Membranes Regulate CD8 T Cell Recognition of Membrane-Bound Toxoplasma gondii Protective Antigen." Cell Rep **13**(10): 2273-2286.

Lourido, S. and S. N. Moreno (2015). "The calcium signaling toolkit of the Apicomplexan parasites Toxoplasma gondii and Plasmodium spp." Cell Calcium **57**(3): 186-193.

Lovett, J. L. and L. D. Sibley (2003). "Intracellular calcium stores in Toxoplasma gondii govern invasion of host cells." J Cell Sci **116**(Pt 14): 3009-3016.

Luft, B. J. and J. S. Remington (1992). "Toxoplasmic encephalitis in AIDS." Clin Infect Dis **15**(2): 211-222.

Luo, S., F. A. Ruiz and S. N. Moreno (2005). "The acidocalcisome Ca²⁺-ATPase (TgA1) of Toxoplasma gondii is required for polyphosphate storage, intracellular calcium homeostasis and virulence." Mol Microbiol **55**(4): 1034-1045.

Luo, S., M. Vieira, J. Graves, L. Zhong and S. N. Moreno (2001). "A plasma membrane-type Ca(2+)-ATPase co-localizes with a vacuolar H(+)-

pyrophosphatase to acidocalcisomes of *Toxoplasma gondii*." EMBO J **20**(1-2): 55-64.

Martin-Iguacel, R., M. G. Ahlstrom, M. Touma, F. N. Engsig, N. B. Staerke, M. Staerkind, N. Obel and L. D. Rasmussen (2017). "Incidence, presentation and outcome of toxoplasmosis in HIV infected in the combination antiretroviral therapy era." J Infect.

Mazzillo, F. F., K. Shapiro and M. W. Silver (2013). "A new pathogen transmission mechanism in the ocean: the case of sea otter exposure to the land-parasite *Toxoplasma gondii*." PLoS One **8**(12): e82477.

McFadden, G. I. and E. Yeh (2017). "The apicoplast: now you see it, now you don't." Int J Parasitol **47**(2-3): 137-144.

Melo, E. J., M. Attias and W. De Souza (2000). "The single mitochondrion of tachyzoites of *Toxoplasma gondii*." J Struct Biol **130**(1): 27-33.

Mercier, C., K. D. Adjogble, W. Daubener and M. F. Delauw (2005). "Dense granules: are they key organelles to help understand the parasitophorous vacuole of all apicomplexa parasites?" Int J Parasitol **35**(8): 829-849.

Mercier, C. and M. F. Cesbron-Delauw (2015). "Toxoplasma secretory granules: one population or more?" Trends Parasitol **31**(2): 60-71.

Mercier, C., M. F. Cesbron-Delauw and L. D. Sibley (1998). "The amphipathic alpha helices of the toxoplasma protein GRA2 mediate post-secretory membrane association." J Cell Sci **111 (Pt 15)**: 2171-2180.

Mercier, C., J. F. Dubremetz, B. Rauscher, L. Lecordier, L. D. Sibley and M. F. Cesbron-Delauw (2002). "Biogenesis of nanotubular network in *Toxoplasma*

parasitophorous vacuole induced by parasite proteins." Mol Biol Cell **13**(7): 2397-2409.

Mercier, C., D. K. Howe, D. Mordue, M. Lingnau and L. D. Sibley (1998). "Targeted disruption of the GRA2 locus in *Toxoplasma gondii* decreases acute virulence in mice." Infect Immun **66**(9): 4176-4182.

Mets, M. B., E. Holfels, K. M. Boyer, C. N. Swisher, N. Roizen, L. Stein, M. Stein, J. Hopkins, S. Withers, D. Mack, R. Luciano, D. Patel, J. S. Remington, P. Meier and R. McLeod (1997). "Eye manifestations of congenital toxoplasmosis." Am J Ophthalmol **123**(1): 1-16.

Miranda, K., D. A. Pace, R. Cintron, J. C. Rodrigues, J. Fang, A. Smith, P. Rohloff, E. Coelho, F. de Haas, W. de Souza, I. Coppens, L. D. Sibley and S. N. Moreno (2010). "Characterization of a novel organelle in *Toxoplasma gondii* with similar composition and function to the plant vacuole." Mol Microbiol **76**(6): 1358-1375.

Mondragon, R. and E. Frixione (1996). "Ca(2+)-dependence of conoid extrusion in *Toxoplasma gondii* tachyzoites." J Eukaryot Microbiol **43**(2): 120-127.

Montoya, J. G. and O. Liesenfeld (2004). "Toxoplasmosis." Lancet **363**(9425): 1965-1976.

Mordue, D. G., N. Desai, M. Dustin and L. D. Sibley (1999). "Invasion by *Toxoplasma gondii* establishes a moving junction that selectively excludes host cell plasma membrane proteins on the basis of their membrane anchoring." J Exp Med **190**(12): 1783-1792.

Mordue, D. G., S. Hakansson, I. Niesman and L. D. Sibley (1999). "Toxoplasma gondii resides in a vacuole that avoids fusion with host cell endocytic and exocytic vesicular trafficking pathways." Exp Parasitol **92**(2): 87-99.

Moreno, S. N., L. Ayong and D. A. Pace (2011). "Calcium storage and function in apicomplexan parasites." Essays Biochem **51**: 97-110.

Moreno, S. N. and L. Zhong (1996). "Acidocalcisomes in Toxoplasma gondii tachyzoites." Biochem J **313 (Pt 2)**: 655-659.

Morlon-Guyot, J., L. Berry, C. T. Chen, M. J. Gubbels, M. Lebrun and W. Daher (2014). "The Toxoplasma gondii calcium-dependent protein kinase 7 is involved in early steps of parasite division and is crucial for parasite survival." Cell Microbiol **16**(1): 95-114.

Moudy, R., T. J. Manning and C. J. Beckers (2001). "The loss of cytoplasmic potassium upon host cell breakdown triggers egress of Toxoplasma gondii." J Biol Chem **276**(44): 41492-41501.

Muniz-Hernandez, S., M. G. Carmen, M. Mondragon, C. Mercier, M. F. Cesbron, S. L. Mondragon-Gonzalez, S. Gonzalez and R. Mondragon (2011). "Contribution of the residual body in the spatial organization of Toxoplasma gondii tachyzoites within the parasitophorous vacuole." J Biomed Biotechnol **2011**: 473983.

Murphy, E., L. R. Berkowitz, E. Orringer, L. Levy, S. A. Gabel and R. E. London (1987). "Cytosolic free calcium levels in sickle red blood cells." Blood **69**(5): 1469-1474.

Nagamune, K. (2009). "[Toxoplasma gondii as a plant: plant hormone and calcium signaling]." Tanpakushitsu Kakusan Koso **54**(8 Suppl): 1047-1052.

Nagamune, K., W. L. Beatty and L. D. Sibley (2007). "Artemisinin induces calcium-dependent protein secretion in the protozoan parasite *Toxoplasma gondii*." Eukaryot Cell **6**(11): 2147-2156.

Nagamune, K., L. M. Hicks, B. Fux, F. Brossier, E. N. Chini and L. D. Sibley (2008). "Abscisic acid controls calcium-dependent egress and development in *Toxoplasma gondii*." Nature **451**(7175): 207-210.

Nair, S. C., C. F. Brooks, C. D. Goodman, A. Sturm, G. I. McFadden, S. Sundriyal, J. L. Anglin, Y. Song, S. N. Moreno and B. Striepen (2011). "Apicoplast isoprenoid precursor synthesis and the molecular basis of fosmidomycin resistance in *Toxoplasma gondii*." J Exp Med **208**(7): 1547-1559.

Neuen-Jacob, E., C. Figge, G. Arendt, B. Wendtland, B. Jacob and W. Wechsler (1993). "Neuropathological studies in the brains of AIDS patients with opportunistic diseases." Int J Legal Med **105**(6): 339-350.

Nichols, B. A. and M. L. Chiappino (1987). "Cytoskeleton of *Toxoplasma gondii*." J Protozool **34**(2): 217-226.

Niedelman, W., D. A. Gold, E. E. Rosowski, J. K. Sprockholt, D. Lim, A. Farid Arenas, M. B. Melo, E. Spooner, M. B. Yaffe and J. P. Saeij (2012). "The rhoptry proteins ROP18 and ROP5 mediate *Toxoplasma gondii* evasion of the murine, but not the human, interferon-gamma response." PLoS Pathog **8**(6): e1002784.

Niesen, F. H., H. Berglund and M. Vedadi (2007). "The use of differential scanning fluorimetry to detect ligand interactions that promote protein stability." Nat Protoc **2**(9): 2212-2221.

Okada, T., D. Marmansari, Z. M. Li, A. Adilbish, S. Canko, A. Ueno, H. Shono, H. Furuoka and M. Igarashi (2013). "A novel dense granule protein, GRA22, is involved in regulating parasite egress in *Toxoplasma gondii*." Mol Biochem Parasitol **189**(1-2): 5-13.

Opitz, C. and D. Soldati (2002). "'The glideosome': a dynamic complex powering gliding motion and host cell invasion by *Toxoplasma gondii*." Mol Microbiol **45**(3): 597-604.

Oray, M., P. C. Ozdal, Z. Cebeci, N. Kir and I. Tugal-Tutkun (2015). "Fulminant Ocular Toxoplasmosis: The Hazards of Corticosteroid Monotherapy." Ocul Immunol Inflamm: 1-10.

Pace, D. A., C. A. McKnight, J. Liu, V. Jimenez and S. N. Moreno (2014). "Calcium entry in *Toxoplasma gondii* and its enhancing effect of invasion-linked traits." J Biol Chem **289**(28): 19637-19647.

Pappas, G., N. Roussos and M. E. Falagas (2009). "Toxoplasmosis snapshots: global status of *Toxoplasma gondii* seroprevalence and implications for pregnancy and congenital toxoplasmosis." Int J Parasitol **39**(12): 1385-1394.

Park, Y. H. (2012). "*Toxoplasma gondii* in the peripheral blood of patients with ocular toxoplasmosis." Br J Ophthalmol **96**(5): 766; author reply 766.

Parker, S. L. and R. E. Holliman (1992). "Toxoplasmosis and laboratory workers: a case-control assessment of risk." Med Lab Sci **49**(2): 103-106.

Parussini, F., I. Coppens, P. P. Shah, S. L. Diamond and V. B. Carruthers (2010). "Cathepsin L occupies a vacuolar compartment and is a protein maturase within the endo/exocytic system of *Toxoplasma gondii*." Mol Microbiol **76**(6): 1340-1357.

Peixoto, L., F. Chen, O. S. Harb, P. H. Davis, D. P. Beiting, C. S. Brownback, D. Ouloguem and D. S. Roos (2010). "Integrative genomic approaches highlight a family of parasite-specific kinases that regulate host responses." Cell Host Microbe **8**(2): 208-218.

Pelletier, L., C. A. Stern, M. Pypaert, D. Sheff, H. M. Ngo, N. Roper, C. Y. He, K. Hu, D. Toomre, I. Coppens, D. S. Roos, K. A. Joiner and G. Warren (2002). "Golgi biogenesis in *Toxoplasma gondii*." Nature **418**(6897): 548-552.

Pfefferkorn, E. R., D. J. Bzik and C. P. Honsinger (2001). "Toxoplasma gondii: mechanism of the parasitostatic action of 6-thioxanthine." Exp Parasitol **99**(4): 235-243.

Pfefferkorn, L. C. and E. R. Pfefferkorn (1980). "Toxoplasma gondii: genetic recombination between drug resistant mutants." Exp Parasitol **50**(3): 305-316.

Pingret, L., J. M. Millot, S. Sharonov, A. Bonhomme, M. Manfait and J. M. Pinon (1996). "Relationship between intracellular free calcium concentrations and the intracellular development of *Toxoplasma gondii*." J Histochem Cytochem **44**(10): 1123-1129.

Porter, S. B. and M. A. Sande (1992). "Toxoplasmosis of the central nervous system in the acquired immunodeficiency syndrome." N Engl J Med **327**(23): 1643-1648.

Pressman, B. C. (1976). "Biological applications of ionophores." Annu Rev Biochem **45**: 501-530.

Prole, D. L. and C. W. Taylor (2011). "Identification of intracellular and plasma membrane calcium channel homologues in pathogenic parasites." PLoS One **6**(10): e26218.

Radke, J. R., B. Striepen, M. N. Guerini, M. E. Jerome, D. S. Roos and M. W. White (2001). "Defining the cell cycle for the tachyzoite stage of *Toxoplasma gondii*." Mol Biochem Parasitol **115**(2): 165-175.

Rain, J. C., L. Selig, H. De Reuse, V. Battaglia, C. Reverdy, S. Simon, G. Lenzen, F. Petel, J. Wojcik, V. Schachter, Y. Chemama, A. Labigne and P. Legrain (2001). "The protein-protein interaction map of *Helicobacter pylori*." Nature **409**(6817): 211-215.

Reed, P. W. and H. A. Lardy (1972). "A23187: a divalent cation ionophore." J Biol Chem **247**(21): 6970-6977.

Ren, J., L. Wen, X. Gao, C. Jin, Y. Xue and X. Yao (2008). "CSS-Palm 2.0: an updated software for palmitoylation sites prediction." Protein Eng Des Sel **21**(11): 639-644.

Rodrigues, C. O., F. A. Ruiz, P. Rohloff, D. A. Scott and S. N. Moreno (2002). "Characterization of isolated acidocalcisomes from *Toxoplasma gondii* tachyzoites reveals a novel pool of hydrolyzable polyphosphate." J Biol Chem **277**(50): 48650-48656.

Rodrigues, C. O., D. A. Scott, B. N. Bailey, W. De Souza, M. Benchimol, B. Moreno, J. A. Urbina, E. Oldfield and S. N. Moreno (2000). "Vacuolar proton

pyrophosphatase activity and pyrophosphate (PPi) in *Toxoplasma gondii* as possible chemotherapeutic targets." Biochem J **349 Pt 3**: 737-745.

Roiko, M. S., N. Svezhova and V. B. Carruthers (2014). "Acidification Activates *Toxoplasma gondii* Motility and Egress by Enhancing Protein Secretion and Cytolytic Activity." PLoS Pathog **10**(11): e1004488.

Rome, M. E., J. R. Beck, J. M. Turetzky, P. Webster and P. J. Bradley (2008). "Intervacuolar transport and unique topology of GRA14, a novel dense granule protein in *Toxoplasma gondii*." Infect Immun **76**(11): 4865-4875.

Rosowski, E. E., D. Lu, L. Julien, L. Rodda, R. A. Gaiser, K. D. Jensen and J. P. Saeij (2011). "Strain-specific activation of the NF-kappaB pathway by GRA15, a novel *Toxoplasma gondii* dense granule protein." J Exp Med **208**(1): 195-212.

Roux, K. J., D. I. Kim and B. Burke (2013). "BioID: a screen for protein-protein interactions." Curr Protoc Protein Sci **74**: Unit 19 23.

Ruggiero, M. A., D. P. Gordon, T. M. Orrell, N. Bailly, T. Bourgoin, R. C. Brusca, T. Cavalier-Smith, M. D. Guiry and P. M. Kirk (2015). "A higher level classification of all living organisms." PLoS One **10**(4): e0119248.

Ruiz, N., S. S. Chng, A. Hiniker, D. Kahne and T. J. Silhavy (2010). "Nonconsecutive disulfide bond formation in an essential integral outer membrane protein." Proc Natl Acad Sci U S A **107**(27): 12245-12250.

Russell, D. G. and R. G. Burns (1984). "The polar ring of coccidian sporozoites: a unique microtubule-organizing centre." J Cell Sci **65**: 193-207.

Saeij, J. P., J. P. Boyle, M. E. Grigg, G. Arrizabalaga and J. C. Boothroyd (2005). "Bioluminescence imaging of *Toxoplasma gondii* infection in living mice reveals dramatic differences between strains." Infect Immun **73**(2): 695-702.

San Miguel, J. M., D. Gutierrez-Exposito, A. Aguado-Martinez, E. Gonzalez-Zotes, J. Pereira-Bueno, M. Gomez-Bautista, P. Rubio, L. M. Ortega-Mora, E. Collantes-Fernandez and G. Alvarez-Garcia (2016). "Effect of Different Ecosystems and Management Practices on *Toxoplasma Gondii* and *Neospora Caninum* Infections in Wild Ruminants in Spain." J Wildl Dis **52**(2): 293-300.

Scholytyseck, E., H. Mehlhorn and B. E. Muller (1974). "[Fine structure of cyst and cyst wall of *Sarcocystis tenella*, *Besnoitia jellisoni*, *Frenkelia* sp. and *Toxoplasma gondii*]." J Protozool **21**(2): 284-294.

Schwab, J. C., C. J. Beckers and K. A. Joiner (1994). "The parasitophorous vacuole membrane surrounding intracellular *Toxoplasma gondii* functions as a molecular sieve." Proc Natl Acad Sci U S A **91**(2): 509-513.

Schwartzman, J. D. and E. C. Krug (1989). "Toxoplasma gondii: characterization of monoclonal antibodies that recognize rhoptries." Exp Parasitol **68**(1): 74-82.

Sheiner, L., J. D. Fellows, J. Ovciarikova, C. F. Brooks, S. Agrawal, Z. C. Holmes, I. Bietz, N. Flinner, S. Heiny, O. Mirus, J. M. Przyborski and B. Striepen (2015). "*Toxoplasma gondii* Toc75 Functions in Import of Stromal but not Peripheral Apicoplast Proteins." Traffic **16**(12): 1254-1269.

Sheiner, L. and D. Soldati-Favre (2008). "Protein trafficking inside *Toxoplasma gondii*." Traffic **9**(5): 636-646.

Sibley, L. D., I. R. Niesman, T. Asai and T. Takeuchi (1994). "Toxoplasma gondii: secretion of a potent nucleoside triphosphate hydrolase into the parasitophorous vacuole." Exp Parasitol **79**(3): 301-311.

Sibley, L. D., I. R. Niesman, S. F. Parmley and M. F. Cesbron-Delauw (1995). "Regulated secretion of multi-lamellar vesicles leads to formation of a tubulo-vesicular network in host-cell vacuoles occupied by Toxoplasma gondii." J Cell Sci **108 (Pt 4)**: 1669-1677.

Slavin, M. A., J. D. Meyers, J. S. Remington and R. C. Hackman (1994). "Toxoplasma gondii infection in marrow transplant recipients: a 20 year experience." Bone Marrow Transplant **13**(5): 549-557.

Sloves, P. J., S. Delhaye, T. Mouveaux, E. Werkmeister, C. Slomianny, A. Hovasse, T. Dilezitoko Alayi, I. Callebaut, R. Y. Gaji, C. Schaeffer-Reiss, A. Van Dorsselear, V. B. Carruthers and S. Tomavo (2012). "Toxoplasma sortilin-like receptor regulates protein transport and is essential for apical secretory organelle biogenesis and host infection." Cell Host Microbe **11**(5): 515-527.

Soete, M., D. Camus and J. F. Dubremetz (1994). "Experimental induction of bradyzoite-specific antigen expression and cyst formation by the RH strain of Toxoplasma gondii in vitro." Exp Parasitol **78**(4): 361-370.

Soete, M., B. Fortier, D. Camus and J. F. Dubremetz (1993). "Toxoplasma gondii: kinetics of bradyzoite-tachyzoite interconversion in vitro." Exp Parasitol **76**(3): 259-264.

Soldati, D. and J. C. Boothroyd (1993). "Transient transfection and expression in the obligate intracellular parasite *Toxoplasma gondii*." Science **260**(5106): 349-352.

Soldati, D., A. Lassen, J. F. Dubremetz and J. C. Boothroyd (1998). "Processing of *Toxoplasma* ROP1 protein in nascent rhoptries." Mol Biochem Parasitol **96**(1-2): 37-48.

Speer, C. A., S. Clark and J. P. Dubey (1998). "Ultrastructure of the oocysts, sporocysts, and sporozoites of *Toxoplasma gondii*." J Parasitol **84**(3): 505-512.

Speer, C. A., M. Tilley, M. E. Temple, J. A. Blixt, J. P. Dubey and M. W. White (1995). "Sporozoites of *Toxoplasma gondii* lack dense-granule protein GRA3 and form a unique parasitophorous vacuole." Mol Biochem Parasitol **75**(1): 75-86.

Srinivas, S. P., A. Ong, L. Goon, L. Goon and J. A. Bonanno (2002). "Lysosomal Ca(2+) stores in bovine corneal endothelium." Invest Ophthalmol Vis Sci **43**(7): 2341-2350.

Stommel, E. W., E. Cho, J. A. Steide, R. Seguin, A. Barchowsky, J. D. Schwartzman and L. H. Kasper (2001). "Identification and role of thiols in *Toxoplasma gondii* egress." Exp Biol Med (Maywood) **226**(3): 229-236.

Stommel, E. W., K. H. Ely, J. D. Schwartzman and L. H. Kasper (1997). "*Toxoplasma gondii*: dithiol-induced Ca²⁺ flux causes egress of parasites from the parasitophorous vacuole." Exp Parasitol **87**(2): 88-97.

Straub, K. W., E. D. Peng, B. E. Hajagos, J. S. Tyler and P. J. Bradley (2011). "The moving junction protein RON8 facilitates firm attachment and host cell invasion in *Toxoplasma gondii*." PLoS Pathog **7**(3): e1002007.

Striepen, B., C. Y. He, M. Matrajt, D. Soldati and D. S. Roos (1998). "Expression, selection, and organellar targeting of the green fluorescent protein in *Toxoplasma gondii*." Mol Biochem Parasitol **92**(2): 325-338.

Suss-Toby, E., J. Zimmerberg and G. E. Ward (1996). "Toxoplasma invasion: the parasitophorous vacuole is formed from host cell plasma membrane and pinches off via a fission pore." Proc Natl Acad Sci U S A **93**(16): 8413-8418.

Tenter, A. M., A. R. Heckeroth and L. M. Weiss (2000). "Toxoplasma gondii: from animals to humans." Int J Parasitol **30**(12-13): 1217-1258.

Tomita, T., D. J. Bzik, Y. F. Ma, B. A. Fox, L. M. Markillie, R. C. Taylor, K. Kim and L. M. Weiss (2013). "The *Toxoplasma gondii* cyst wall protein CST1 is critical for cyst wall integrity and promotes bradyzoite persistence." PLoS Pathog **9**(12): e1003823.

Tomita, T., T. Yamada, L. M. Weiss and A. Orlofsky (2009). "Externally triggered egress is the major fate of *Toxoplasma gondii* during acute infection." J Immunol **183**(10): 6667-6680.

Tran, J. Q., J. C. de Leon, C. Li, M. H. Huynh, W. Beatty and N. S. Morrissette (2010). "RNG1 is a late marker of the apical polar ring in *Toxoplasma gondii*." Cytoskeleton (Hoboken) **67**(9): 586-598.

Travier, L., R. Mondragon, J. F. Dubremetz, K. Musset, M. Mondragon, S. Gonzalez, M. F. Cesbron-Delauw and C. Mercier (2008). "Functional domains of

the Toxoplasma GRA2 protein in the formation of the membranous nanotubular network of the parasitophorous vacuole." Int J Parasitol **38**(7): 757-773.

Treeck, M., J. L. Sanders, J. E. Elias and J. C. Boothroyd (2011). "The phosphoproteomes of Plasmodium falciparum and Toxoplasma gondii reveal unusual adaptations within and beyond the parasites' boundaries." Cell Host Microbe **10**(4): 410-419.

Tyler, J. S. and J. C. Boothroyd (2011). "The C-terminus of Toxoplasma RON2 provides the crucial link between AMA1 and the host-associated invasion complex." PLoS Pathog **7**(2): e1001282.

van Dooren, G. G., C. Tomova, S. Agrawal, B. M. Humbel and B. Striepen (2008). "Toxoplasma gondii Tic20 is essential for apicoplast protein import." Proc Natl Acad Sci U S A **105**(36): 13574-13579.

van Dooren, G. G., L. M. Yeoh, B. Striepen and G. I. McFadden (2016). "The Import of Proteins into the Mitochondrion of Toxoplasma gondii." J Biol Chem **291**(37): 19335-19350.

Varberg, J. M., L. R. Padgett, G. Arrizabalaga and W. J. Sullivan, Jr. (2016). "TgATAT-Mediated alpha-Tubulin Acetylation Is Required for Division of the Protozoan Parasite Toxoplasma gondii." mSphere **1**(1).

Vivier, E. and A. Petitprez (1969). "[The outer membrane complex and its development at the time of the formation of daughter cells in Toxoplasma gondii]." J Cell Biol **43**(2): 329-342.

Wan, K. L., V. B. Carruthers, L. D. Sibley and J. W. Ajioka (1997). "Molecular characterisation of an expressed sequence tag locus of Toxoplasma

gondii encoding the micronemal protein MIC2." Mol Biochem Parasitol **84**(2): 203-214.

Warring, S. D., Z. Dou, V. B. Carruthers, G. I. McFadden and G. G. van Dooren (2014). "Characterization of the chloroquine resistance transporter homologue in *Toxoplasma gondii*." Eukaryot Cell **13**(11): 1360-1370.

Weiss, L. M. and K. Kim (2000). "The development and biology of bradyzoites of *Toxoplasma gondii*." Front Biosci **5**: D391-405.

Weiss, L. M. and K. Kim (2014). *Toxoplasma gondii* the model apicomplexan - perspectives and methods. Amsterdam, Elsevier/AP: xxi, 1085 pages.

Weiss, L. M., D. Laplace, P. M. Takvorian, H. B. Tanowitz, A. Cali and M. Wittner (1995). "A cell culture system for study of the development of *Toxoplasma gondii* bradyzoites." J Eukaryot Microbiol **42**(2): 150-157.

Wilson, C. B., J. S. Remington, S. Stagno and D. W. Reynolds (1980). "Development of adverse sequelae in children born with subclinical congenital *Toxoplasma* infection." Pediatrics **66**(5): 767-774.

Wojcik, J., I. G. Boneca and P. Legrain (2002). "Prediction, assessment and validation of protein interaction maps in bacteria." J Mol Biol **323**(4): 763-770.

Yung, S. and N. Lang-Unnasch (1999). "Targeting of a nuclear encoded protein to the apicoplast of *Toxoplasma gondii*." J Eukaryot Microbiol **46**(5): 79S-80S.

Curriculum Vitae

Kaice Arminda LaFavers

Education

Doctor of Philosophy

Indiana University (Indianapolis, IN)

November 2017

Thesis: A Forward Genetic Approach to Identifying Novel Calcium Regulators in

Toxoplasma gondii

Mentor: Gustavo Arrizabalaga

Master of Public Health

Indiana University School of Medicine (Indianapolis, IN)

August 2012

Major: Epidemiology

Cumulative GPA: 3.979/4.000

Bachelor of Science

Purdue University (West Lafayette, IN)

May 2009

Majors: Microbiology, Honors Biochemistry, Genetic Biology; Cell,

Developmental and Molecular Biology

Minors: Chemistry, Forensic Science, Psychology

Cumulative GPA: 3.79/4.00

Research Experience

Graduate Student

Department of Pharmacology and Toxicology, Indiana University School of
Medicine (Indianapolis, IN)

Mentor: Gustavo Arrizabalaga, Ph.D.

May 2013 – November 2017

Area of study: Calcium signaling in the obligate intracellular parasite *Toxoplasma gondii*

Undergraduate Researcher

Department of Biology, Purdue University (West Lafayette, IN)

Mentor: Richard Kuhn, Ph.D.

January 2006 – October 2008

Area of study: Non-structural protein function in Sindbis virus

Professional Experience

Biochemist

Kelly Scientific Resources, on site at Dow AgroSciences, LLC (Indianapolis, IN)

March 2011 – August 2012

- Created and maintained the structure of a protein “pharmacy” which provided fully characterized, proprietary protein standards to internal and external users.
- Worked with other members of the Plant Biology and Biochemistry group to perform biochemical studies required to register genetically modified plant products with global regulators.

- Developed proficiency in ELISA, SDS-PAGE, Western Blotting, tissue extraction, and seed devitalization techniques

Teaching Experience

Research Mentor

Arrizabalaga Laboratory, Indiana University School of Medicine (Indianapolis, IN)

January 2016 – August 2017

- Mentored an undergraduate biology student on a project identifying and characterizing novel calcium binding proteins in the *T. gondii* parasitophorous vacuole.

Research Mentor

Arrizabalaga Laboratory, Indiana University School of Medicine (Indianapolis, IN)

May 2014 – July 2014

- Mentored a medical student as part of the Student Research Program in Academic Medicine.

Tutor

Biology Resource Center (West Lafayette, Indiana)

January 2008 – May 2009

- Provided free one-on-one and group tutoring for students in core biology courses
- Worked with biology professors to provide necessary resources for underclassmen students to succeed

Publications

LaFavers KA, Marquez Noguerras K, Coppens I, Moreno S, Arrizabalaga A. (2017) A novel dense granule protein, GRA41, regulates timing of egress and calcium sensitivity in *Toxoplasma gondii*. Cellular Microbiology

Roiko MS, **LaFavers KA**, Arrizabalaga G. (2017) *Toxoplasma gondii*-positive human sera recognize intracellular tachyzoites and bradyzoites with diverse patterns of immunoreactivity, submitted.

Varberg J, **LaFavers KA**, Arrizabalaga G, Sullivan WJ. (2017) Characterization of Plasmodium Atg3-Atg8 interaction inhibitors identifies novel alternative mechanisms of action in *Toxoplasma gondii*, submitted.

Treeck M, Sanders JL, Gaji, RY, **LaFavers KA**, Child MA, Arrizabalaga G, Elias JE, Boothroyd JC (2014) The calcium-dependent protein kinase 3 of toxoplasma influences basal calcium levels and functions beyond egress as revealed by quantitative phosphoproteome analysis. PLoS Pathogens. 10(6): e1004197

Zhang J, Luo M, Marasco D, Logsdon D, **LaFavers KA**, Chen Q, Reed A, Kelley MR, Gross ML, Georgiadis MM. (2013) Inhibition of apurinic/aprimidinic endonuclease I's redox activity revisited. Biochemistry. 52(17):2955-66

Grants

T32 AI060519

12/01/2014-12/31/2015

National Institutes of Health

Role: Program trainee

Immunology and Infectious Disease Training Program

16PRE27260042

01/01/2016-12/31/2017

American Heart Association

Role: Principal Investigator

The role of a novel dense granule protein in calcium-dependent signaling in
Toxoplasma gondii

Talks

LaFavers, KA, Gaji, R, Arrizabalaga, GA (2015) A Novel Dense Granule Protein Plays a Role in Calcium-dependent Signaling Events in *Toxoplasma gondii*. Talk given at 2015 Midwest Neglected Infectious Disease Meeting at Notre Dame University.

LaFavers, KA, Gaji, R, Arrizabalaga, GA (2016) A Novel Dense Granule Protein Plays a Role in Calcium-dependent Signaling Events in *Toxoplasma gondii*. Teaser talk and poster given at 2016 Molecular Parasitology Meeting in Woods Hole, MA.

Posters

LaFavers, KA, Gaji, R, Arrizabalaga, GA (2013) Genetic Dissection of Calcium Signaling in *Toxoplasma gondii*. Poster presented at 2013 Midwest Neglected Infectious Disease Meeting at Notre Dame University.

LaFavers, KA, Gaji, R, Arrizabalaga, GA (2013) Genetic Dissection of Calcium Signaling in *Toxoplasma gondii*. Poster presented at the 2013 Molecular Parasitology Meeting in Woods Hole, MA.

LaFavers, KA, Gaji, R, Arrizabalaga, GA (2014) A Novel Dense Granule Protein Plays a Role in Calcium-dependent Signaling Events in *Toxoplasma*

gondii. Poster presented at 2014 Midwest Neglected Infectious Disease Meeting at Notre Dame University.

LaFavers, KA, Arrizabalaga, GA (2015) A Novel Dense Granule Protein Plays a Role in Calcium-dependent Signaling Events in *Toxoplasma gondii*. Poster presented at The 13th International Congress on Toxoplasmosis and *T. gondii* Biology.

Awards and Honors

Recipient of Paradise Travel Award to attend the 2013 Molecular Parasitology Meeting in Woods Hole, MA.

Outstanding Poster Award for “A Novel Dense Granule Protein Plays a Role in Calcium-dependent Signaling Events in *Toxoplasma gondii*” at The 13th International Congress on Toxoplasmosis and *T. gondii* Biology in 2015.

Inducted into Phi Beta Kappa in May 2009.

Recipient of National Merit Scholar scholarship award in May 2005.

Recipient of Howard Hughes Research Internship in June 2006.